

National Institute of Public Health and the Environment (RIVM)
Bilthoven, the Netherlands

Report no. 722108017

**Deposition of base-cations in Europe
and its role in acid neutralization and
forest nutrition**

G.P.J. Draaijers*, E.P. Van Leeuwen,
P.G.H de Jong, and J.W. Erisman

June 1996

* *present address*: TNO Institute of
Environmental Sciences, Energy
Research and Process Innovation.
P.O. box 6011, 2600 JA Delft, the
Netherlands, tel.: +31 15 2696036;
fax: +31 15 2617217.

This investigation has been performed in order and for the account of the Directorate-General for Environmental Protection, Directorate Air and Energy (DGM/LE), within the framework of project 722108.

National Institute of Public Health and the Environment, P.O. box 1, 3720 BA Bilthoven, the Netherlands, tel.: +31 30 2749111; fax: +31 30 2742971

MAILING LIST

1. Ir. G.M. van der Slikke, Directeur Lucht en Energie, DGM
2. Dr. ir. B.C.J. Zoeteman, Plv. Directeur-Generaal Milieubeheer
3. Drs. R.J.T. van Lint, Hoofd afd. Luchtkwaliteit en Verzuring, DGM
4. Dr. B. Achermann (FOEFL, Switzerland)
5. Dr. W.A.H. Asman (RISφ, Denmark)
6. Ir. H.P. Baars (TNO-MEP)
7. Dr. J. Bak (NERI, Denmark)
8. Prof. dr. V.N. Bashkin (RAS-ISSP, Russian Federation)
9. Dr. C. Beier (DFLRI, Denmark)
10. Dr. J.J.M. Berdowski (TNO-MEP)
11. Dr. E. Berge (DNMI, Norway)
12. Dr. R. Bobbink (KUN)
13. Dr. P. Borrell (Fraunhofer Institute, Germany)
14. Drs. F.C. Bosveld (KNMI)
15. Dr. A.W. Boxman (KUN)
16. Dr. A. Branding (Kiel University, Germany)
17. Dr. S. Braun (IAPB, Switzerland)
18. Prof. dr. N. van Breemen (LUW-BG)
19. Dr. J.R. Brook (AES, Canada)
20. Dr. K. Bull (ITE, United Kingdom)
21. Dr. H.G. van Dobben (IBN-DLO)
22. Dr. ing. J.H. Duyzer (TNO-MEP)
23. Dr. L.J.M. van der Eerden (IPO-DLO)
24. Drs. R. van Ek (RIZA)
25. Dr. A. Eliassen (DNMI, Norway)
26. Dr. M. Forsius (FEA, Finland)
27. Dr. F. Fowler (ITE, United Kingdom)
28. Dr. Th. Gauger (Stuttgart University, Germany)
29. Dr. G. Gravenhorst (Göttingen University, Germany)
30. Dr. H.D. Gregor (UBA, Germany)
31. Dr. P. Grennfelt (IVL, Sweden)
32. Dr. R. Guicherit (TNO-MEP)
33. Dr. J.R. Hall (ITE, United Kingdom)
34. Dr. K. Hansen (DFLRI, Denmark)
35. Dr. C.M.A. Hendriks (SC-DLO)
36. Dr. A. Henriksen (NIWR, Norway)
37. Ir. P. Hofschreuder (LUW-LH&V)
38. Ir. M. Hootsmans (DGM)
39. Dr. M. Hornung (ITE, United Kingdom)
40. Dr. K.D. van den Hout (TNO-MEP)
41. Dr. ir. L.W.A. van Hove (LUW-LH&V)
42. Dr. H. Hultberg (IVL, Sweden)
43. Dr. W.P.M.F. Ivens (OU)
44. Dr. T. Iversen (Oslo University, Norway)
45. Dr. M. Johansson (FEA, Finland)
46. Dr. P. Kauppi (Forest Research Institute, Finland)
47. Mr. V.G Keizer (DGM)

48. Dr. K. Kindbom (IVL, Sweden)
49. Ir. J.M. Klap (SC-DLO)
50. Dr. S. Kleemola (FEA, Finland)
51. Dr. R. Köble (Stuttgart University, Germany)
52. Dr. G. Landmann (INFRA, France)
53. Dr. S.E. Lindberg (ORNL, USA)
54. Dr. G. Lövblad (IVL, Sweden)
55. Dr. G.M. Lovett (NYBG, USA)
56. Dr. W. Mill (IEIA, Poland)
57. Dr. G.M.J. Mohren (IBN-DLO)
58. Dr. H.D. Nagel (ÖNU-GmbH, Germany)
59. Dr. T. Paces (CGI, Czech Republic)
60. Dr. L. Rasmussen (DFLRI, Denmark)
61. Drs. G.J. Reinds (SC-DLO)
62. Dr. B. Rihm (METEOTEST, Switzerland)
63. Dr. J.G.M. Roelofs (KUN)
64. Dr. H. Rodhe (Stockholm University, Sweden)
65. Dr. F. G. Römer (KEMA)
66. Ir. W. Ruijgrok (KEMA)
67. Mr. L. Saare (EEIC, Estonia)
68. Dr. J. Schaug (NILU, Norway)
69. Dr. J. Schneider (FEA, Austria)
70. Dr. A. Semb (NILU, Norway)
71. Dr. D. Simpson (DNMI, Norway)
72. Dr. I. Skorepová (CEI, Czech Republic)
73. Prof. dr. J. Slanina (ECN)
74. Drs. S. Smeulders (DGM)
75. Dr. G. Smiatek (Stuttgart University, Germany)
76. Dr. T. Spranger (UBA, Germany)
77. Dr. H. Staaf (IVL, Sweden)
78. Mr. dr. E.G Steingröver (IBN-DLO)
79. Dr. M. Sutton (ITE, United Kingdom)
80. Dr. H. Sverdrup (Lund University, Sweden)
81. Ir. G. van Tol (IKC-NBLF)
82. Dr. E. Ulrich (ONF, France)
83. Dr. A.C. Veltkamp (ECN)
84. Prof. dr. K. Verstraten (FGBL-UvA)
85. Drs. J.O. Voshaar (SC-DLO)
86. Dr. ir. W. de Vries (SC-DLO)
87. Dr. B. Werner (UBA, Germany)
88. Dr. G.P. Wijers (ECN)
89. Dr. B.L.B. Wiman (Lund University, Sweden)
90. Depot Nederlandse Publicaties en Nederlandse Bibliografie
91. Drs. ir. R.B.J. van Noort, Directeur-Generaal RIVM
92. Prof. dr. R. Kroes, Plv. Directeur-Generaal RIVM
93. Prof. Ir. N.D. van Egmond, Directeur Milieu RIVM
94. Prof. dr. G. Elzinga, Directeur Volksgezondheid RIVM
95. Ir. F. Langeweg, Directeur Sector 7 RIVM
96. Drs. J.A.M. Lijdsman, Hoofd Bureau Voorlichting en Public Relations

- 97. Dr. R.M. van Aalst (RIVM-LLO)
- 98. Dr. J. Aben (RIVM-LLO)
- 99. Ir. J.P. Beck (RIVM-LLO)
- 100. Ing. A. Bleeker (RIVM-LLO)
- 101. Ir. L.J.M. Boumans (RIVM-LBG)
- 102. Ir. A.H.M. Bresser (RIVM-LWD)
- 103. Drs. J. Burn (RIVM-LLO)
- 104. Drs. E. Buijsman (RIVM-LLO)
- 105. Dr. A.L.M. Dekkers (RIVM-CWM)
- 106. Ir. H.S.M.A. Diederer (RIVM-LLO)
- 107. Drs. H. Eleveld (RIVM-LLO)
- 108. Dr. ir. J.J.M. van Grinsven (RIVM-LBG)
- 109. Ir. G.J. Heij (RIVM-LWD)
- 110. Dr. J.P. Hettelingh (RIVM-CCE)
- 111. Dr. ing. J.A. van Jaarsveld (RIVM-LLO)
- 112. Dr. L.H.J.M. Janssen (RIVM-LLO)
- 113. Drs. L.H.M. Kohsiek (RIVM-LAE)
- 114. Drs. J. Latour (RIVM-LBG)
- 115. Dr. F.A.A.M. de Leeuw (RIVM-LLO)
- 116. Dr. ir. D. van Lith (RIVM-LLO)
- 117. Drs. R.J.M. Maas (RIVM-MNV)
- 118. E.A.M. Mathijssen-Spiekman (RIVM-ECO)
- 119. Drs. R. Meijers (RIVM-LBG)
- 120. Dr. M.G. Mennen (RIVM-LLO)
- 121. Dr. D. Onderdelinden (RIVM-LLO)
- 122. Dr. M. Posch (RIVM-CCE)
- 123. Ing. C.J.M. Potma (RIVM-LLO)
- 124. Dr. ir. W.A.J. van Pul (RIVM-LLO)
- 125. Drs. R. Reiling (RIVM-LBG)
- 126. Ir. F.J. Sauter (RIVM-CWM)
- 127. Dr. ir. T. Schneider (RIVM-NOP)
- 128. Drs. R.J.C.F. Sluyter (RIVM-LLO)
- 129. Ir. P.A.M. de Smet (RIVM-CCE)
- 130. Dr. A. Tiktak (RIVM-LBG)
- 131. Dr. R. van de Velde (RIVM-LBG)
- 132. Drs. D. de Zwart (RIVM-ECO)
- 133. Bureau rapportenregistratie RIVM
- 133-134. Bibliotheek RIVM
- 135. Bibliotheek RIVM-LLO
- 136-139. Auteurs
- 140-160. Bureau Rapportenbeheer RIVM
- 161-175. Reserve exemplaren

CONTENTS		Page
	Mailing list	2
	Summary	6
	Samenvatting	8
1	Introduction	10
2	Emission sources, profiles and trends	12
3	Modeling and mapping deposition	16
	3.1 Wet deposition	16
	3.2 Dry deposition	22
	3.3 Total deposition	36
4	Acid neutralization capacity	42
	4.1 Amount of acid in precipitation neutralized by base-cations	42
	4.2 Amount of potential acid deposition counteracted by deposition of base-cations	45
5	Contribution to forest nutrition	47
6.	Uncertainty analysis	49
	6.1 Evaluation with independent field data	49
	6.2 Error propagation	56
	6.2.1 Wet deposition	57
	6.2.2 Dry deposition	58
	6.2.3 Total deposition	61
	6.2.4 Acid neutralization capacity	61
	6.2.5 Contribution to forest nutrition	62
7	Conclusions	63
	Acknowledgments	64
	References	65
	Appendices	73

SUMMARY

In considering acidification problems, emphasis is seldom placed on the role of deposition of base-cations such as Na^+ , Mg^{2+} , Ca^{2+} and K^+ . Besides their ability to neutralize acid input, base-cations are found to be important nutrient elements for ecosystems. Up to now no accurate estimates of base-cation deposition are available on a European scale, despite their indispensability for the estimation of critical loads as well as exceedances. In this report, maps of total (i.e. wet and dry) base-cation deposition in Europe, based on the so-called inferential modeling technique are presented. Wet deposition is mapped on the basis of field measurements made at approximately 600 sites scattered over Europe. Dry deposition is calculated using air concentrations estimated from rain chemistry data and a scavenging model, together with deposition velocities derived from land use and meteorological information using a detailed parametrisation of the dry deposition process.

Generally, deposition fields found resemble the geographic variability of sources, land use and climate. For Na^+ and Mg^{2+} , a clear pattern of increasing deposition with decreasing distance to seas, in particular the Atlantic Ocean, is observed, reflecting their sea-salt origin. Large Na^+ deposition is also found e.g. northwest of the Black Sea, probably originating from wind erosion of salt containing soils. Large Mg^{2+} , Ca^{2+} and K^+ deposition in southern and south-eastern Europe results from a combination of wind erosion of calcareous and salt-containing soils, agricultural tillage practices, traffic on unpaved roads, and supply of Saharan dust. Relatively large Ca^{2+} deposition found in the border area between Germany, Poland and the Czech Republic, as well as in Lithuania and Latvia, can be attributed to intensive industrial activity. Dry deposition constitutes on average 45% of the total deposition of non-sea salt $\text{Mg}^{2+}+\text{Ca}^{2+}+\text{K}^+$ in Europe. Mg^{2+} , Ca^{2+} and K^+ contribute on average 21, 66 and 13%, respectively, to the total deposition of non-sea salt $\text{Mg}^{2+}+\text{Ca}^{2+}+\text{K}^+$ in Europe.

In large parts of southern Europe more than 50% of the potential acid deposition is found to be counteracted by deposition of non-sea salt $\text{Mg}^{2+}+\text{Ca}^{2+}+\text{K}^+$. In central and northwestern Europe base-cation deposition usually amounts to less than 25% of the acid input. The lowest base-cation deposition relative to potential acid deposition is found in southern Scandinavia, Denmark, northern Germany and the Netherlands. A similar spatial pattern is found for the neutralization of acid anions in precipitation. Whereas in Scandinavia weathering is found the dominant supplier of base-cations to forest soils, in eastern and southern Europe forests mainly rely on atmospheric deposition for the supply of base-cations.

Modeled deposition estimates compare reasonably well with deposition estimates derived from throughfall and bulk-precipitation measurements made at 174 sites scattered over Europe, taking into account the relatively large uncertainty in both estimates. On average, no significant differences are found, but the model seems to underestimate dry deposition of base-cations near local sources. Using error propagation, the random and systematic errors in total deposition for an average grid cell of 10x20 km were estimated to equal 35-50% and 25-40%, respectively. Wet and dry deposition contribute to the same extent to the random error in total deposition. The systematic error in total deposition, however, is dominated by the systematic error in dry deposition. The latter depends on the systematic uncertainty in dry deposition velocity and air concentration. The parametrisation of the dry deposition velocity is based on a model only tested with results of micrometeorological measurements over

forest in the Netherlands. Validation for other surfaces and climates is necessary to ensure its applicability for the whole of Europe. The parametrisation can be improved by taken into account the impact of size distribution. Relatively large uncertainty is introduced by using precipitation concentrations and a relatively simple scavenging model to estimate air concentrations. The scavenging model can be improved by e.g. incorporating the effect of relative humidity on particle size.

The uncertainty in dry deposition estimates will be reduced considerably if information on the temporal and spatial variability of base-cation air concentration and/or emission becomes available through which air concentrations can be modeled more accurately. Emission-related deposition estimates will provide the opportunity of predicting the loads to be expected in association with specific economic scenarios. In this report, results for 1989 are presented. It may be expected that, due to emission reductions in particularly eastern Europe, deposition of base-cations will have been lower in more recent years. Deposition for the years 1986-1988 and 1990-1994 will be estimated in the near future. An uncertainty analysis using Monte Carlo sampling and simulation is foreseen.

SAMENVATTING

In relatie tot de verzuringsproblematiek wordt meestal weinig aandacht besteed aan de rol van basische kationen zoals Na^+ , Mg^{2+} , Ca^{2+} en K^+ . Echter, door depositie van basische kationen kan een deel van de zure depositie geneutraliseerd worden. Daarnaast zijn basische kationen belangrijke nutriënten voor ecosystemen. Tot op heden zijn geen betrouwbare depositieschattingen voor basische kationen aanwezig op Europese schaal, alhoewel dat deze informatie nodig is voor het bepalen van kritische depositiewaarden en haar overschrijdingen. In dit rapport worden kaarten van de totale (natte en droge) depositie in Europa gepresenteerd welke zijn gebaseerd op de zogenaamde 'inferentie' modellering. De natte depositie is gekarteerd op basis van resultaten van veldmetingen op meer dan 600 lokaties verspreid over Europa. De droge depositie is berekend door vermenigvuldiging van luchtconcentraties en droge depositiesnelheden. Luchtconcentraties zijn bepaald aan de hand van concentraties in neerslag gebruik makend van een scavenging model, terwijl droge depositiesnelheden zijn afgeleid uit landgebruik en meteorologische informatie gebruik makend van een gedetailleerde parametrisatie van het droge depositieproces.

De berekende depositievelden weerspiegelen de geografische variatie in bronnen, landgebruik en klimaat. Voor Na^+ en Mg^{2+} is een duidelijk patroon van toenemende depositie in de richting van zeeën, in het bijzonder de Atlantische Oceaan, gevonden. Hoge Na^+ depositie is ook berekend voor een gebied ten noorden van de Zwarte Zee, welke waarschijnlijk zijn oorsprong vindt in winderosie van zouthoudende bodems. Hoge Mg^{2+} , Ca^{2+} en K^+ depositie gevonden in Zuid-Europa is een gevolg van een combinatie van winderosie van kalk- en/of zouthoudende bodems, emissies samenhangend met agrarische bodembehandelingen en verkeer op onverharde wegen, alsmede toevoer van woestijnstof uit de Sahara. Relatief hoge Ca^{2+} depositie gevonden in het grensgebied tussen Duitsland, Polen en Tjechië, alsmede in bijvoorbeeld Litouwen en Letland, kunnen worden toegeschreven aan industriële emissies. Droge depositie draagt gemiddeld in Europa 45% bij aan de totale depositie van niet-zeezout afkomstig $\text{Mg}^{2+} + \text{Ca}^{2+} + \text{K}^+$. Gemiddeld dragen Mg^{2+} , Ca^{2+} en K^+ in Europa respectievelijk 21, 66 en 13% bij aan de totale depositie van niet-zeezout $\text{Mg}^{2+} + \text{Ca}^{2+} + \text{K}^+$.

Vergelijking met berekende potentieel zure deposities laat zien dat in Zuid-Europa over het algemeen meer dan 50% van de potentieel zure depositie geneutraliseerd wordt door depositie van basische kationen. In Centraal- en Noordwest-Europa bedraagt de depositie van basische kationen in de regel minder dan 25% van de totale depositie van potentieel zuur. De laagste depositie van basische kationen in verhouding tot de depositie van potentieel zuur vindt plaats in Zuid-Scandinavië, Denemarken, Noord-Duitsland en Nederland. Voor de neutralisatie van zuurvormende anionen in neerslag werd een vergelijkbaar ruimtelijk patroon gevonden. Terwijl in Scandinavië de toevoer van basische kationen naar bosbodems voornamelijk plaatsvindt via bodemverwerking, is in Oost- en Zuid-Europa atmosferische depositie de belangrijkste bron van basische kationen.

De gemodelleerde deposities komen goed overeen met depositieschattingen gemaakt voor 174 locaties verspreid over Europa op basis van doorval- en neerslagmetingen, zeker gezien de relatief grote onzekerheid in beide schattingen. Gemiddeld bestonden er geen verschillen tussen beide depositieschattingen. Wel bleek het model de droge depositie op bossen gelegen nabij lokale bronnen systematisch te onderschatten. Met behulp van foutenvoortplantings-technieken is

voor een gemiddelde gridcel van 10x20 km in Europa de toevallige en systematische fout in de totale depositie van basische kationen geschat op 35-50%, respectievelijk 25-40%. Natte en droge depositie dragen in gelijke mate bij aan de toevallige fout. De systematische fout in de depositieschatting wordt echter door de systematische fout in de droge depositie gedomineerd. Laatstgenoemde is afhankelijk van de systematische fout in zowel droge depositie snelheid als luchtconcentratie. De parametrisatie van de depositiesnelheid is gebaseerd op een model dat, tot op heden, alleen getest is met micrometeorologische metingen boven bos in Nederland. Validatie voor andere soorten landgebruik en klimaten is nodig om er zeker van te zijn dat deze parametrisatie voor geheel Europa toepasbaar is. De parametrisatie van de depositiesnelheid kan verbeterd worden door de invloed van de deeltjesgrootteverdeling mee te nemen. De relatief grote onzekerheid in droge depositie hangt mede samen met het gebruik van neerslagconcentraties in samenhang met een scavenging model voor het bepalen van luchtconcentraties. Het scavenging model kan verbeterd worden door bijvoorbeeld het effect van relatieve vochtigheid op de massa-mediane diameters van aerosolen in te bouwen.

De onzekerheid in de berekende droge depositie kan drastisch verminderd worden indien informatie over de temporele en ruimtelijke variatie in luchtconcentraties en/of emissies van basische kationen beschikbaar komt, waardoor de luchtconcentraties nauwkeuriger gemodelleerd kunnen worden. Emissie-gerelateerde depositieschattingen zullen het mogelijk maken toekomstige deposities te voorspellen in afhankelijkheid van specifieke economische scenario's. In dit rapport zijn resultaten voor 1989 gepresenteerd. Verwacht wordt dat nadien, door emissiereducties in met name Oost-Europa, de depositie van basische kationen lager is geworden. In de nabije toekomst zullen depositieschattingen voor de jaren 1986-1988 en 1990-1994 gemaakt worden. Daarbij zullen onzekerheidsschattingen worden gemaakt gebruik makend van Monte Carlo simulaties.

INTRODUCTION

Acid deposition is widely recognized as an environmental problem, the chief causes of which are oxides of sulfur and nitrogen emitted during fossil fuel combustion and metal smelting, and ammonia emitted from animal manure (e.g. Heij and Schneider, 1991; Rodhe *et al.*, 1995). Usually little emphasis is placed on the role of base-cations such as Na^+ , Mg^{2+} , Ca^{2+} and K^+ in relation to acid deposition. Base-cations play an integral role in the chemical processes of acid deposition since the acidity of any material is a function of both its acidic and basic compounds. Besides their ability to neutralize acid, base-cations are important nutrient elements for ecosystems. Deposition of physiologically active base-cations (Mg^{2+} , Ca^{2+} and K^+) may improve the nutrient status of ecosystems with respect to eutrophication by nitrogen inputs (TFM, 1996). The depletion of exchangeable base-cations in sensitive soils is currently thought to represent a major detrimental effect of acid deposition on terrestrial ecosystems (e.g. De Vries, 1994; Rodhe *et al.*, 1995). Atmospheric input of alkaline particles may be a quantitatively important source of base-cations in soils where the mineral content and weathering rate of base-cations is small. Due to the large mass median diameters of alkaline particles and consequently high dry deposition velocities, most alkaline particles are likely to deposit near the area of origin (Milford and Davidson, 1985), although under specific meteorological conditions long-range transport of, for example, desert dust has also been reported (e.g. Ganor *et al.*, 1991; Swap *et al.*, 1992).

For estimation of critical loads or their exceedances (used as a basis for emission control strategies) actual and future base-cation deposition amounts in Europe have to be mapped (Hettelingh *et al.*, 1991; Hornung *et al.*, 1995; Posch *et al.*, 1995; TFM, 1996). Wet deposition maps of base-cations on a European scale have been compiled by Van Leeuwen *et al.* (1995, 1996). Several studies have shown that dry deposition may be quantitatively equally or even more important than wet deposition as a source of base-cations to vegetation (Lannefors *et al.*, 1983; Driscoll *et al.*, 1989; Johnson and Lindberg, 1992; Erisman *et al.*, 1994), stressing the importance to map dry deposition in addition to wet deposition to assess total inputs. Very crude estimates of base-cation dry deposition in Europe have been made by Downing *et al.* (1993) and De Vries *et al.* (1993) (for details see Appendix 1). If emission or concentration estimates are available, dry deposition can be mapped using long-range transport models (e.g. by means of the EMEP model, Iversen *et al.*, 1991). However, up to now there is lack of knowledge on the spatial and temporal variation of base-cation emissions and concentrations.

In this report, base-cations total (wet+dry) deposition maps of Europe are presented which are based on the so-called inferential modeling technique. Deposition fields for 1989 are calculated with a spatial resolution of $1/6^\circ$ latitude x $1/6^\circ$ longitude which equals $\sim 10 \times 20$ km in central Europe (Lambert-Azimuthal projection). Wet deposition is estimated on the basis of field measurements made at a large number of sites scattered over Europe (Van Leeuwen *et al.*, 1995; 1996). Dry deposition is estimated using air concentrations estimated from rain chemistry and scavenging ratios, and deposition velocities calculated using the scheme of Ruijgrok *et al.* (1994) which was based on the model of Slinn (1982). An uncertainty analysis is presented, including all the different steps in the calculation procedure. Furthermore, model results are evaluated using independent field data. Base-cation deposition is compared to the deposition of potential acid as estimated from the EDACS model. The latter is

described in detail in Erisman *et al.* (1995) and Van Pul *et al.* (1995). Moreover a comparison is made with soil weathering rates of base-cations to see to what extent atmospheric deposition contributes to forest nutrition. Soil weathering rates are taken from De Vries *et al.* (1993).

2 EMISSION SOURCES, PROFILES AND TRENDS

In this chapter the different sources of alkaline particles are described and for each source category a characterization is given of the chemical composition of the alkaline particles (i.e. the emission profile). Moreover, trends in emission and deposition are discussed.

Emissions sources

Base-cations in the atmosphere originate from both natural and anthropogenic sources (Gorham, 1994). *Natural* sources of base-cations are associated with wind erosion of arid soils, volcanic eruptions, natural forest fires and biological mobilization (e.g. pollen, weathered leaf cuticle, leaf hairs). Especially soils on calcareous bedrock may emit large amounts of alkaline particles to the atmosphere. Important factors influencing the suspension of soil dust are wind speed and soil moisture content. As long as soil is wet or snow-covered, suspension will practically not occur (Sehmel, 1980). Saharan dust is an important source of alkaline particles in the atmosphere of southern Europe. Episodes with red- or ochre-stained deposition of Saharan dust have been observed even in northern Europe (Semb *et al.*, 1995). There are also historical reports of dustfall in Scandinavia which appeared to have been caused by dust storms near the Black Sea (Semb *et al.*, 1995). In maritime areas, sea spray is an important source of Na^+ and Mg^{2+} -containing particles. *Anthropogenic* sources of alkaline particles include wind erosion of arable land, agricultural tillage practices (ploughing, liming, planting, harvesting), biomass burning, traffic on unpaved roads, construction and demolition of buildings and roads, and oil/coal burning generating fly ash. Non-fossil fuel combustion (wood and peat) is found an important source for alkaline particles in e.g. Scandinavia (Antilla, 1990). Limestone quarries as well as cement and concrete factories are local sources of Ca^{2+} , whereas road de-icing may be a source of Na^+ and Ca^{2+} containing particles in the atmosphere (Bernard *et al.*, 1987).

In the USA more than 90% of the emissions of alkaline particles were attributed to *open sources*, with the remainder due to industrial and miscellaneous sources (NAPAP, 1987). Of the open sources, traffic on unpaved roads was found the largest (67%), followed by wind erosion (28%), and agricultural tilling (5%). Locally, however, anthropogenic sources were found to dominate. For Europe, no information is available on the contribution of open sources and industrial sources, respectively, to the total emission of alkaline particles.

Emission profiles

In soil-derived dust, base-cations have been found predominantly associated with carbonates (e.g. calcite and dolomite) or aluminum silicates having a hydroxyl group, i.e. clay minerals such as montmorillonite and illite (Bernard *et al.*, 1987; Gomes and Gillette, 1993; Andronova *et al.*, 1993). Potassium feldspars and plagioclase have been found too (e.g. Schütz and Sebert, 1987). Feldspars usually dissolve quickly yielding cations and bicarbonate, thus imparting alkalinity to the solution (Bernard *et al.*, 1987). Base-cations with carbonate as counter-ion or present as clay mineral will fully contribute to neutralization, which can either take place in the atmosphere or after deposition. In depressions near desert or steppe lakes having no discharge, marine lagoons as well as in low-level coastal zones near deserts, soil-derived dust may contain considerable amounts of evaporites. Evaporites consist of

soluble chlorides and sulfates (and to a lesser extent carbonates) of Na^+ , Mg^{2+} , Ca^{2+} and K^+ (Pannekoek, 1976). If associated with Cl^- or SO_4^{2-} , base-cations do not have the ability (anymore) to neutralize acid compounds.

Soil-derived material within the size range of particles with radii smaller than $10\ \mu\text{m}$ are usually found in crustal proportions (Schütz and Rahn, 1982), which means that their composition generally reflects the mineral content of the upper-soil. Schütz and Sebert (1987) showed that the aerosol over the Sahara desert is a rather homogeneous mixture of materials from different sources without showing strong regional characteristics. It is found a product of long-range transport from a number of dust producing regions, rather than from more local sources. Stronger deviations from the average compositional pattern is only observed during sandstorms when relatively large particles containing some local characteristics are injected into the air. In general, however, a thoroughly mixed background mineral aerosol exists.

In sea spray base-cations are mainly associated with Cl^- , and thus do not contribute to neutralization of atmospheric acid. The chemical composition of material derived from forest fires and biological mobilization will show considerable spatial and temporal variation but will always be relatively rich in K^+ (Antilla, 1990). Limestone quarries and cement factories will generate carbonates of calcium and magnesium into the atmosphere. Nilsson and Timm (1983) found base-cations originating from wood (and peat) combustion mainly associated with silicates and oxides. The mineral content of fly-ash from chimneys will be very diverse: industrial processes may generate sulfates, carbonates, silicates, oxides as well as organic material. It is generally assumed, however, that most of the trace elements from combustion sources are present in the form of oxides (Olmez *et al.*, 1988). In the presence of water these oxides will react to form hydroxides (Stelson and Seinfeld, 1981). In waste incinerators trace elements also occur in the form of chlorides (Schroeder *et al.*, 1987) while fly ash from coal combustion mainly consist of silicate particles (Mamane *et al.*, 1986). Fly ash consisting of base-cations associated with sulfate (e.g. gypsum) or chloride does not have the ability (anymore) to neutralize acid compounds.

Emission trends

Hedin *et al.*, (1994) found particulate emissions from urban and industrial point sources in Europe significantly reduced during recent years. Regression fits of emission data of the sum of Na^+ , Mg^{2+} , Ca^{2+} and K^+ with time showed declines of 63% in the Netherlands for the period 1970-1990 (CBS, personal communication), 75% in former West Germany for the period 1966-1990 (UBA, 1992), 24% in former East Germany for the period 1975-1990 (UBA, 1992), 56% in France for the period 1965-1990 (Ulrich and Williot, 1993), 51% in the United Kingdom for the period 1970-1990 (Gilham *et al.*, 1992), and 82% in Sweden for the period 1960-1980 (Lövblad, 1987). Figure 1 presents the temporal variation of alkaline dust emissions from point sources in Sweden for the period 1900-1990. Especially emissions associated with energy production and cement and limestone industry were found reduced. Although this is poorly known, Hedin *et al.* (1994) assume emissions of base-cations from non-point sources to have declined too due to e.g. the pavement of dust roads.

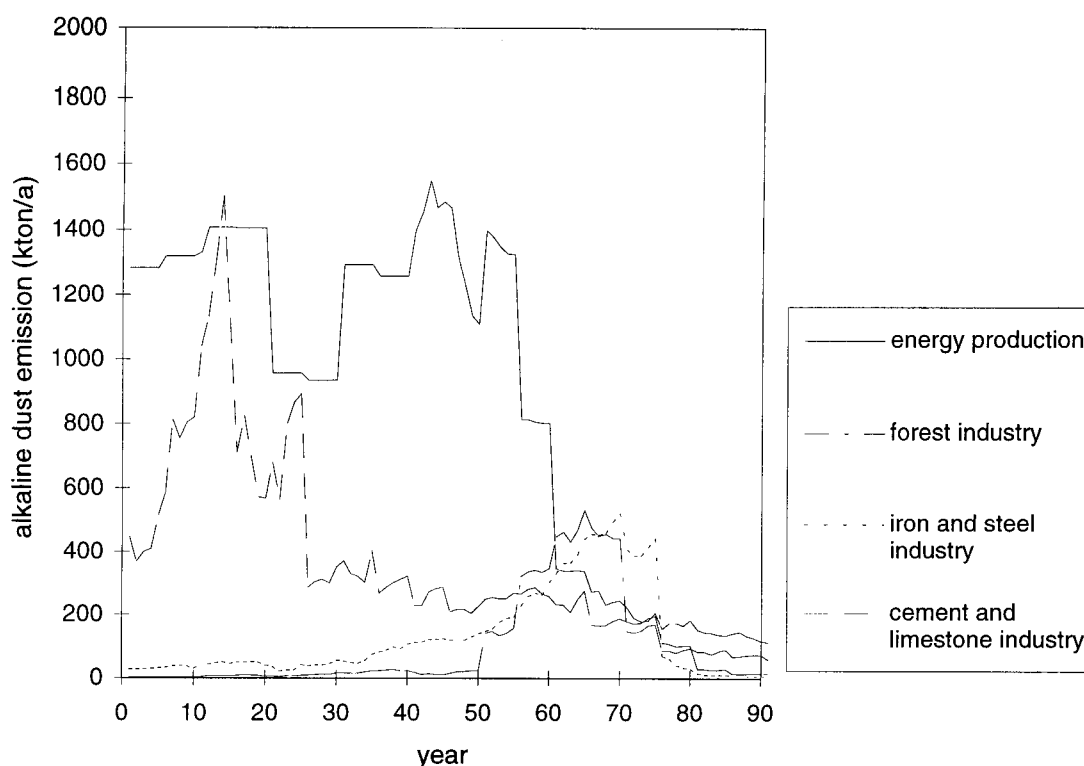


Figure 1 Alkaline dust emissions in Sweden associated with energy production, forest industry, iron and steel industry and cement and limestone industry for the period 1900-1990 (after Kindbom *et al.*, 1993).

Hedin *et al.* (1994) reported a significant decline in total base-cation (i.e. sum of non-sea salt Na^+ , Mg^{2+} , Ca^{2+} and K^+) wet deposition during the last 10 to 20 years in several parts of Europe and North America. The decline was dominated by Ca^{2+} which contributed, on the basis of charge equivalents, about 48-81% to the total base-cation wet deposition decline (Hedin *et al.*, 1994; Buishand and Montfort, 1989). For a site in Sweden a 74% reduction in total base-cation wet deposition was reported for the time period 1971-1989. For several sites in the Netherlands a 32-47% decline was found between 1978 and 1989. Erisman and Draaijers (1995) analyzed long-term measurements of precipitation at Leiduin near the Dutch coast and found the concentrations of Ca^{2+} and Mg^{2+} reduced by 70% since 1932 (Figure 2). Reported declines in wet deposition are similar to reported urban and industrial emission reductions, suggesting urban and industrial point sources in these countries are (or have been) at least as important as semi-natural sources in emitting alkaline particles to the atmosphere. Declines in the deposition of base-cations will have lessened the efficiency of sulfur-dioxide emission control in mitigating acid deposition (Gorham, 1994). So, the expected improvements in nutrient balances in forests due to reduced SO_2 emissions may not be fully realized. In some areas (e.g. directly around smelters on the Kola peninsula), the deposition of alkaline fly ash have been found to neutralize acid deposition completely (Rodhe *et al.*, 1995).

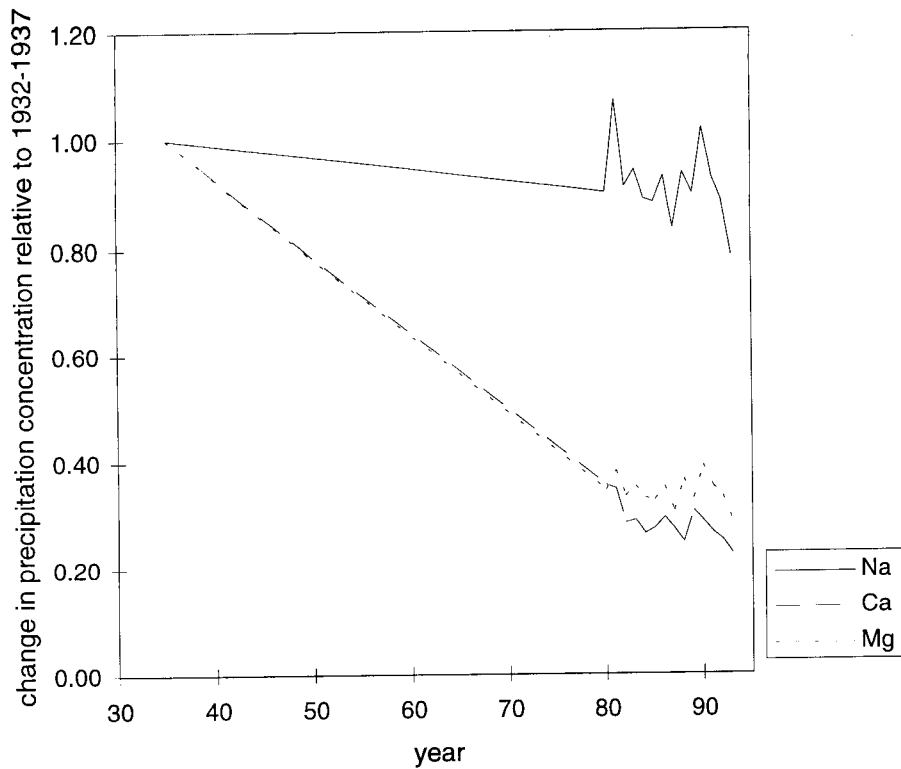


Figure 2 Temporal variation of Na⁺, Mg²⁺ and Ca²⁺ concentrations in precipitation at Leiduin near the Dutch coast. Annual average concentrations for the period 1980-1993 are obtained from the National Precipitation Monitoring Network (RIVM, 1994). They are presented relative to the average concentrations for the period 1932-1937, obtained from Leeftang (1938).

3 MODELING AND MAPPING DEPOSITION

3.1 Wet deposition

The wet deposition flux of base-cations is calculated as the product of precipitation concentration and precipitation amount.

Precipitation concentrations

Precipitation concentration data for base-cations were obtained from national organizations responsible for wet deposition monitoring in their countries and from the EMEP database (Van Leeuwen *et al.*, 1995; 1996). In total, results from around 600 monitoring locations scattered over Europe were obtained. Annual mean concentrations were corrected for the contribution of dry deposition onto funnels of bulk samplers. For this, correction factors were derived from parallel measurements with bulk and wet-only samplers made in the Netherlands, the United Kingdom, Germany, Sweden, Italy and the Czech Republic. Spatial analysis based on the 'regionalized variable theory' revealed autocorrelation for all ion concentrations and reasonable bounded models could be fitted to the experimental variograms. Effective ranges of the variogram models varied between 500 km for K^+ to 750 km for Mg^{2+} . Concentration maps were compiled using the block-kriging interpolation technique with blocks of 50x50 km.

In these maps (Figure 3) the different sources of base-cations can easily be recognized. For Na^+ and Mg^{2+} , a clear pattern of increasing precipitation concentrations with decreasing distance to seas, in particular the Atlantic Ocean, can be observed, reflecting their sea-salt origin. Large Na^+ concentrations are also found e.g. northwest of the Black Sea, where they probably originate from wind erosion of salt containing soils. Large Mg^{2+} , Ca^{2+} and K^+ concentrations in southern and south-eastern Europe result from a combination of wind erosion of calcareous and salt-containing soils, agricultural tillage practices, traffic on unpaved roads, and supply of Saharan dust. In this part of Europe, the prevalence of warm and dry conditions in the summer period enhances the suspension of alkaline particles in the atmosphere. In some areas, Saharan 'red dust' will be the dominating source of alkaline particles in the atmosphere. For example, Loye-Pilot *et al.* (1986) found more than 80% of the wet deposition of particulate matter in Corsica caused by Saharan dust. The relatively large Ca^{2+} concentrations in the border area between Germany, Poland and the Czech Republic (the so-called Black Triangle), as well as in e.g. Latvia and Lithuania, can be attributed to intensive industrial activity. In the Black Triangle, considerable Ca^{2+} emissions occur from the use of brown coal for energy production (Marquadt and Ihle, 1988), and in Latvia and Lithuania Ca-rich oil-shale is used for energy production (Antilla, 1990).

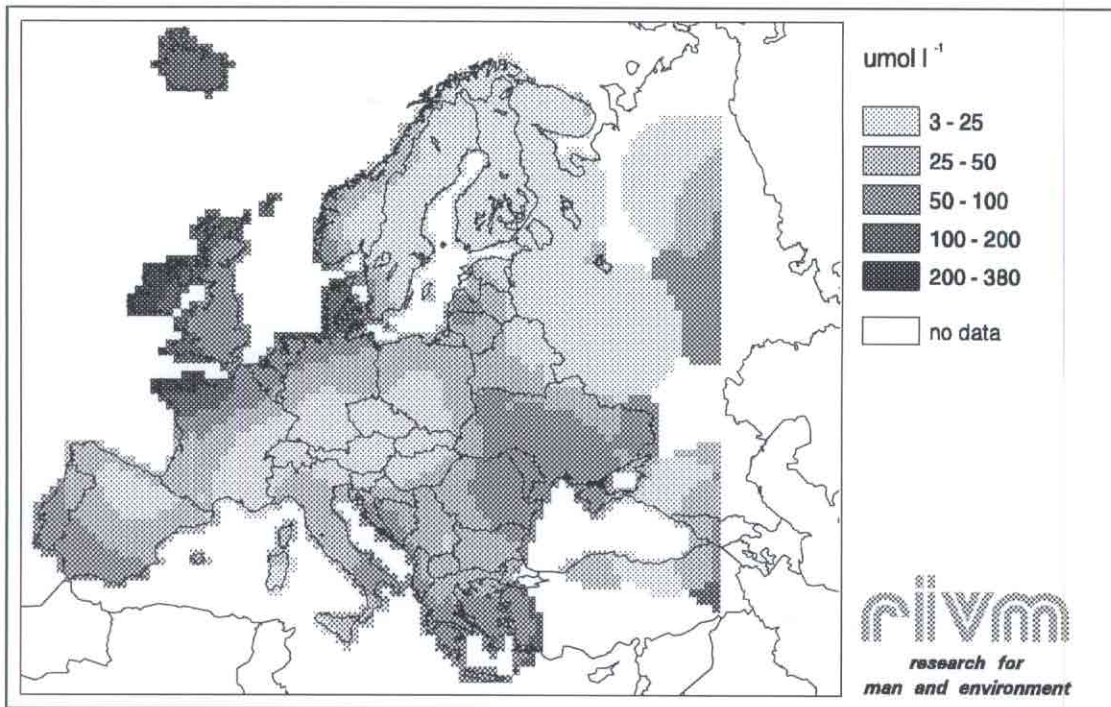


Figure 3a Annual mean concentrations of Na^+ in precipitation in Europe ($\mu\text{mol l}^{-1}$) (after Van Leeuwen *et al.*, 1995; 1996).

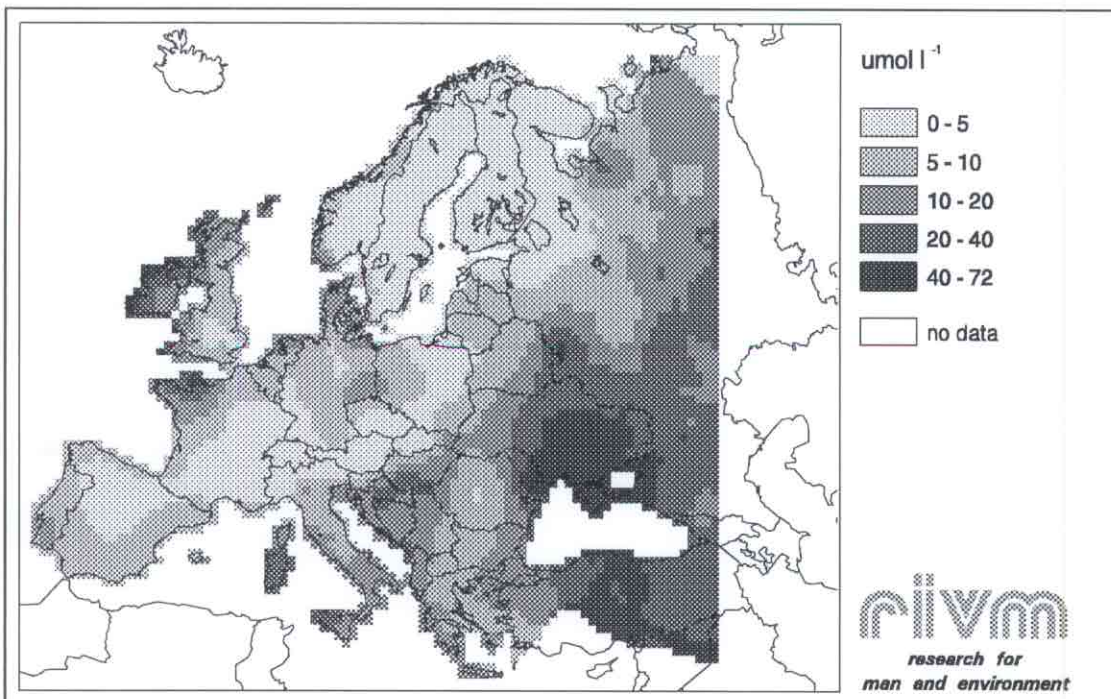


Figure 3b Annual mean concentrations of Mg^{2+} in precipitation in Europe ($\mu\text{mol l}^{-1}$) (after Van Leeuwen *et al.*, 1995; 1996).

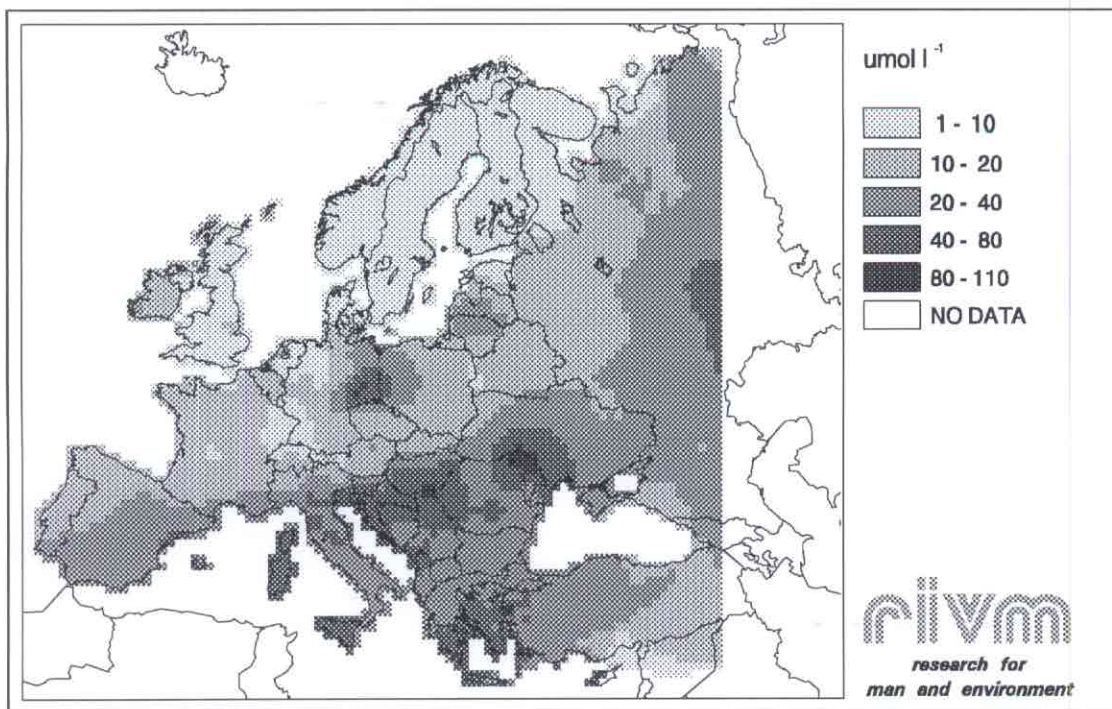


Figure 3c Annual mean concentrations of Ca^{2+} in precipitation in Europe ($\mu\text{mol l}^{-1}$) (after Van Leeuwen *et al.*, 1995; 1996).

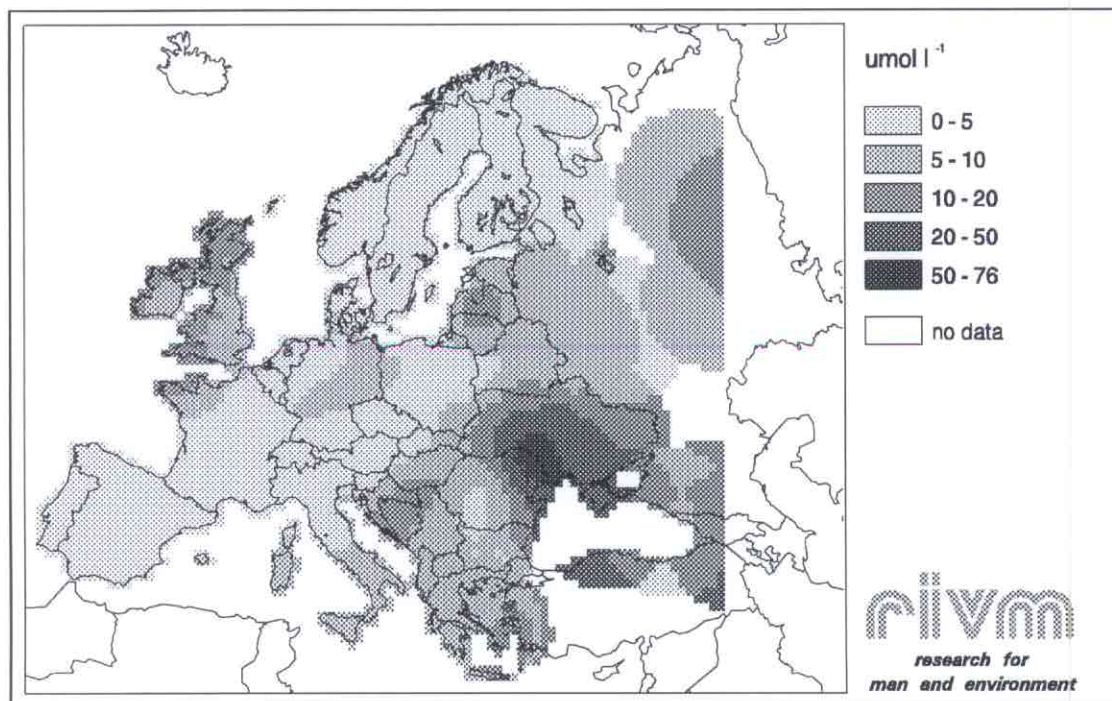


Figure 3d Annual mean concentrations of K^{+} in precipitation in Europe ($\mu\text{mol l}^{-1}$) (after Van Leeuwen *et al.*, 1995; 1996).

Precipitation amounts

Long-term mean precipitation amounts were obtained from a database of the USA Environmental Protection Agency (EPA). This EPA database contains validated monthly mean precipitation amounts measured from 1920 to 1980 at a several thousands of measurement sites scattered over Europe which were interpolated to a $0.5^\circ \times 0.5^\circ$ lat./long. (approx. 30×60 km) grid (Legates and Willmott, 1990). EPA used a procedure for correcting gauge-induced biases to remove systematic errors caused by wind, wetting on the internal walls of the gauge, and evaporation from the gauge.

Precipitation amounts in Europe as obtained from the EPA database are presented in Figure 4. Relatively large precipitation amounts are found in *i*) mountainous areas due to orographic effects, *ii*) an area situated between 40° and 65° latitude due to the frequent passage of low-pressure systems, and *iii*) some continental areas as a result of convection processes.

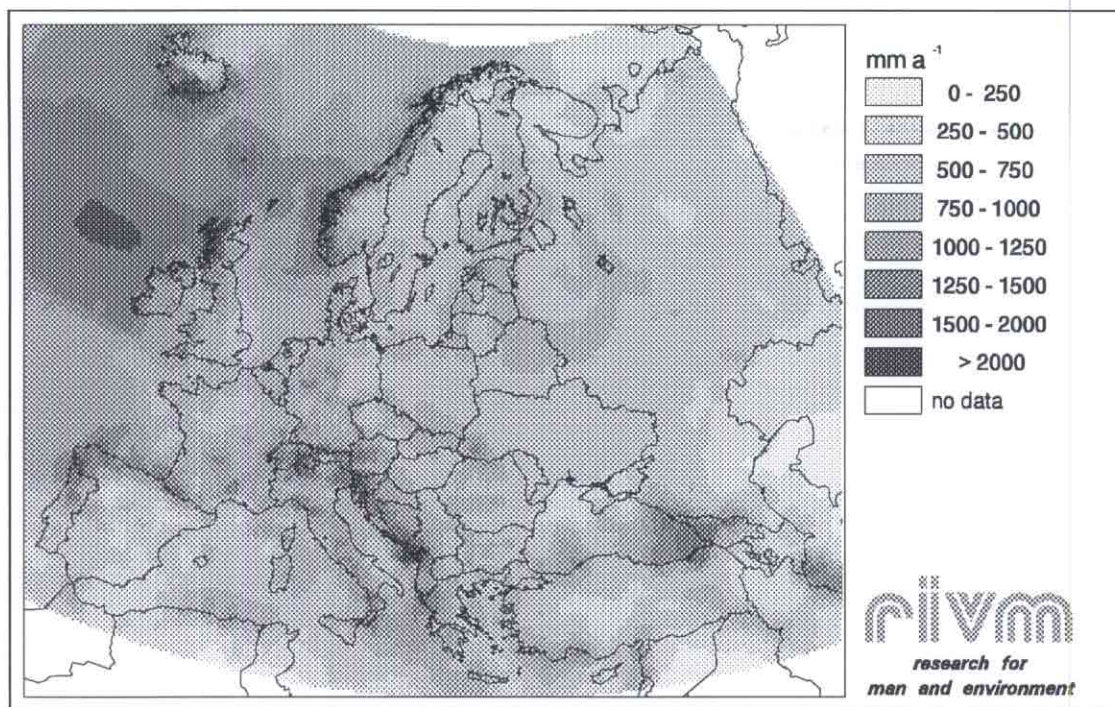


Figure 4 Precipitation amounts in Europe averaged for the period 1920-1980 (mm a^{-1}) (after Legates and Willmott, 1990).

Wet deposition fluxes

In Figure 5 wet deposition fluxes of base-cations are presented. Fluxes clearly resemble the European climate (i.e. precipitation amount) and emission (reflected by precipitation concentration) pattern. Largest Na^+ wet deposition fluxes are found along the Irish and the British west coast and in Iceland, whereas lowest Na^+ fluxes appear in central Europe, central Spain, Sweden, Finland and the Russian Federation. Besides areas bordering sea, Ukraine and Turkey experience relatively large Mg^{2+} wet deposition fluxes. Largest Ca^{2+} wet deposition fluxes are found in Italy, the Baltic States, Moldavia and the Black Triangle. Very low Ca^{2+} fluxes appear in Scandinavia. Largest K^+ fluxes are found along the Irish and British west coast and in Croatia, Bosnia-Herzegovina, Moldavia and Ukraine.

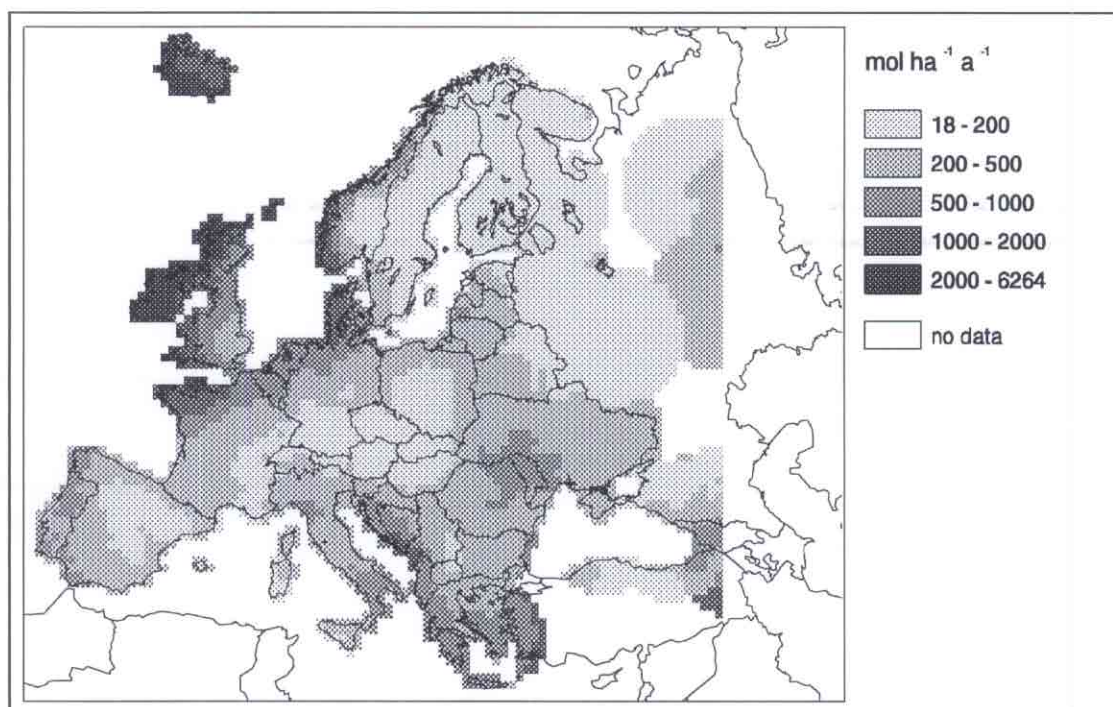


Figure 5a Wet deposition of Na^+ over Europe (in $\text{mol ha}^{-1} \text{a}^{-1}$) (after Van Leeuwen *et al.*, 1995; 1996).

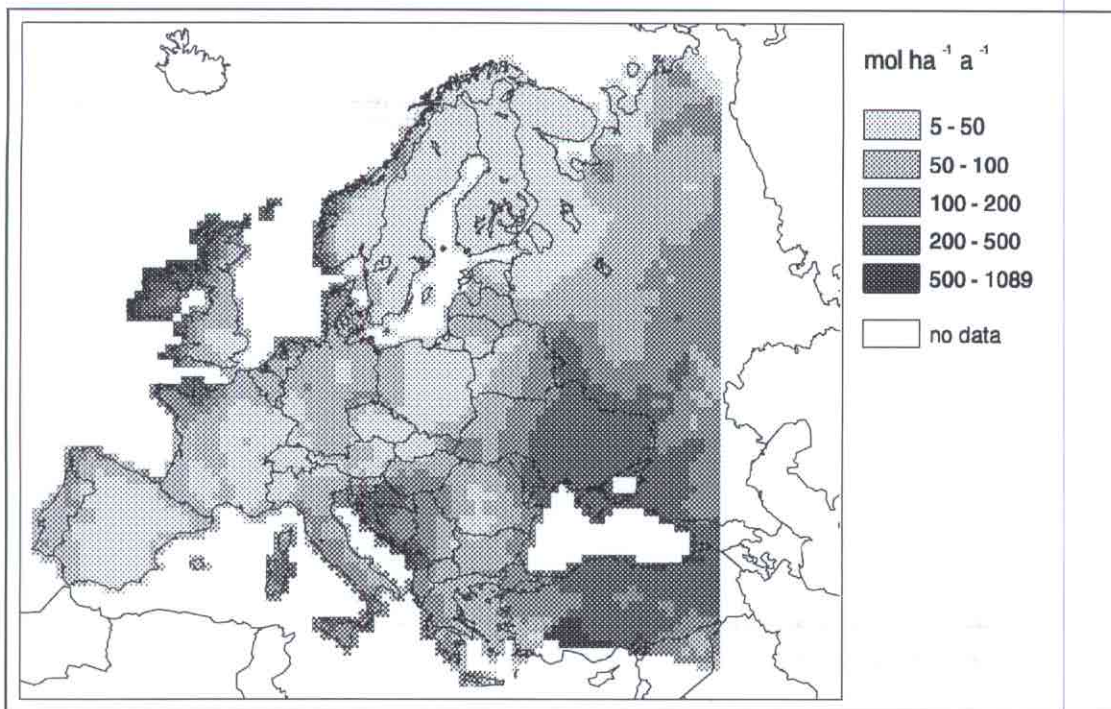


Figure 5b Wet deposition of Mg²⁺ over Europe (in mol ha⁻¹ a⁻¹) (after Van Leeuwen *et al.*, 1995; 1996).

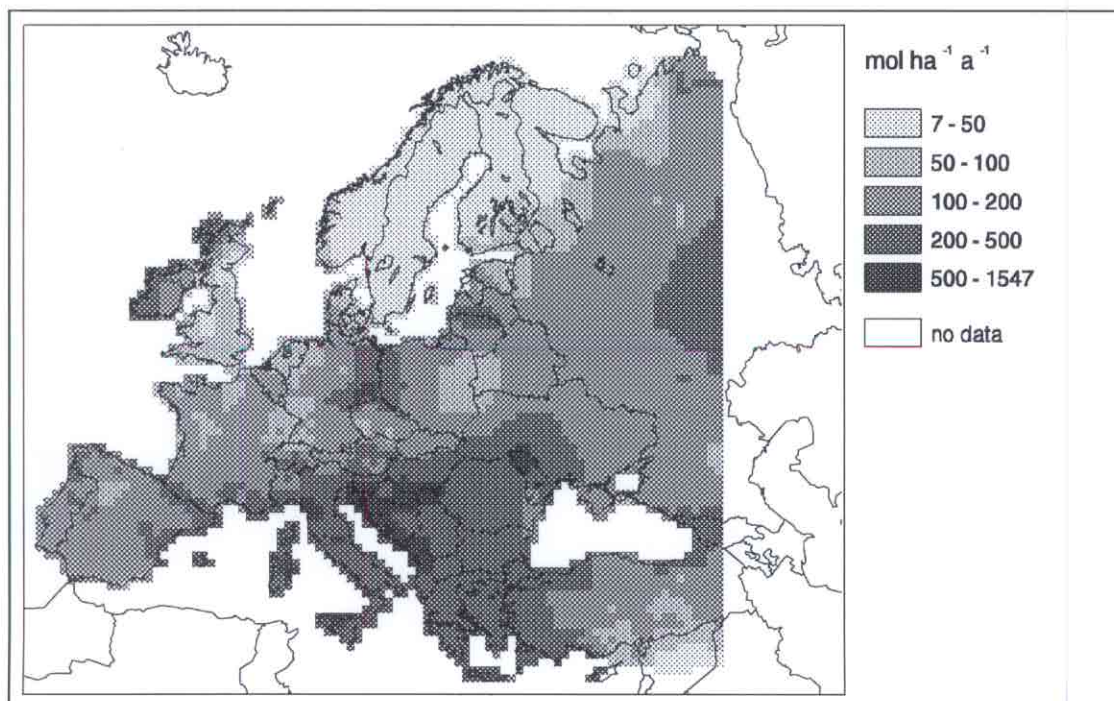


Figure 5c Wet deposition of Ca²⁺ over Europe (in mol ha⁻¹ a⁻¹) (after Van Leeuwen *et al.*, 1995; 1996).

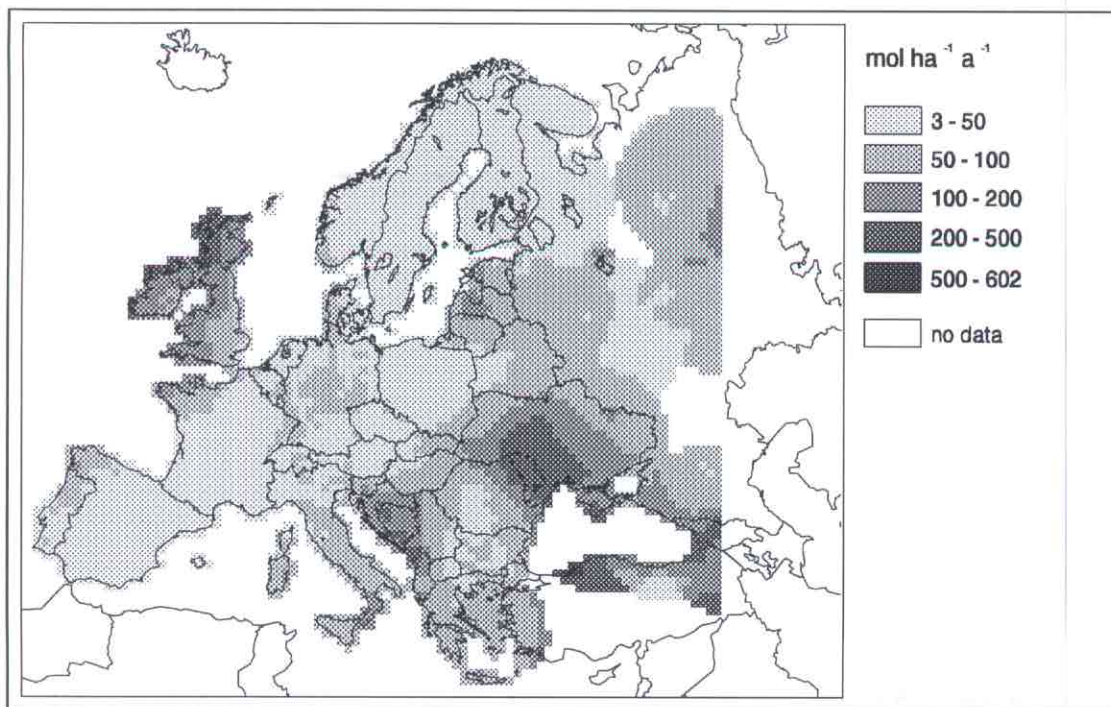


Figure 5d Wet deposition of K⁺ over Europe (in mol ha⁻¹ a⁻¹) (after Van Leeuwen *et al.*, 1995; 1996).

3.2 Dry deposition

The dry deposition flux of base-cations is calculated as the product of dry deposition velocity and ambient concentration at a reference height above the surface. In the inferential technique, the choice for a reference height (50 m) is a compromise between the height where the concentration is not severely affected by local deposition or emission and is still within the constant flux layer (Erisman, 1992). For this height, dry deposition velocity fields over Europe are constructed for every six hours from land use and meteorological information, using a detailed parametrisation of the dry deposition process. Dry deposition velocity fields are aggregated to annual means before they are combined with annual mean air concentration fields, yielding dry deposition estimates on a small scale over Europe.

Land use information, based on topographical maps and satellite observations, was available on a 1/6°x1/6° lat./long. (approx. 10x20 km) grid (Van de Velde *et al.*, 1994; Veldkamp *et al.*, 1996). Land use categories distinguished include: *i*) temporary crops (arable land), *ii*) permanent crops (e.g. vineyards, olives, fruits), *iii*) grassland for agricultural use, *iv*) natural areas and extensive agricultural areas, *v*) coniferous and mixed forest, *vi*) deciduous forest, *vii*) inland water and *viii*) urban areas. The area of each land use category is stored per unit grid cell. From the land use map, roughness lengths for the summer and winter season were derived using the classification presented by Wieringa (1992). In turn, roughness lengths were used for the estimation of aerodynamic transport to the receptor surface.

Meteorological information was obtained from the Observational Data Set (ODS) which is a product of the European Center for Medium-range Weather Forecasts (ECMWF). The ODS dataset contains observational meteorological data

averaged over six hours at 00, 06, 12 and 18 hours UT for 1297 measurement sites spread over Europe (Potma, 1993). Meteorological parameters include among others, surface pressure, temperature, wind speed, wind direction, cloud cover, precipitation amount and relative humidity. Meteorological data were interpolated over Europe on a 1.0°x0.5° lat./long. (approx. 60x60 km) grid.

Dry deposition velocities

The parametrisation of the dry deposition velocity was based on the model of Slinn (1982) which was tested with micrometeorological measurements performed at the Speulder forest in the Netherlands (Ruijgrok *et al.*, 1994; Erisman *et al.*, 1994). It includes both turbulent exchange and sedimentation of coarse particles. The general form for V_d at a height of 50 m equals:

$$V_d = 1/[1/V_{da} + 1/V_{ds}] + V_s \quad [1]$$

where following Slinn's (1982) approach, turbulent exchange is split in an aerodynamic and a surface deposition velocity (V_{da} and V_{ds} , respectively). Deposition as a result of sedimentation due to the earth's gravitational force is represented by V_s . The aerodynamic deposition velocity equals the inverse of the aerodynamic resistance (R_a):

$$V_{da} = 1/R_a(z=50) \quad [2]$$

R_a is approximated following procedures presented by Garland (1978) and Beljaars and Holtslag (1990). The surface deposition velocity depends on the collection efficiency of the surface which, in turn, is determined by the various deposition processes, the size of the depositing aerosol, atmospheric conditions and surface properties. Ruijgrok *et al.* (1994) showed from theoretical considerations that V_{ds} has the following limiting form:

$$V_{ds} = E * (u_*^2/u_h) \quad [3]$$

in which E represents an overall collection efficiency, u_* the friction velocity and u_h the wind speed at canopy height. The collection efficiency will depend on atmospheric and surface conditions. Ruijgrok *et al.* (1994) showed that values of V_{ds} show a different response to the driving force u_*^2/u_h for different wetness conditions of the surface and ambient relative humidity (rh). Their parametrisations of the collection efficiency under different conditions are presented in Table I.

The sedimentation velocity of particles can be computed using Stoke's Law and equals 0.0067 m.s⁻¹ when assuming a mean particle density of 1700 kg.m⁻³. At relative humidities larger than 80%, the effect of hygroscopic particle growth has to be taken into account. Ruijgrok *et al.* (1994) parametrised this effects based on work of Fitzgerald (1975):

$$V_s = 0.0067 * 1.89 * \exp[(0.00066*rh)/(1.058-rh*0.01)] \quad [4]$$

Table I Parametrisations of the collection efficiency under different conditions (after Ruijgrok *et al.*, 1994). The surface is considered wet during and a few hours after precipitation.

E	Condition
$0.679 * u_*^{0.56}$	wet surface, $rh \leq 80$
$0.679 * u_*^{0.56} * [1 + 0.37 * e^{(rh-80)/20}]$	wet surface, $rh > 80$
$0.140 * u_*^{0.12}$	dry surface, $rh \leq 80$
$0.140 * u_*^{0.12} * [1 + 0.09 * e^{(rh-80)/20}]$	dry surface, $rh > 80$

The V_d calculated with the parametrisation described above (equation 4) hold for Na^+ , Mg^{2+} and Ca^{2+} containing particles with MMDs representative for the Speulder forest. For K^+ containing particles the outcome should be halved, because of the smaller MMD of such particles (Ruijgrok *et al.*, 1994). The parametrisation does not account for variation of MMD over Europe.

The annual mean dry deposition velocity of Na^+ , Mg^{2+} and Ca^{2+} containing particles over Europe is presented in Figure 6. Relatively large dry deposition velocities are found in forested areas generating high turbulence. Largest dry deposition velocities are found in the coastal areas of Scotland and Scandinavia as a result of the co-occurrence of high wind velocities, high relative humidities and prolonged periods with surface wetness.

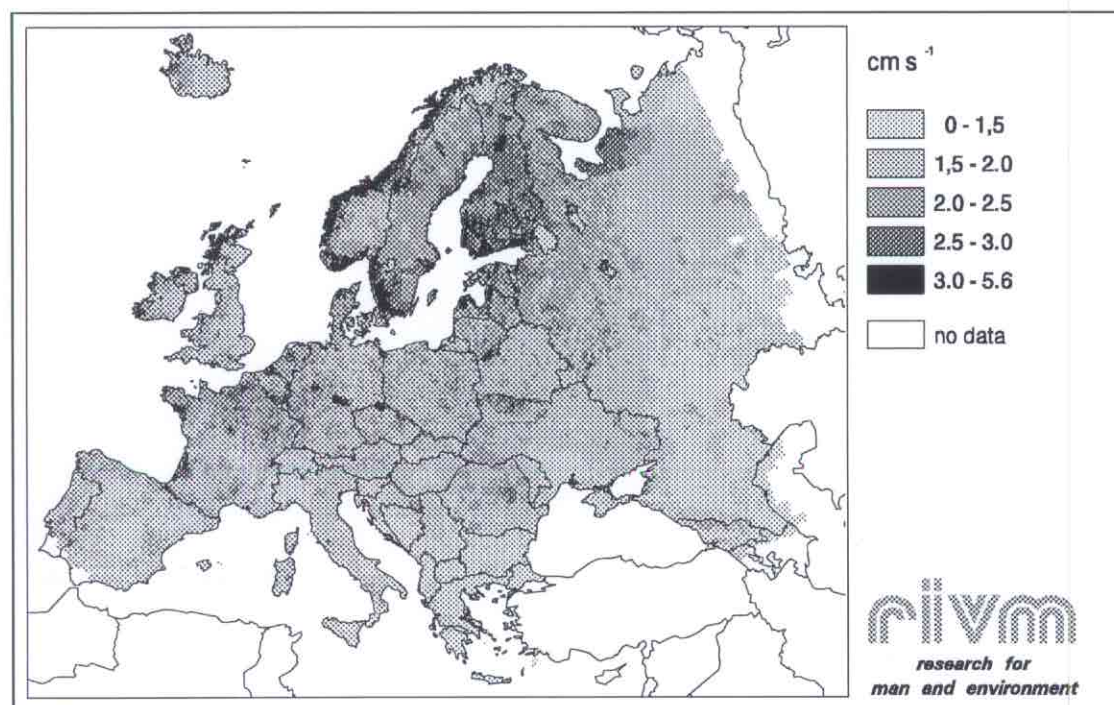


Figure 6 Annual mean dry deposition velocity of Na^+ , Mg^{2+} and Ca^{2+} containing particles over Europe (in $m s^{-1}$). For K^+ containing particles the value needs to be halved.

Ambient air concentrations

Air concentrations of alkaline particles were estimated from precipitation concentrations using scavenging ratios. The latter were derived from simultaneous measurements of base-cation concentrations in precipitation and surface-level air, using a relatively simple scavenging process model (see below). This approach to estimate air concentrations is based on the premise that cloud droplets and precipitation efficiently scavenge particles resulting in a strong correlation between concentrations in precipitation and the surface-level air (Eder and Dennis, 1990). This assumption will only be valid for well-mixed conditions at sufficient distance from sources. Particles will be scavenged when they serve as cloud condensation nuclei (in-cloud scavenging) or when they are intercepted by falling hydrometeors (below-cloud scavenging). Experiments of Jaffrezo and Colin (1988) indicate in-cloud processes to be the dominant scavenging pathway for Na^+ , whereas for Mg^{2+} , Ca^{2+} and K^+ both in-cloud and below-cloud scavenging is important.

Factors that will influence the magnitude and variability of scavenging ratios include particle size distribution (Kane *et al.*, 1994; Jaffrezo and Colin, 1988; Buat-Menard and Duce, 1986) and to a lesser extent particle solubility (e.g. Slinn *et al.*, 1978; Jaffrezo and Colin, 1988), precipitation amount (Barrie, 1985; Savoie *et al.*, 1987), precipitation rate (Slinn, 1977; Scott, 1981), droplet accretion process (Scott, 1981) and storm type (Barrie, 1992). Event scavenging ratios can range several orders of magnitude even for single species at a single location. However, scavenging ratios have been found reasonably consistent when averaged over one year or longer (Galloway *et al.*, 1993). For this reason, annual mean precipitation concentrations were used to infer annual mean air concentrations of Na^+ , Mg^{2+} , Ca^{2+} and K^+ . Precipitation concentration data were taken from Van Leeuwen *et al.* (1995). They compiled measurement results from about 600 sites scattered over Europe (see also section 2.1). Ambient air concentrations derived this way will reflect the large scale background situation. Large sub-grid concentration gradients are likely to exist, especially when point sources and/or many scattered sources such as agricultural fields and unpaved roads are present. In emission areas, surface-level air concentrations will be larger than concentrations at 50m height, whereas in (more) background situations surface-level concentrations will be lower as a result of dry deposition.

Simultaneous measurements of base-cation concentrations in precipitation and surface-level air were performed by Stevenson (1967), Harrison and Pio (1983), Derrick *et al.* (1984), Pratt and Krupa (1985), Savoie *et al.* (1987), Jaffrezo and Colin (1988), Eder and Dennis (1990), RIVM (1993), Galloway *et al.* (1993), Kane *et al.* (1994), Römer and Te Winkel (1994) and Guerzoni *et al.* (1995). Results are presented in Figure 7.

The scavenging ratio (SR) is defined as:

$$\text{SR} = [\text{C}]_{\text{rain}} * \rho / [\text{C}]_{\text{air}} \quad [5]$$

where $[\text{C}]_{\text{rain}}$ denotes the concentration in precipitation (mg/l), $[\text{C}]_{\text{air}}$ the concentration in ambient air (in $\mu\text{g}/\text{m}^3$) and ρ the density of air, taken as 1200 g m^{-3} . For the size range alkaline particles usually occur in, the following relationship between the scavenging ratio and the mass median diameter (MMD, in μm) can be derived from data of Kane *et al.* (1994):

$$SR = 188 * e^{(0.227 * MMD)} \quad [6]$$

Rearranging equation [5] and [6] gives a simple empirical model describing the relationship between air concentration on the one hand and precipitation concentration and mass median diameter on the other hand:

$$[C]_{air} = ([C]_{rain} * 1200) / (188 * e^{0.227 * MMD}) \quad [7]$$

The MMD of aerosols will depend, among others, on the distance to sources. More efficient removal by dry and wet deposition of the larger particles results in decreasing MMD's with source distance. As no information was available on the distribution of MMD of alkaline particles over Europe, it was assumed to cover the variation in precipitation concentration. Both MMD and $[C]_{rain}$ will increase with decreasing distance to source areas. Linear relationships between MMD and $[C]_{rain}$ were derived assuming coinciding 'means', 'means $\pm \sigma_g$ ' and 'means $\pm 2\sigma_g$ ' in which σ_g represents the geometric standard deviation (Table II). Mean and σ_g of MMD were assumed equal to the ones reported by Milford and Davidson (1985), and mean and σ_g of $[C]_{rain}$ in Europe were taken from Van Leeuwen *et al.* (1995). Model predictions fitted results of simultaneous measurements of $[C]_{air}$ and $[C]_{rain}$ very well (Figure 7). The impact of relative humidity on the MMD of aerosols is not taken into account. This will result in a slight overestimation of air concentrations in areas with above-average relative humidities and vice versa.

Table II Relationships between mass median diameters of alkaline aerosols (MMD, in μm) and precipitation concentrations ($[C]_{rain}$, in mg l^{-1}) in Europe.

Component	Relationship between MMD and $[C]_{rain}$
Na^+	$\text{MMD} = 0.574 * [C]_{rain} + 6.082$
Mg^{2+}	$\text{MMD} = 2.778 * [C]_{rain} + 5.694$
Ca^{2+}	$\text{MMD} = 1.520 * [C]_{rain} + 6.316$
K^+	$\text{MMD} = 2.740 * [C]_{rain} + 4.096$

Annual mean ambient air concentrations of Na^+ , Mg^{2+} , Ca^{2+} and K^+ derived from precipitation concentrations using equation [7] in combination with the equations presented in Table II, are displayed in Figure 8. A similar pattern as for precipitation concentrations (Figure 3) can be seen, with the exception that peak values are to some extent leveled-off. However, in the maps the sources of base-cations can still be recognized. A detailed description of the spatial distribution of the different sources of base-cations is presented in section 2.1.

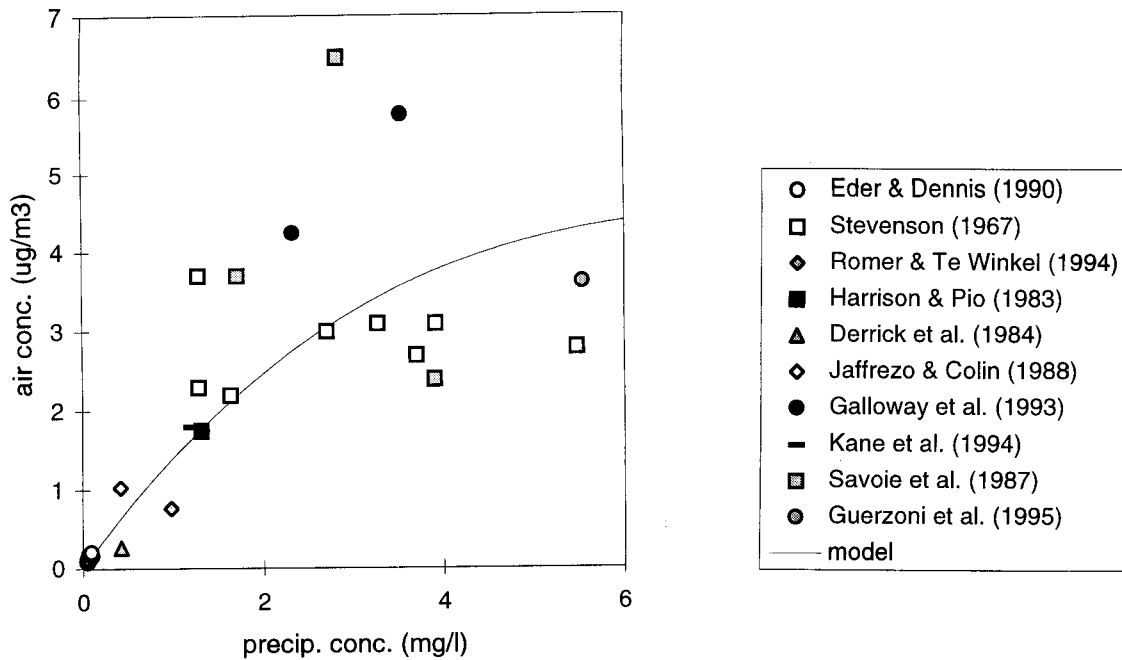


Figure 7a Results of simultaneous measurements of concentrations in precipitation and surface-level air for Na⁺. In Appendix 2 an overview is presented of site characteristics and measurement methods used by mentioned authors. Modeled relationships between [C]_{air} and [C]_{rain} (see text for more details) are also presented.

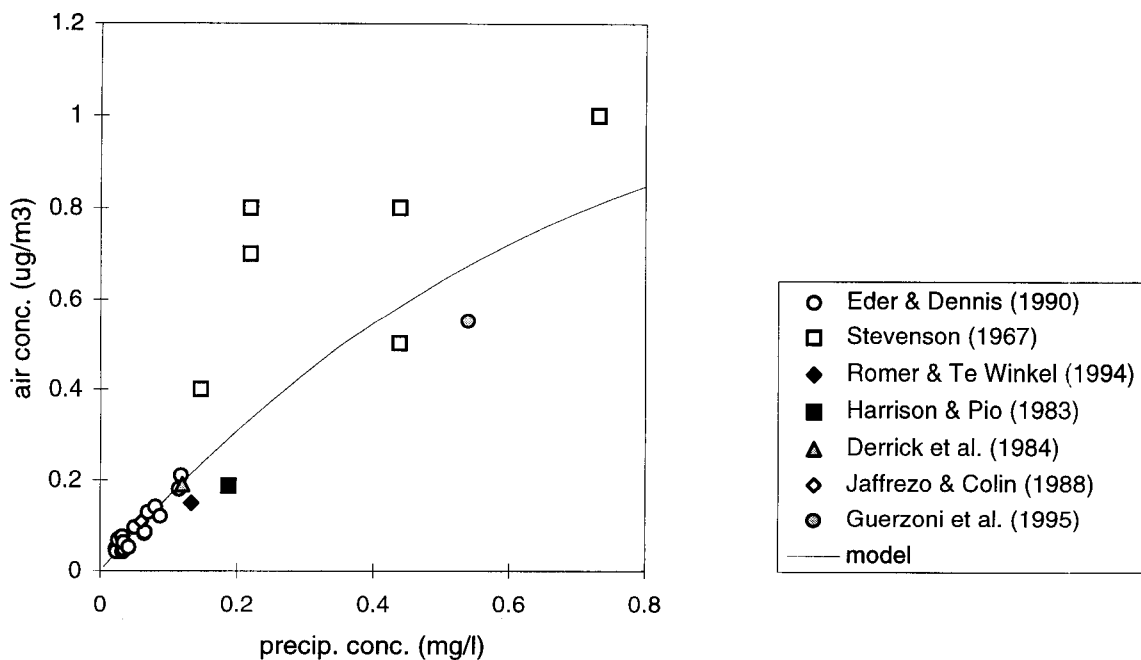


Figure 7b Results of simultaneous measurements of concentrations in precipitation and surface-level air for Mg²⁺. In Appendix 2 an overview is presented of site characteristics and measurement methods used by mentioned authors. Modeled relationships between [C]_{air} and [C]_{rain} (see text for more details) are also presented.

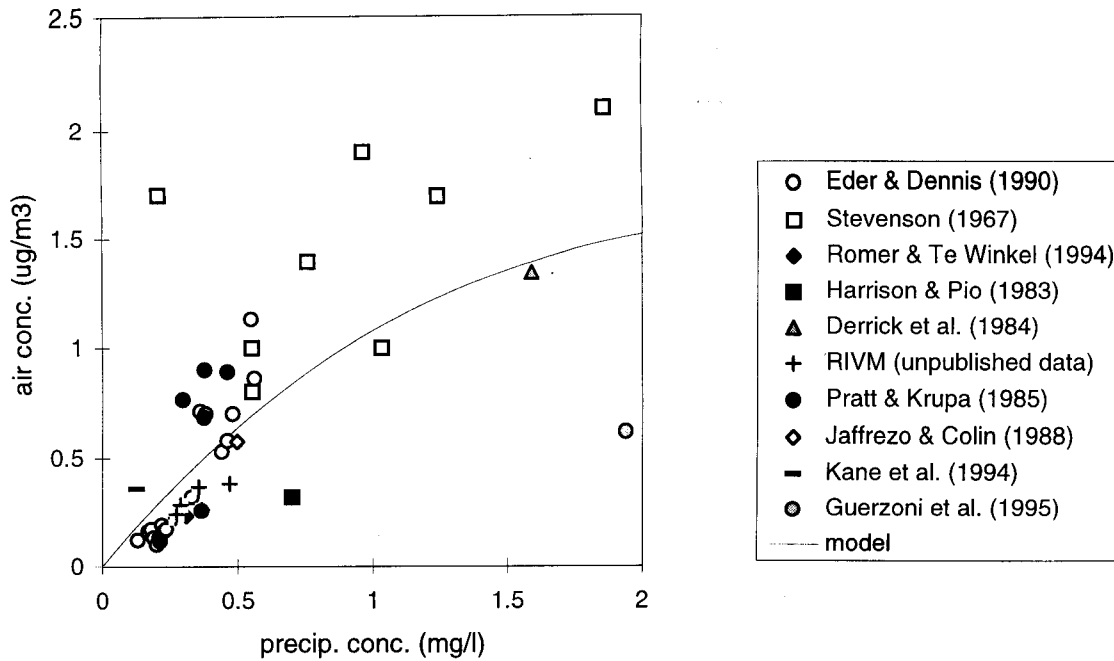


Figure 7c Results of simultaneous measurements of concentrations in precipitation and surface-level air for Ca²⁺. In Appendix 2 an overview is presented of site characteristics and measurement methods used by mentioned authors. Modeled relationships between [C]_{air} and [C]_{rain} (see text for more details) are also presented.

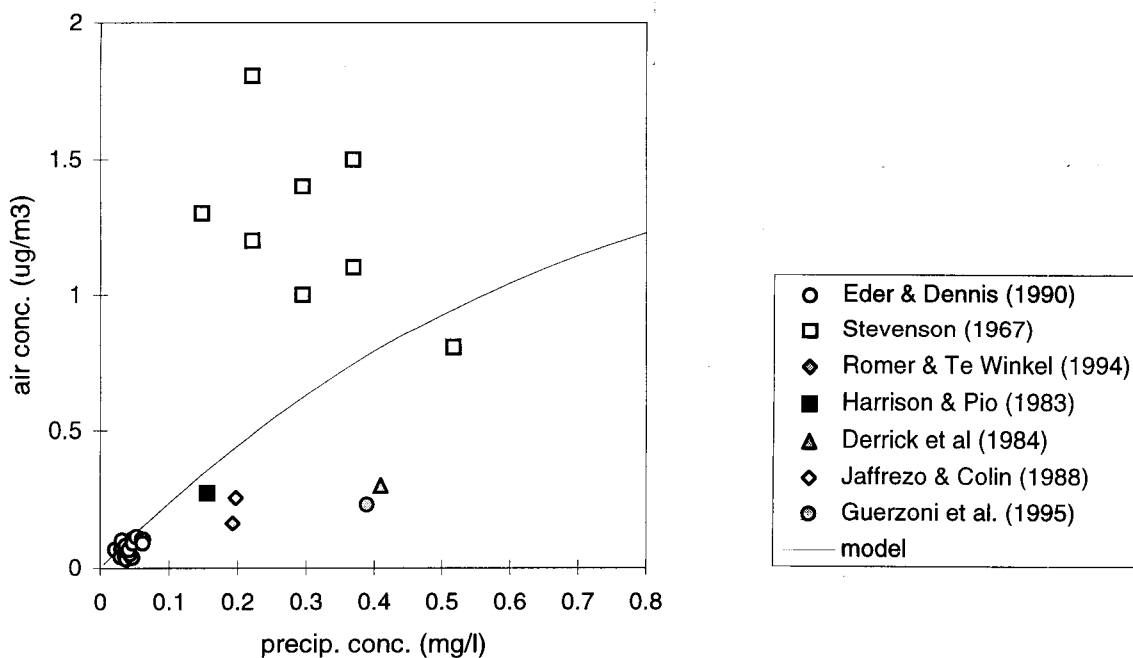


Figure 7d Results of simultaneous measurements of concentrations in precipitation and surface-level air for K⁺. In Appendix 2 an overview is presented of site characteristics and measurement methods used by mentioned authors. Modeled relationships between [C]_{air} and [C]_{rain} (see text for more details) are also presented.

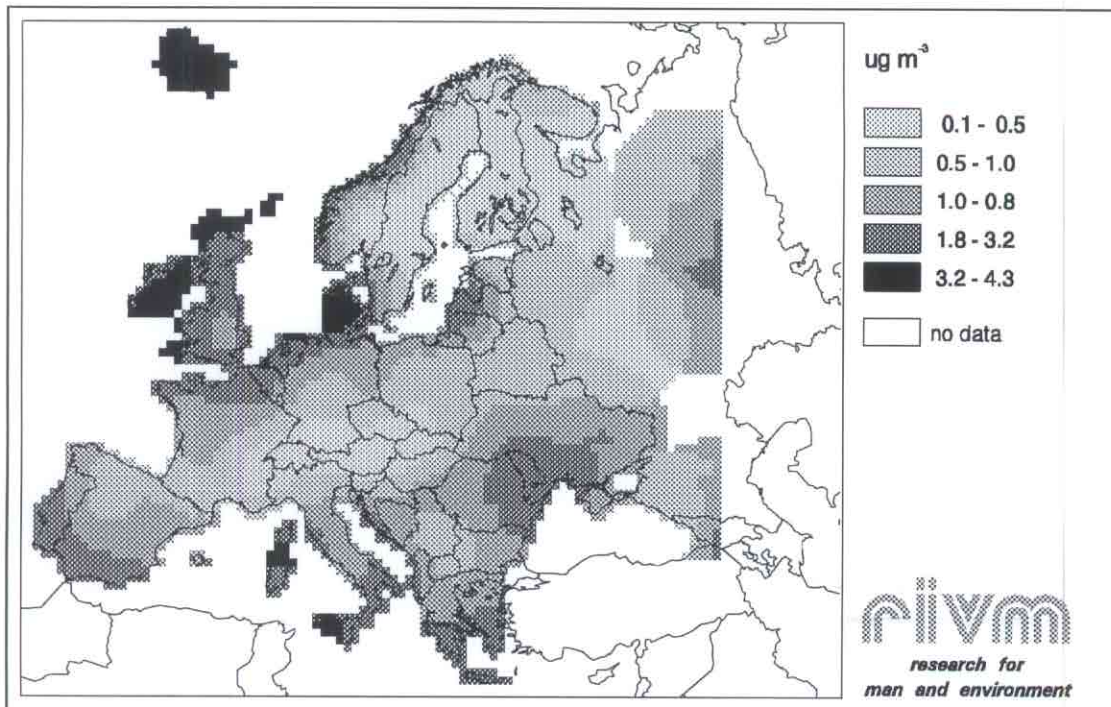


Figure 8a Annual mean concentrations of Na^+ in ambient air over Europe (in $\mu\text{g m}^{-3}$).

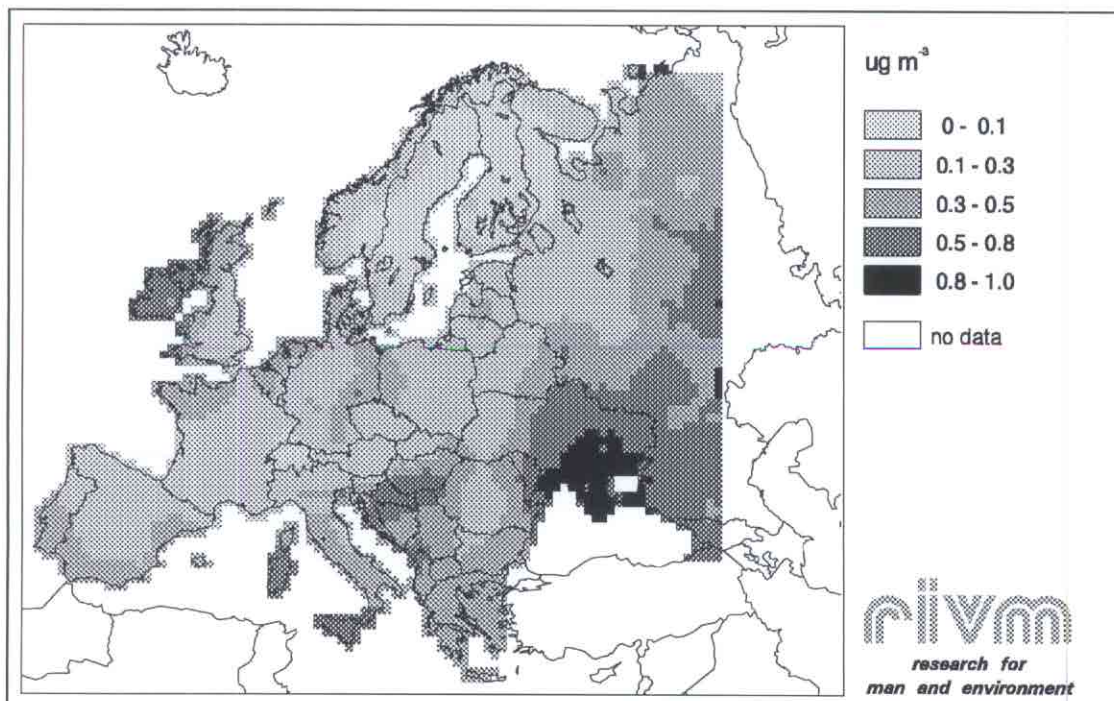


Figure 8b Annual mean concentrations of Mg^{2+} in ambient air in Europe (in $\mu\text{g m}^{-3}$).

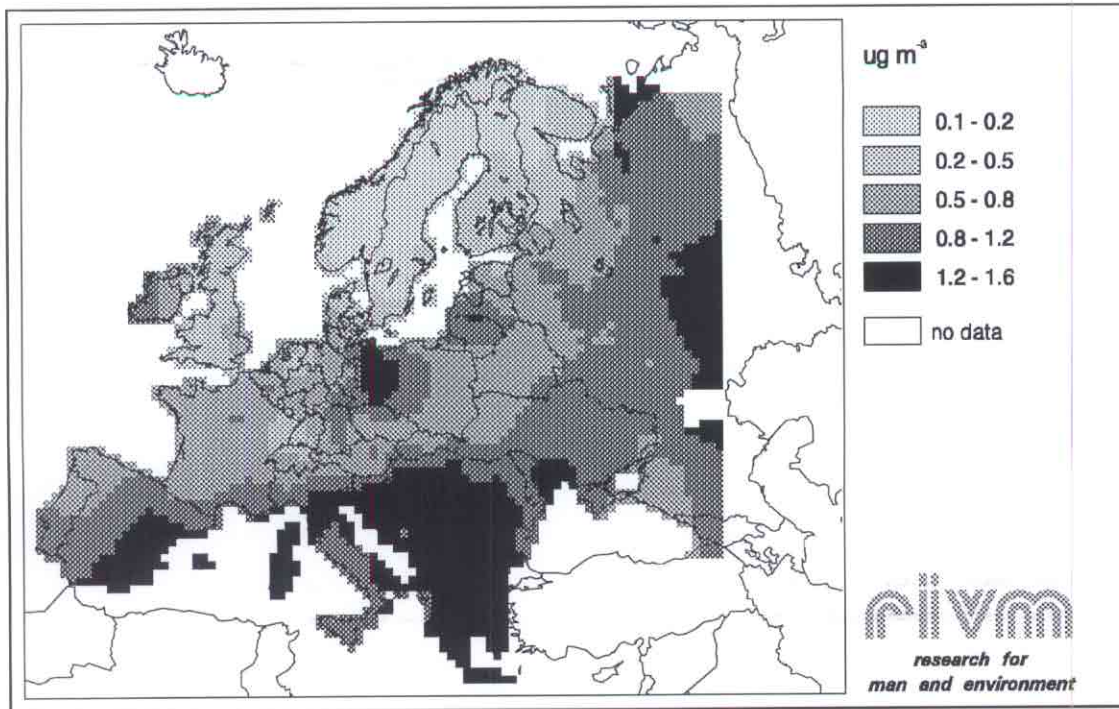


Figure 8c Annual mean concentrations of Ca^{2+} in ambient air over Europe (in $\mu\text{g m}^{-3}$).

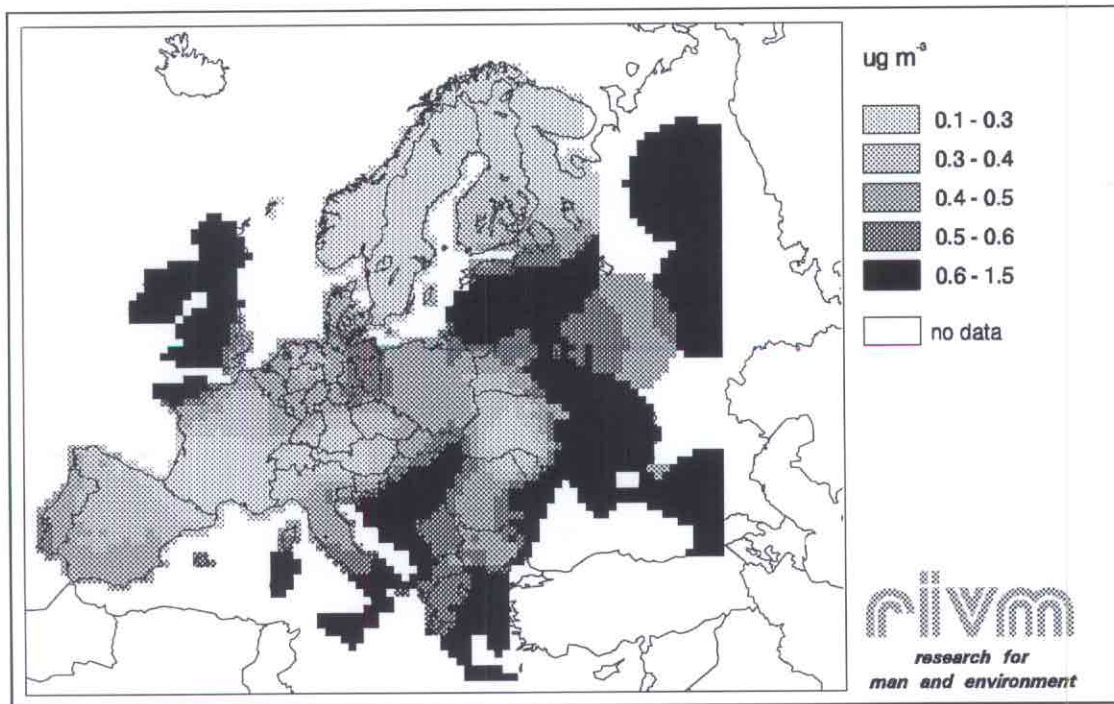


Figure 8d Annual mean concentrations of K^{+} in ambient air over Europe (in $\mu\text{g m}^{-3}$).

Dry deposition fluxes

In Figure 9 dry deposition fluxes of base-cations are presented. Fluxes clearly resemble the European climate/land use (i.e. dry deposition velocity) and emission (i.e. air concentration) pattern. Large Na^+ dry deposition fluxes are found in the coastal areas of northwest Europe, and relatively low Na^+ dry deposition fluxes in the Alps. Large Mg^{2+} dry deposition fluxes are found in the coastal areas of northwest Europe and in the Black Triangle, Sardinia, Croatia, Hungary and north of the Black Sea. Largest Ca^{2+} dry deposition fluxes appear in eastern Spain, Sardinia, Croatia, Hungary, Romania, the Black Triangle and Latvia. K^+ dry deposition is notably high in 'hot spots' located in the United Kingdom, Croatia, Latvia and north of the Black Sea.

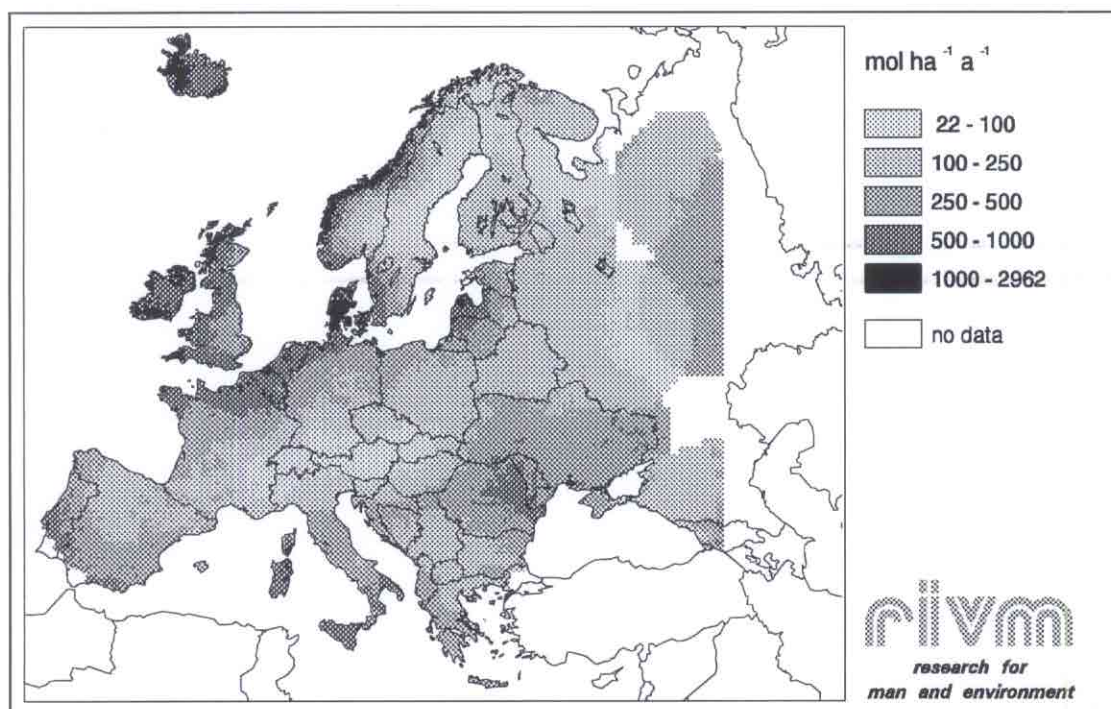


Figure 9a Dry deposition of Na^+ over Europe in 1989 (in mol ha⁻¹ a⁻¹).

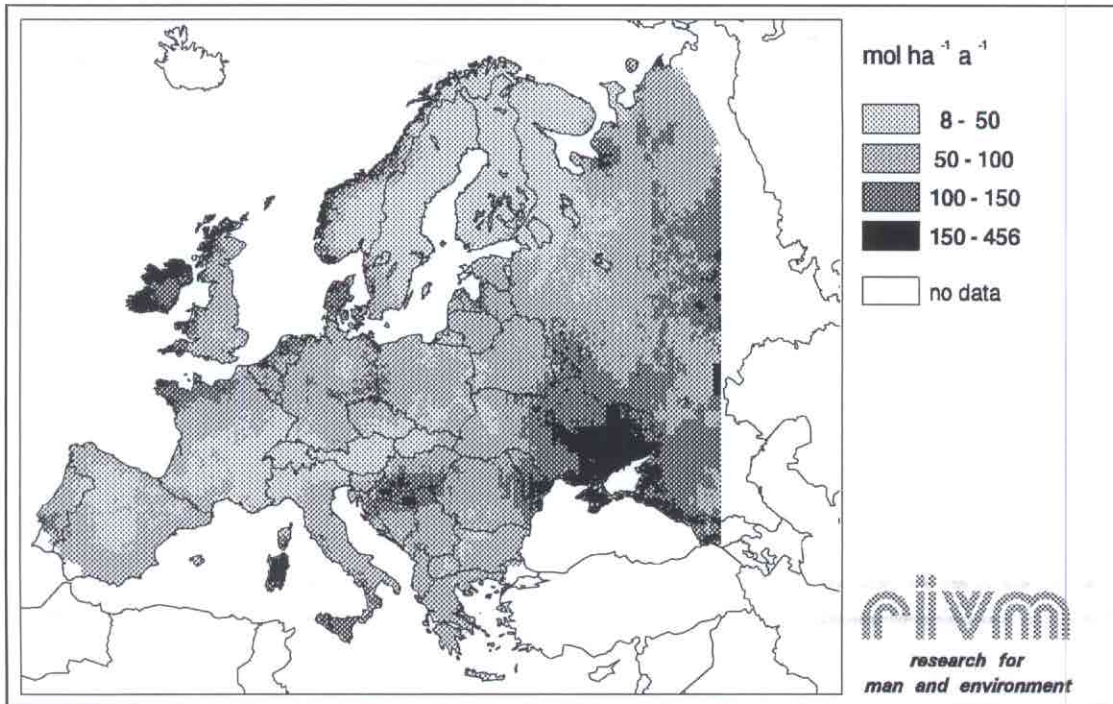


Figure 9b Dry deposition of Mg^{2+} over Europe in 1989 (in $mol\ ha^{-1}\ a^{-1}$).

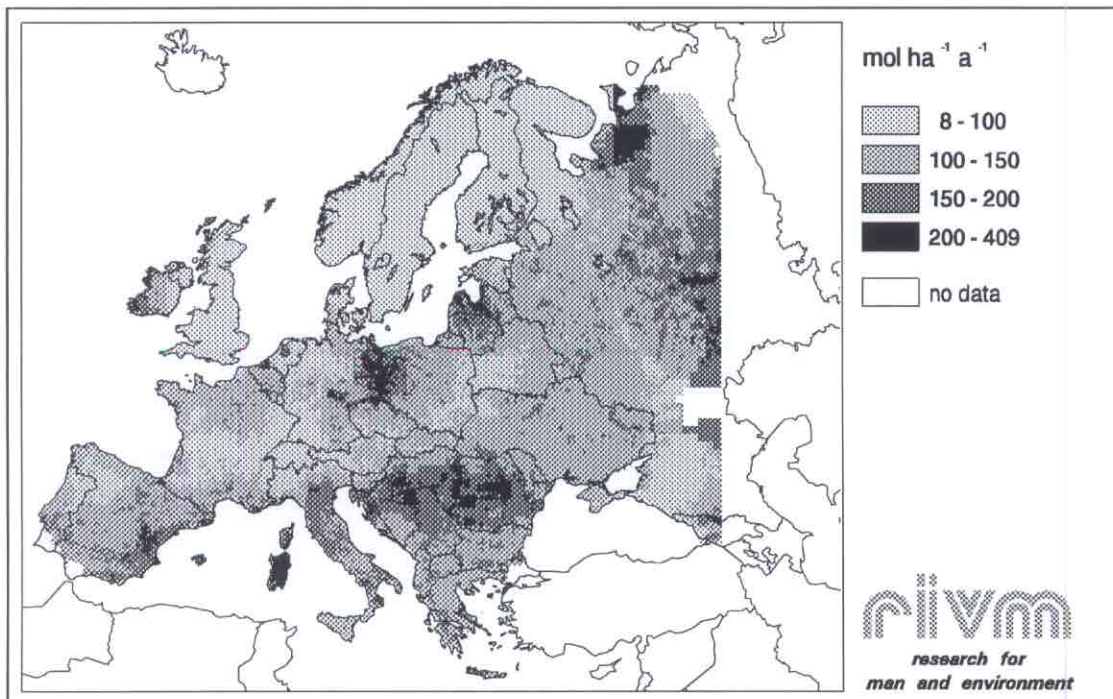


Figure 9c Dry deposition of Ca^{2+} over Europe in 1989 (in $mol\ ha^{-1}\ a^{-1}$).

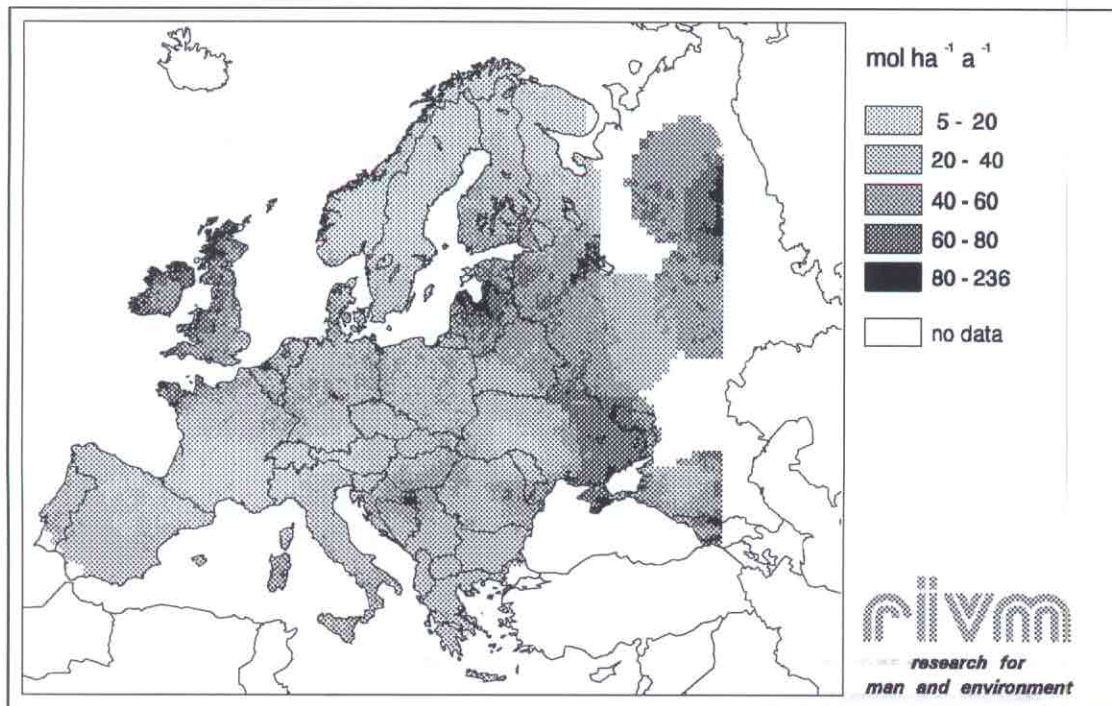


Figure 9d Dry deposition of K^+ over Europe in 1989 (in $\text{mol ha}^{-1} \text{a}^{-1}$).

Seasonal variation

An indication of seasonal differences in dry deposition was obtained by multiplying monthly mean air concentrations with monthly mean dry deposition velocities. Monthly mean air concentrations, in turn, were derived from monthly mean precipitation concentrations calculated from EMEP data at 90 sites scattered over Europe (Schaug *et al.*, 1991) and monthly mean scavenging ratios derived from measurements made by Galloway *et al.* (1993). Na^+ and Mg^{2+} concentrations in precipitation are found largest in the winter period which can be addressed to the frequent occurrence of westerly storms in this time of year bringing relatively large amounts of sea salt particles into the atmosphere (Figure 10). In contrast, Ca^{2+} and K^+ concentrations are largest in early summer which is most probably due to a combination of soil tillage and large areas of fallow land, and the prevalence of warm and dry conditions enhancing the suspension of soil particles into the atmosphere. Galloway *et al.* (1993) investigated at three coastal sites the temporal variability of scavenging ratios of Na^+ . There was a tendency for scavenging ratios to be larger in the winter period resulting primarily from increases in precipitation concentrations probably because storms are often accompanied by high winds which increase Na^+ concentrations in precipitation relative to aerosols, due to turbulent mixing in the lower troposphere (Figure 10).

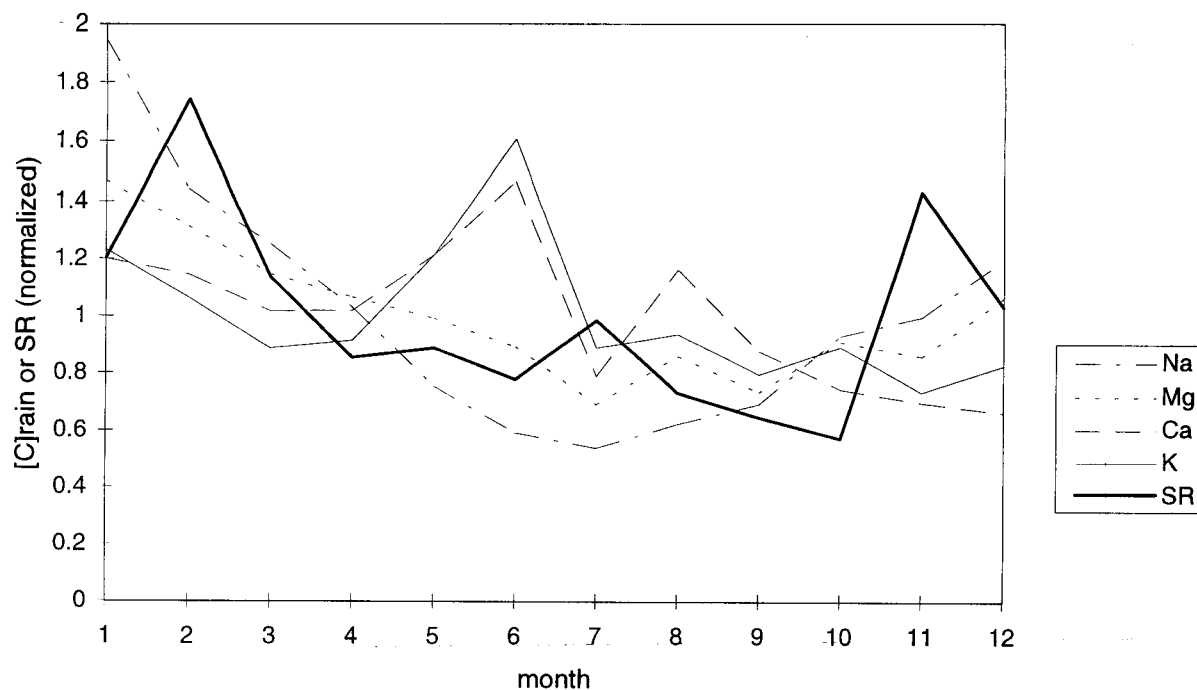


Figure 10 Monthly mean precipitation concentrations of Na^+ , Mg^{2+} , Ca^{2+} and K^+ in Europe in 1989 calculated from EMEP data at 90 sites scattered over Europe (Schaug *et al.*, 1991), as well as monthly mean scavenging ratios of Na^+ derived from measurements at three coastal sites performed by Galloway *et al.* (1993). All values are normalized assuming the annual average equal to 1.0.

Monthly mean air concentrations were calculated assuming that the variation in scavenging ratio found by Galloway *et al.* (1993) holds for other base-cations as well and is the same all over Europe (Figure 11). A similar seasonal trend is found as in precipitation concentrations. Relatively large Na^+ , Mg^{2+} , Ca^{2+} and K^+ air concentrations estimated for autumn can be attributed to the low scavenging ratios in this period. European average monthly mean dry deposition velocities, calculated using the parametrisation of the dry deposition velocity described before, are found largest in the winter period reflecting relatively high wind velocities, high relative humidities and prolonged periods with surface wetness (Figure 11). In comparison to the summer period, dry deposition velocities are about 50% larger in the winter period.

Dry deposition fluxes of Na^+ in the winter period are approximately three times larger in comparison to summer fluxes (Figure 12). A similar but less pronounced seasonal trend is found for Mg^{2+} . Dry deposition fluxes of Ca^{2+} and K^+ experience less clear seasonal trends but peak fluxes are found in early summer and autumn.

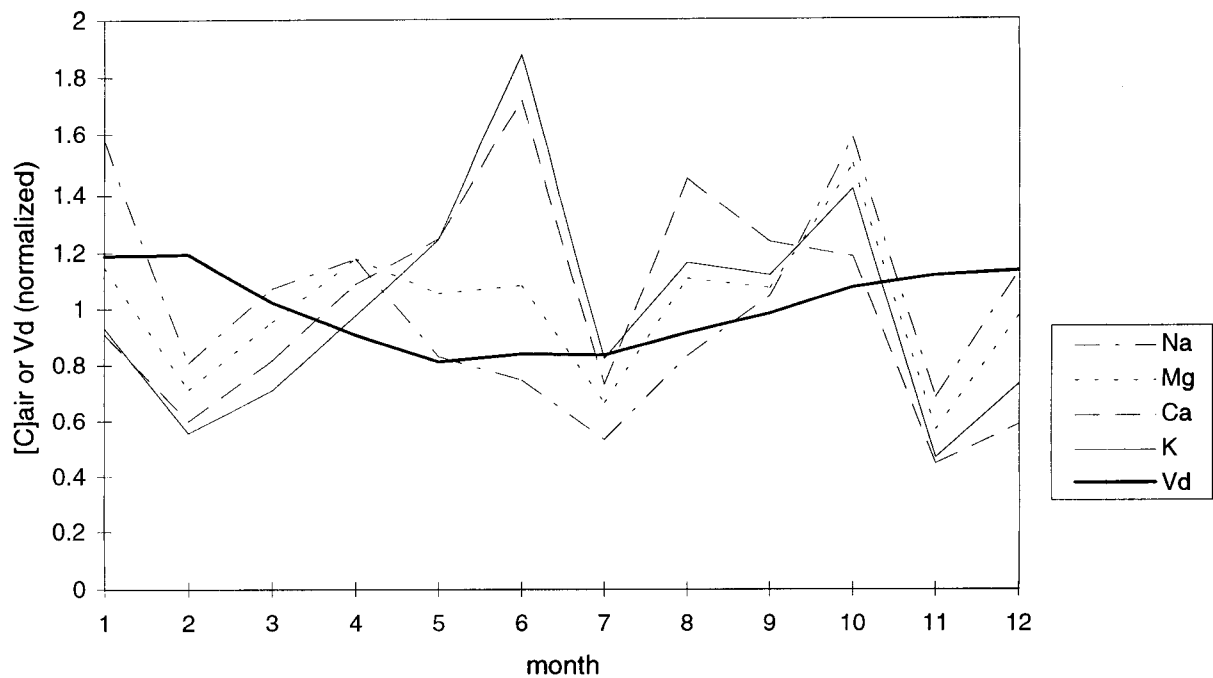


Figure 11 Monthly mean air concentrations of Na^+ , Mg^{2+} , Ca^{2+} and K^+ in Europe in 1989 derived from monthly mean precipitation concentrations and scavenging ratios presented in Figure 10, as well as monthly mean dry deposition velocities of base-cation containing particles in Europe. All values are normalized assuming the annual average equal to 1.0.

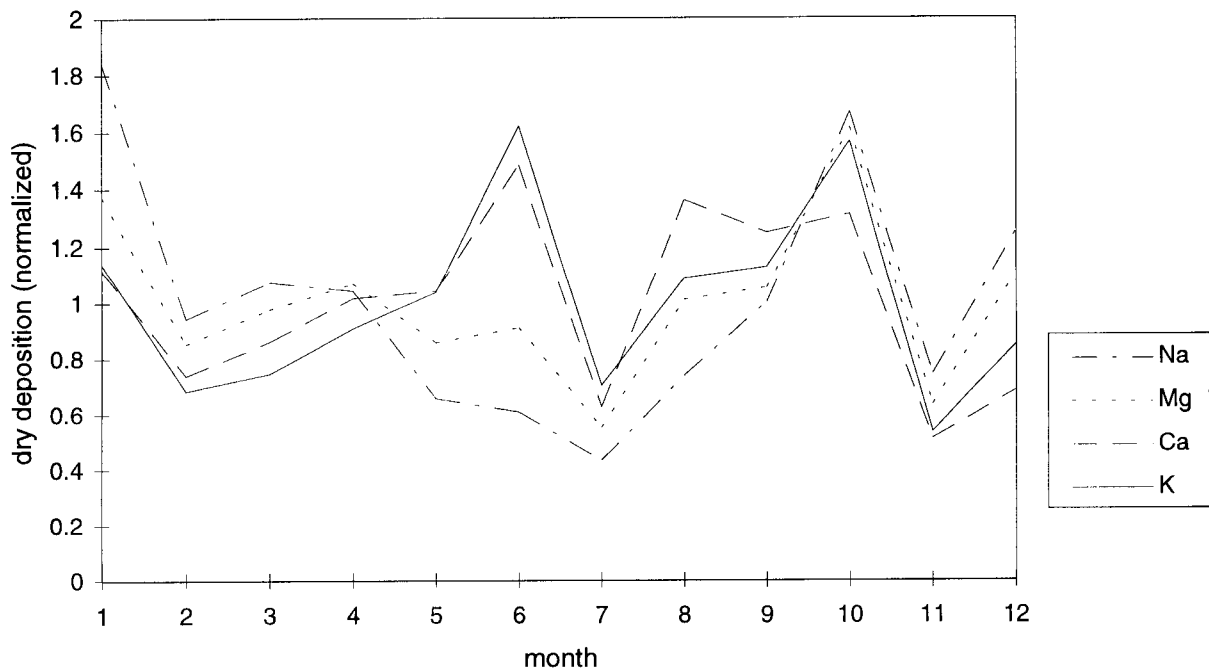


Figure 12 Dry deposition calculated by multiplying monthly mean air concentrations with monthly mean dry deposition as presented in Figure 11. All values are normalized assuming the annual average equal to 1.0.

3.3 Total deposition

Besides climate and land use pattern, calculated total deposition fields of base-cations clearly reflect the geographic variability of sources over Europe (Figure 13). Total deposition of Na^+ is relatively large ($>1000 \text{ mol ha}^{-1} \text{ a}^{-1}$) in the coastal areas of western Europe, Croatia, Bosnia-Herzegovina and Serbia as well as in some areas in Romania and Moldavia. Low Na^+ total deposition fluxes ($< 250 \text{ mol ha}^{-1} \text{ a}^{-1}$) are found in the Alps and the eastern part of Scandinavia. Total deposition of Mg^{2+} appears large ($>400 \text{ mol ha}^{-1} \text{ a}^{-1}$) in the coastal areas of Ireland, Scotland, Sardinia and Serbia. However, notably large Mg^{2+} deposition is also estimated for a large area north of the Black Sea. Very low Mg^{2+} deposition ($<100 \text{ mol ha}^{-1} \text{ a}^{-1}$) is found in some areas in central Spain and in the Alps, Poland and eastern Scandinavia. Total deposition of Ca^{2+} is relatively large ($>400 \text{ mol ha}^{-1} \text{ a}^{-1}$) in Italy, the Baltic States, Moldavia, Ukraine, the Black Triangle and Lithuania, and low ($<100 \text{ mol ha}^{-1} \text{ a}^{-1}$) in Scandinavia and part of the United Kingdom. Large total deposition of K^+ ($>200 \text{ mol ha}^{-1} \text{ a}^{-1}$) is found in part of Ireland, the United Kingdom, Croatia, Bosnia-Herzegovina, Serbia, Moldavia and Ukraine. Very low total K^+ deposition ($<50 \text{ mol ha}^{-1} \text{ a}^{-1}$) is calculated for eastern Scandinavia and for central Spain and southern France. Country average total deposition fluxes of base-cations are presented in Appendix 3.

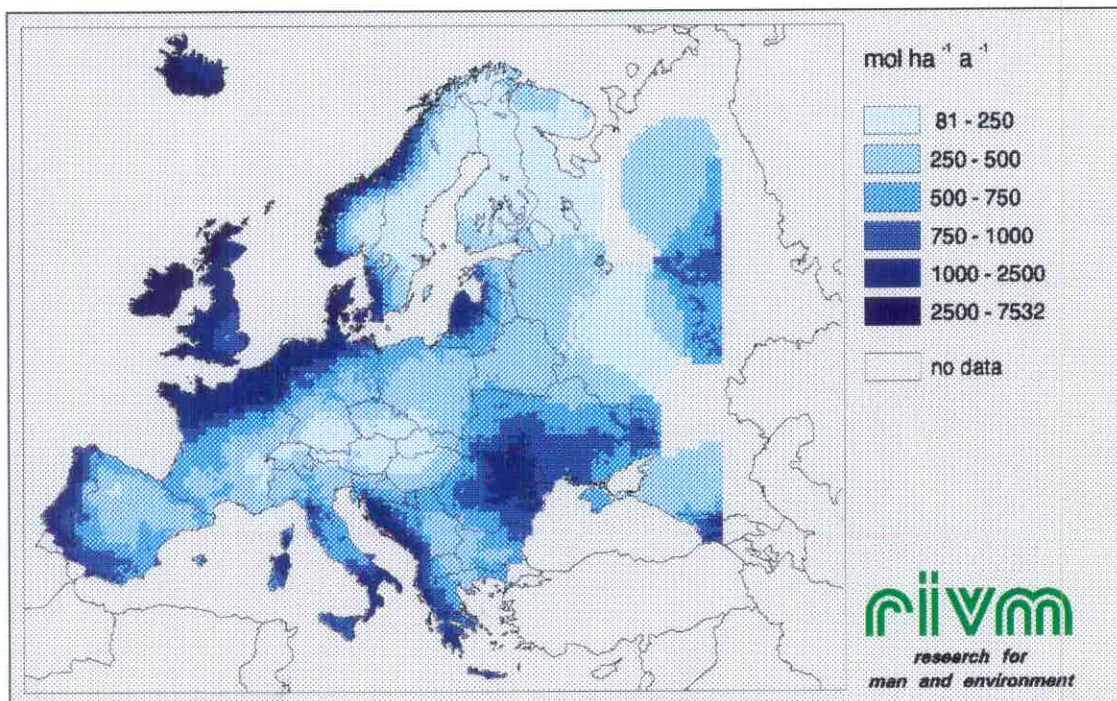


Figure 13a Total deposition of Na^+ over Europe in 1989 (in $\text{mol ha}^{-1} \text{ a}^{-1}$).

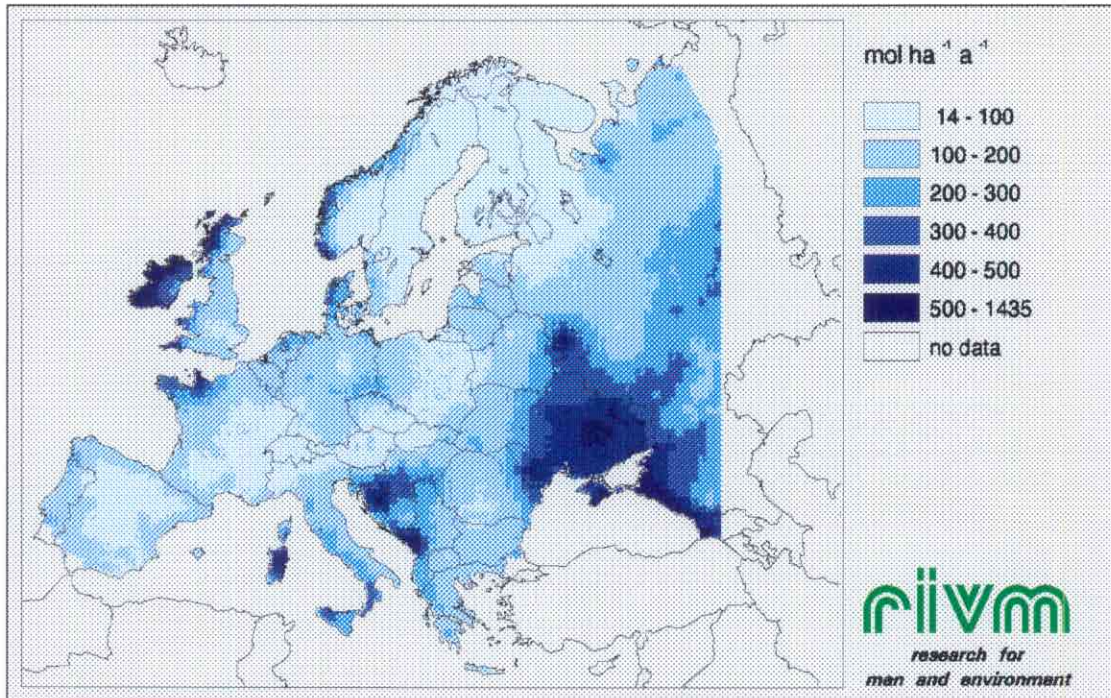


Figure 13b Total deposition of Mg²⁺ over Europe in 1989 (in mol ha⁻¹ a⁻¹).

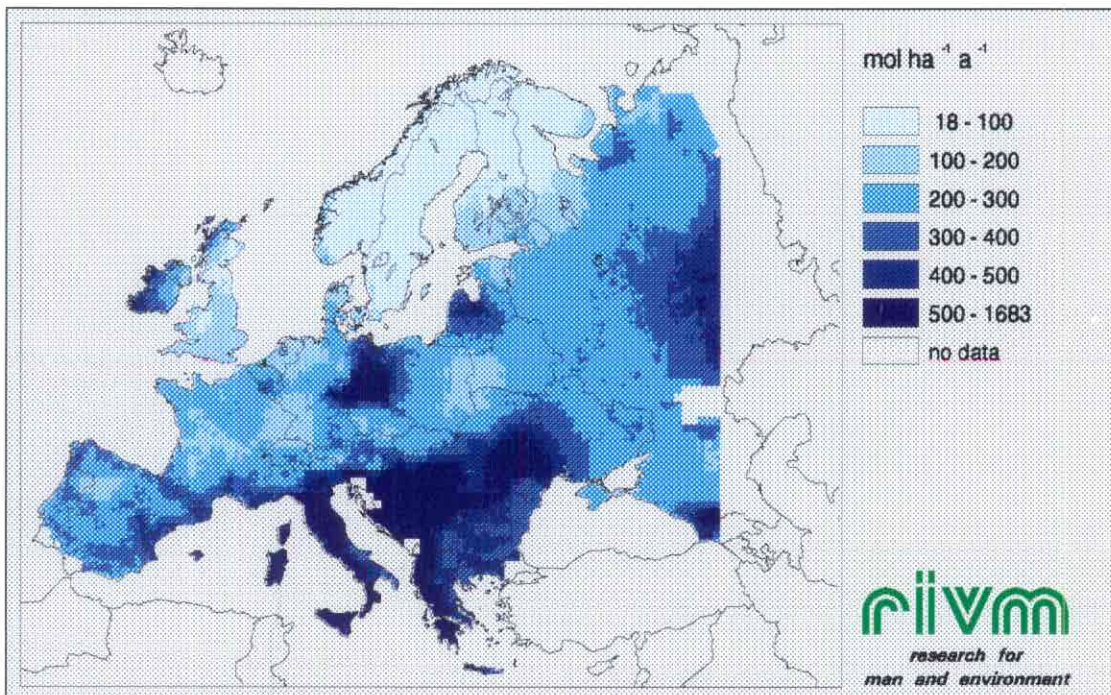


Figure 13c Total deposition of Ca²⁺ over Europe in 1989 (in mol ha⁻¹ a⁻¹).

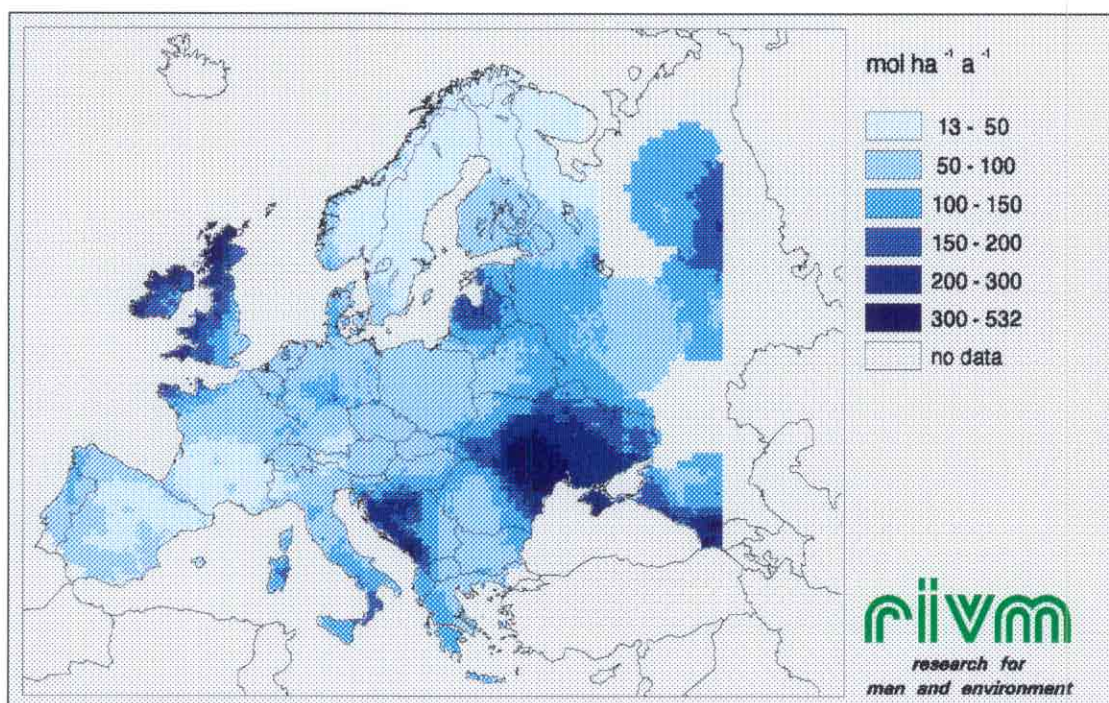


Figure 13d Total deposition of K^+ over Europe in 1989 (in $\text{mol ha}^{-1} \text{a}^{-1}$).

Part of the deposition of Na^+ , Mg^{2+} , Ca^{2+} and K^+ will be the result of sea spray. To estimate what fraction of Mg^{2+} , Ca^{2+} and K^+ is of non-sea salt origin, correction factors have been derived based on the composition of sea water (Asman *et al.*, 1981). It is assumed that Na^+ originates exclusively from sea spray and that the ratio between the concentration in sea spray for the component to be corrected and Na^+ is the same as in bulk sea water. The corrected concentration $[X]_c$ of component X can subsequently be calculated by:

$$[X]_c = [X] - f_x \cdot [\text{Na}^+] \quad [8]$$

where $[X]$ is the uncorrected concentration and f_x is the correction factor for this component. Using average concentrations in sea water (in mol l^{-1}) as presented by Weast (1975), f_x equals 0.1131, 0.0218 and 0.0212 for Mg^{2+} , Ca^{2+} and K^+ , respectively. Using such a correction will only yield reliable estimates of non-sea salt Mg^{2+} , Ca^{2+} and K^+ in areas where sea salt is the only source of Na^+ in ambient air. This generally will be the case in western and northern Europe. In some parts of southern and south-eastern Europe, however, significant quantities of Na^+ in the atmosphere originate from wind-blown evaporites. Applying the sea salt correction there will result in underestimated non-sea salt Mg^{2+} , Ca^{2+} and K^+ concentrations.

Total deposition of non-sea salt $\text{Mg}^{2+} + \text{Ca}^{2+} + \text{K}^+$, used to quantify the amount of potential acid deposition counteracted by base-cation deposition (section 4.2) and for the estimation of critical loads and critical load exceedances (TFM, 1996) is displayed in Figure 14. It is found relatively high ($>1000 \text{ eq ha}^{-1} \text{a}^{-1}$) in Italy, the Baltic States, Moldavia, Ukraine, the Black Triangle and Lithuania. Low fluxes of non-sea salt $\text{Mg}^{2+} + \text{Ca}^{2+} + \text{K}^+$ ($<150 \text{ eq ha}^{-1} \text{a}^{-1}$) occur in Scandinavia. Country average total deposition fluxes of non-sea salt $\text{Mg}^{2+} + \text{Ca}^{2+} + \text{K}^+$ are presented in Appendix 3.

In Europe, dry deposition constitutes on average 45% of the total deposition of non-sea salt $Mg^{2+}+Ca^{2+}+K^+$ (Figure 15). This value corresponds well with estimates made by Lannefors *et al.* (1983), Driscoll *et al.* (1989), Johnson and Lindberg (1992) and Erisman *et al.* (1994) for individual sites. The contribution of dry deposition is relatively large (>60%) in Sweden and Finland which is explained by the co-occurrence of forests and large wind speeds resulting in large dry deposition velocities. A low dry deposition contribution (<30%) is found in parts of Norway, Germany (Saxony), Switzerland, Italy, Slovenia, Croatia, Bosnia-Herzegovina, Serbia, Moldavia and Ukraine.

Mg^{2+} , Ca^{2+} and K^+ constitute on average 21%, 66% and 13%, respectively of the total deposition of non-sea salt $Mg^{2+}+Ca^{2+}+K^+$ in Europe (Figure 16). The contribution of non-sea salt Mg^{2+} to the total deposition of non-sea salt $Mg^{2+}+Ca^{2+}+K^+$ is relatively large (>40%) north from the Black Sea. The relatively large percentages found in the coastal areas of Ireland and Norway suggest that for these areas the correction factor applied for the conversion of bulk to wet-only precipitation concentrations probably was too small. The contribution of non-sea salt Ca^{2+} is markedly large (>80%) in Spain, Italy, some areas in France and Belgium, northern Germany, Denmark, Lithuania, Latvia, Romania, and Greece, whereas the contribution of non-sea salt K^+ is relatively large (>20%) in the United Kingdom, part of Scandinavia, Ukraine and, probably due to open (kali-)mining in France, also in the border area between France, Germany and Switzerland.

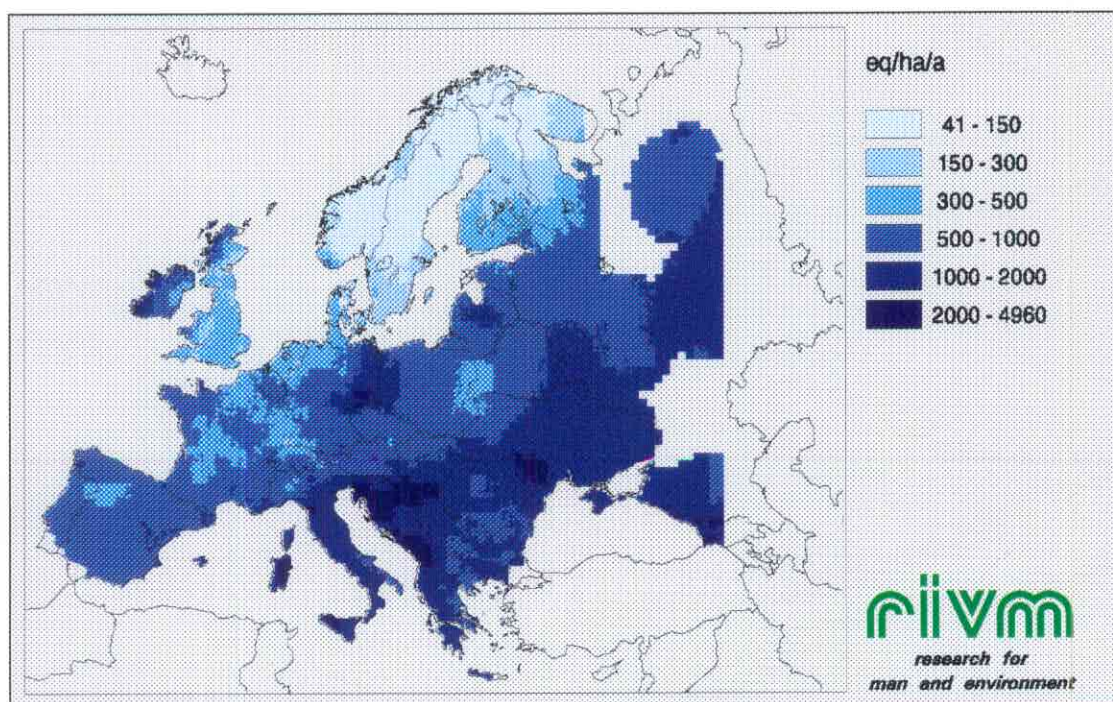


Figure 14 Total deposition of non-sea salt $Mg^{2+}+Ca^{2+}+K^+$ over Europe in 1989 (in $eq\ ha^{-1}\ a^{-1}$).

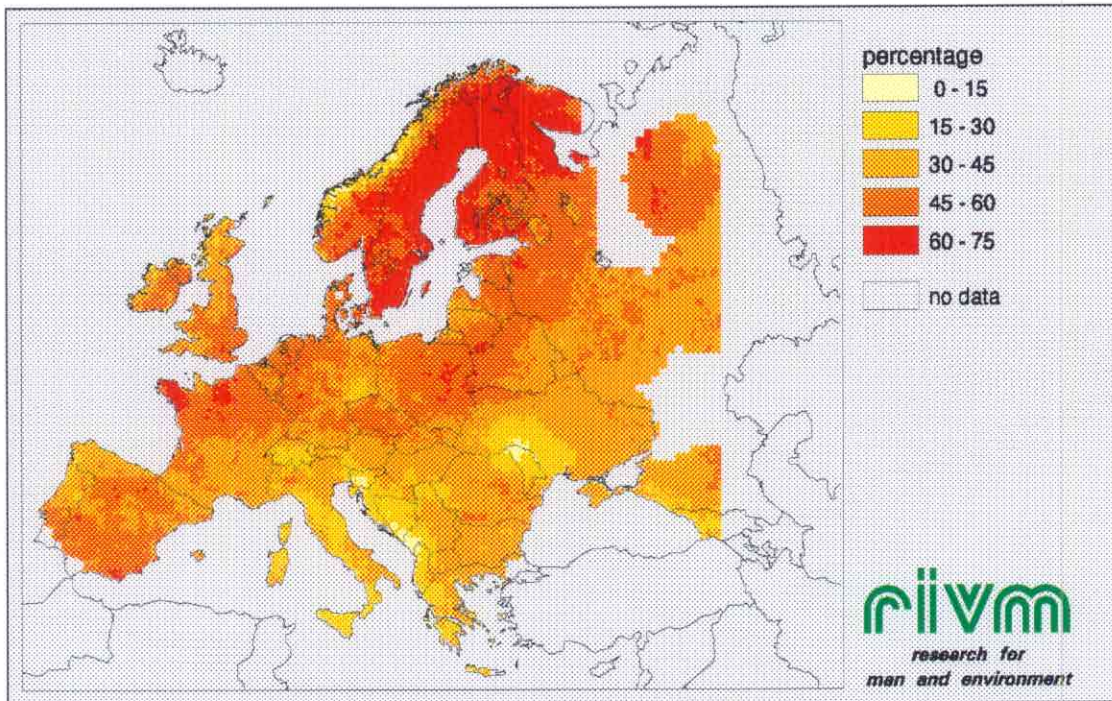


Figure 15 Dry deposition of non-sea salt $Mg^{2+}+Ca^{2+}+K^+$ expressed as percentage of the total deposition of non-sea salt $Mg^{2+}+Ca^{2+}+K^+$ over Europe in 1989 (in %).

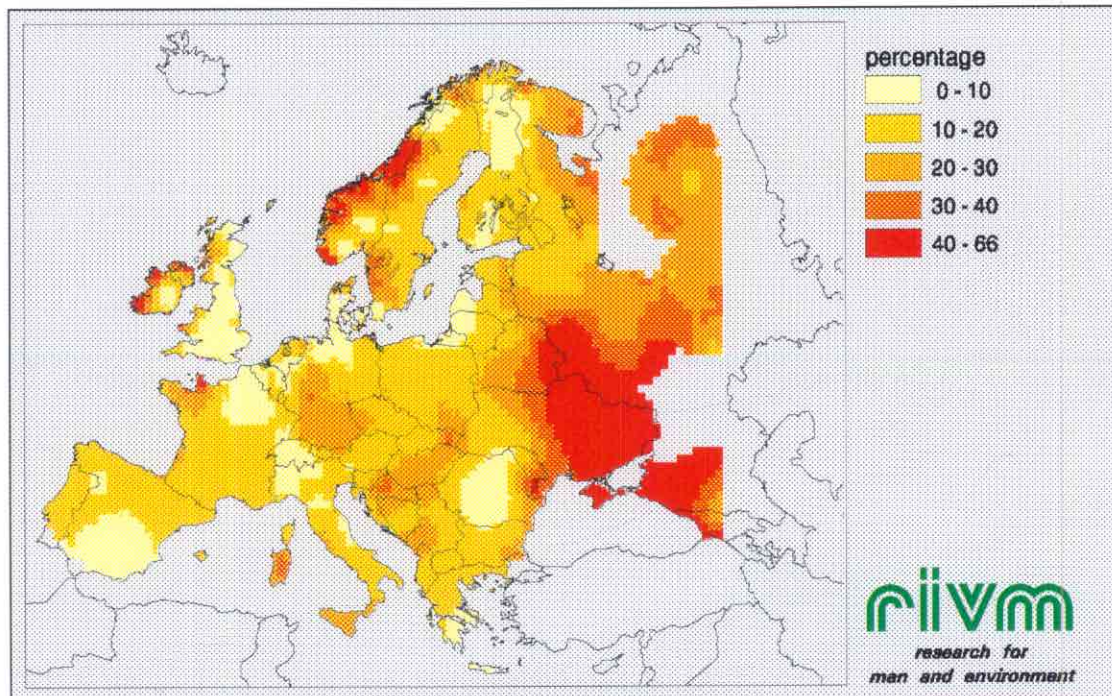


Figure 16a Total deposition of non-sea salt Mg^{2+} expressed as percentage of the total deposition of non-sea salt $Mg^{2+}+Ca^{2+}+K^+$ over Europe in 1989 (in %).

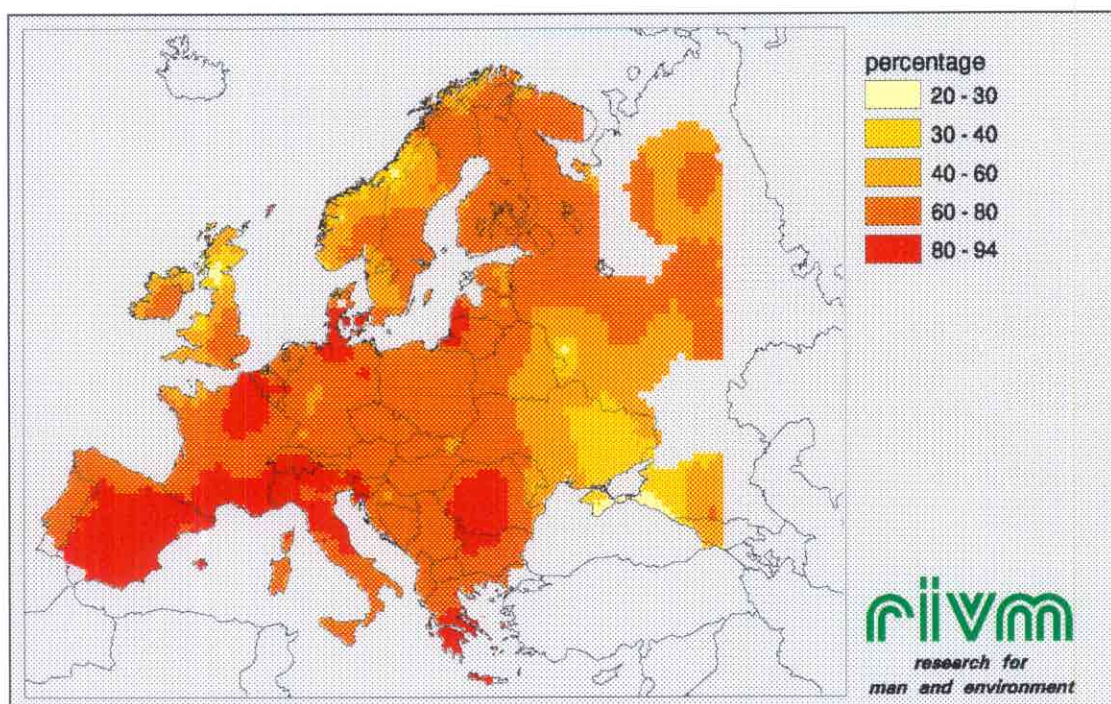


Figure 16b Total deposition of non-sea salt Ca^{2+} expressed as percentage of the total deposition of non-sea salt $\text{Mg}^{2+} + \text{Ca}^{2+} + \text{K}^{+}$ over Europe in 1989 (in %).

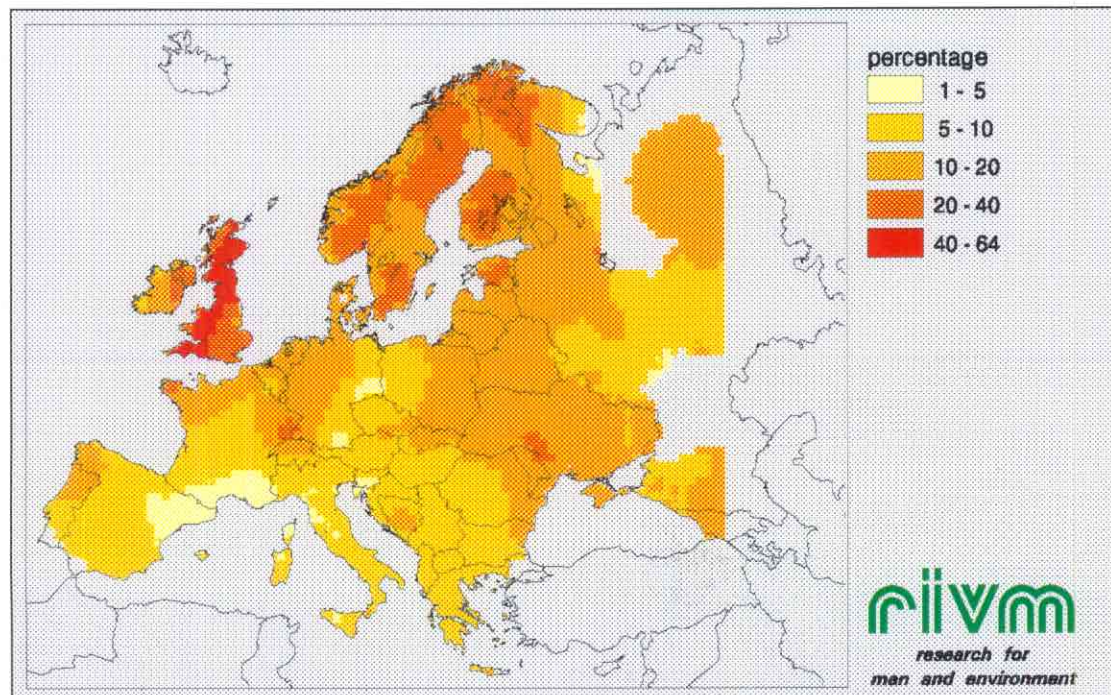


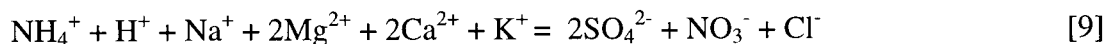
Figure 16c Total deposition of non-sea salt K^{+} expressed as percentage of the total deposition of non-sea salt $\text{Mg}^{2+} + \text{Ca}^{2+} + \text{K}^{+}$ over Europe in 1989 (in %).

4 ACID NEUTRALIZATION CAPACITY

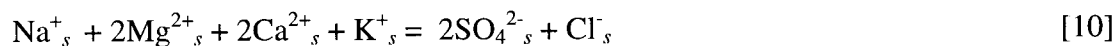
Base-cations contribute to neutralization of acid anions in precipitation and soil. The acid neutralization capacity (ANC) of alkaline particles will depend on the chemical composition of the particles (see chapter 2) and their solubility. Only the soluble part will contribute to neutralization. The dissolution of alkaline particles will be a function of time, solution pH and aerosol mass loading (Williams *et al.*, 1988). The major H⁺ ion removal reactions in clouds or precipitation water and soil include *i*) ion exchange, in which cations adsorbed by clay minerals or other substances are exchanged for H⁺ ions in solution, and *ii*) mineral weathering (dissolution). Cation exchange reactions are essentially instantaneous, reaction rates being usually diffusion limited. Mineral weathering, on the other hand, may be relatively rapid, as in the case of finely divided CaCO₃ particles, or quite slow (days to weeks/months), as in the case of silicate minerals (Gatz *et al.*, 1986). In many field studies, it is found that the rainwater pH increased between the field and the laboratory, or during storage (e.g. Slanina *et al.*, 1987). This may be attributed to mineral weathering of base-cation containing particles. The ANC attributed to a base-cation in precipitation will be less than or equal to the total concentration of the element in precipitation, since elements can also occur in essentially insoluble phases. The insoluble fraction is generally not analyzed in precipitation, but a few measurements made by Cawse (1974) and Gatz *et al.* (1986) suggest that Na and Ca are about 95 to 100% soluble in precipitation, Mg about 80% and K near 50%. A strong spatial variation in insoluble fraction may be expected. Semb *et al.* (1995) found for a site in Norway a much higher Ca to K ratio in precipitation samples in comparison to air samples. This was partly explained by the better solubility of calcium silicates in comparison to potassium silicates. The ANC attributed to base-cations in the soil will not depend on their solubility as eventually even the insoluble fraction will be available for neutralization through mineral weathering.

4.1 Amount of acid in precipitation neutralized by base-cations

The most abundant components in rainwater are NH₄⁺, H⁺, Na⁺, Mg²⁺, Ca²⁺ and K⁺ as cations and SO₄²⁻, NO₃⁻, and Cl⁻ as anions. Because rain water is electrically neutral the following equilibrium must hold (concentrations expressed in mol l⁻¹):



In sea spray, the bulk components are Na⁺, Mg²⁺, Ca²⁺ and K⁺ as cations and SO₄²⁻ and Cl⁻ as anions. The amount of NH₄⁺, H⁺ and NO₃⁻ is negligible. Because of electroneutrality the following equilibrium exists:



where *s* denotes 'in sea spray'. By assuming Na⁺ and Cl⁻ originating exclusively from sea spray, and negligible amounts of HCO₃⁻, formic and acetic acid present, the following relationship can be derived by combining equations [9] and [10]:



where * denotes that the concentration is corrected for the contribution of sea salt. The percentage neutralization of acid anions (SO_4^{2-} and NO_3^-) by base-cations in precipitation can then be computed according to (Asman *et al.*, 1981):

$$100 * \{ 2\text{Mg}^{2+*} + 2\text{Ca}^{2+*} + \text{K}^{+*} \} / \{ 2\text{SO}_4^{2-*} + \text{NO}_3^- \} \quad [12]$$

By computing the percentage neutralization of acid by base-cations in precipitation according to equation [12] it is assumed that all elements are 100% soluble. Taking the insoluble fraction as estimated by Cawse (1974) and Gatz *et al.* (1986) and considering the contribution of the different base-cations, it can be calculated that by assuming all elements 100% soluble the percentage neutralization will usually be overestimated by less than 20%.

Results are displayed in Figure 17. In southern European countries usually more than 50% of the $\text{SO}_4^{2-} + \text{NO}_3^-$ present in precipitation is found neutralized by base-cations. In southern Portugal, southern Spain, part of Italy and the Baltic States, Moldavia and Ukraine the amount of neutralization is even larger than 75%. The percentage neutralization calculated for these countries will to some extent be overestimated as the impact of HCO_3^- is not taken into account in the calculation scheme. HCO_3^- will certainly be present in precipitation in this part of Europe.

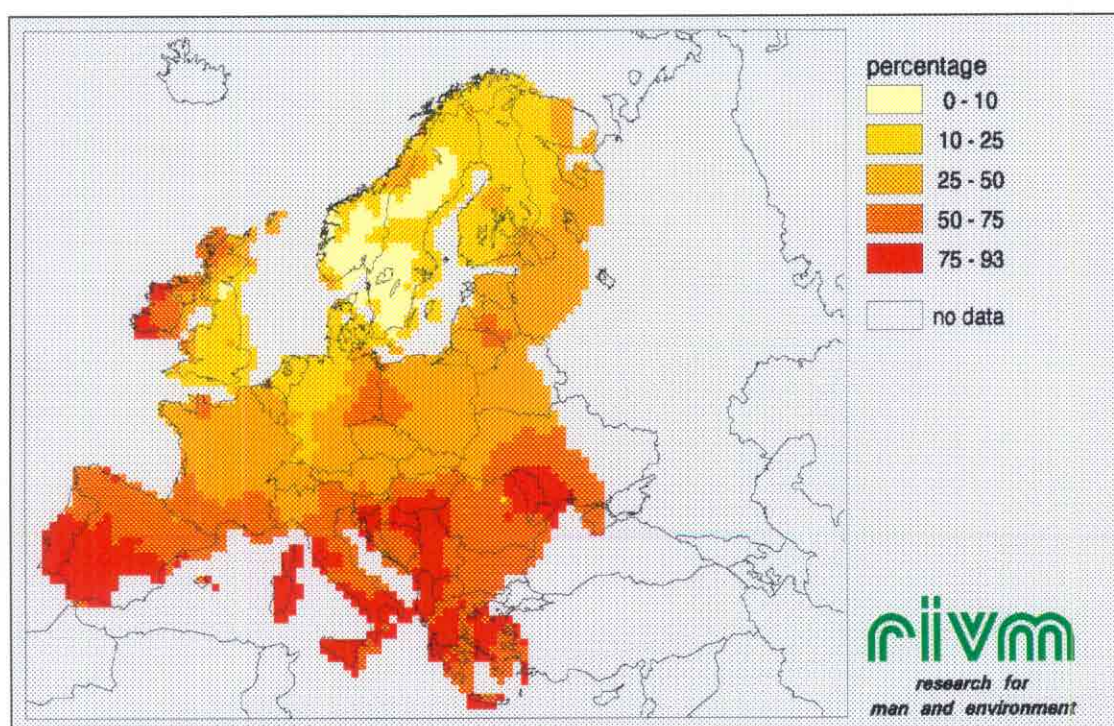


Figure 17 The percentage $\text{SO}_4^{2-} + \text{NO}_3^-$ in precipitation neutralized by base-cations over Europe in 1989 (in %), calculated according to equation [12].

The percentage neutralization will also be overestimated in remote areas in Europe due to formic and acetic acid contributing to rainfall acidity (Keene *et al.*, 1983) which is not taken into account in the calculation procedure. The same holds for areas where HCl contributes to the rainfall acidity. In Scandinavia, Denmark, northern and western Germany, the Netherlands and the southeast of the United Kingdom, the

percentage neutralization by base-cations is very low (<25%). In Scandinavia most of the sulfate and nitrate in precipitation is counteracted by H⁺ while in e.g. the Netherlands NH₄⁺ is the dominant counter-ion.

The latter is illustrated in Table III, showing results of constrained non-linear multiple regression analysis performed on precipitation samples collected at De Bilt during the period 1992-1994. Such an analysis has been found very useful for the determination of cation-anion relationships in precipitation samples, which, in turn, are very useful for the determination and chemical characterization of sources (Slanina *et al.*, 1983; Dekkers and Sauter, 1996; Appendix 4). Of the SO₄²⁻+NO₃⁻ present in precipitation at De Bilt, on average 70% is found associated with NH₄⁺. Only about 17% is counteracted by base-cations, i.e. Na⁺ and Ca²⁺. Mg²⁺ and K⁺ did not contribute to the neutralization of SO₄²⁻+NO₃⁻. These results agree well with results obtained by Slanina *et al.* (1983) analyzing cation-anion relationships in precipitation in Lelystad (The Netherlands) using essentially the same mathematical procedure. From Table III it can be concluded that of all Na⁺ present in precipitation about 88% is associated with Cl⁻ and about 12% with SO₄²⁻. These percentages are exactly the same as those found in sea water (Weast, 1975), clearly indicating its sea-salt origin. Only about 0.3% of the sodium is found associated to HCO₃⁻ and may be considered available for acid neutralization. Mg²⁺ is also found mainly connected to SO₄²⁻ and Cl⁻. In contrast, Ca²⁺ is associated to SO₄²⁻ and NO₃⁻, and K⁺ to SO₄²⁻ and HCO₃⁻. Ca²⁺ and K⁺ thus contribute or have contributed fully to the neutralization of acid anions in precipitation.

Table III The percentage anions are connected to the various cations, and vice versa, in precipitation at De Bilt (The Netherlands) during the period 1992-1994. Details on the method used to derive these values, as well as on the uncertainties involved, are presented in Appendix 4.

	NH ₄ ⁺	H ⁺	Na ⁺	Mg ²⁺	Ca ²⁺	K ⁺
SO ₄ ²⁻	64.1	11.8	9.4	0	14.7	0
NO ₃ ⁻	84.3	10.4	0	0	5.3	0
Cl ⁻	0	0.5	78.3	21.2	0	0
PO ₄ ³⁻	97.5	0	0	0	0	2.5
HCO ₃ ⁻	0	0	0	0	0	100
F ⁻	100	0	0	0	0	0

	SO ₄ ²⁻	NO ₃ ⁻	Cl ⁻	PO ₄ ³⁻	HCO ₃ ⁻	F ⁻
NH ₄ ⁺	59.3	34.5	0	2.9	2.2	0.9
H ⁺	0	52.5	47.5	0	0	0
Na ⁺	11.9	0	87.8	0	0.3	0
Mg ²⁺	31.7	0	67.7	0	0.6	0
Ca ²⁺	56.6	42.6	0	0	0.8	0
K ⁺	71.1	0	0	0	28.9	0

4.2 Amount of potential acid deposition counteracted by deposition of base-cations

Deposition of potential acid has been mapped on a small scale over Europe by Erisman *et al.* (1995) and Van Pul *et al.* (1995) using essentially the same method as described in this report for base-cations. Air concentrations of acidifying gases and aerosols are based on result of the EMEP long-range transport model. Transport to and absorption or uptake of a component by the surface is described using the resistance framework (Hicks *et al.*, 1987). Resistances are calculated using observations of meteorological parameters and parametrisation of surface exchange processes for different receptor surfaces and pollution climates as described in Erisman *et al.* (1994). Dry deposition is calculated using 6 hour average concentrations and dry deposition velocities. Total deposition of potential acid is calculated by:

$$\text{Total potential acid} = 2\text{SO}_x^* + \text{NO}_y + \text{NH}_x \quad [13]$$

where SO_x^* denotes the total (dry + wet) deposition of sulfur compounds corrected for the contribution of sea salt, NO_y the total deposition of oxidized nitrogen compounds and NH_x the total deposition of reduced nitrogen compounds. With respect to soil acidification it is assumed that 1 mol of SO_x is forming 2 moles of H^+ , and 1 mol of NO_y and NH_x each 1 mol of H^+ . NH_x is assumed to contribute fully to soil acidification through the process of nitrification in the soil (Van Breemen *et al.*, 1982). Under the influence of oxygen, nitrifying bacteria may transform reduced nitrogen compounds in the soil into nitrate and acid. If NH_x is completely nitrified the potential acid load equals the actual acid load. HCl deposition also contributes to a (very) small extent to the deposition of potential acid but up to now it has been found impossible to accurately quantify HCl deposition on a European scale. For this reason, in this study its contribution is neglected. The contribution of e.g. HF, PAN and organic acids to the total deposition of potential acid is assumed negligible.

The percentage neutralization of potential acid by deposition of base-cations is calculated by:

$$100 * \{ 2\text{Mg}^{2+*} + 2\text{Ca}^{2+*} + \text{K}^{+*} \} / \{ 2\text{SO}_x^* + \text{NO}_y + \text{NH}_x \} \quad [14]$$

where * denotes that the Ca^{2+} , Mg^{2+} , K^+ and SO_x deposition flux is corrected for the contribution of sea salt. Deposition rates in equation [13] and [14] need to be expressed in $\text{mol ha}^{-1} \text{a}^{-1}$.

In Figure 18 the total deposition of potential acid is presented. Largest potential acid deposition ($>7500 \text{ eq ha}^{-1} \text{a}^{-1}$) is found in the Black Triangle area. In northern Scandinavia and part of Scotland, Portugal and Spain the potential acid deposition is very low ($<500 \text{ eq ha}^{-1} \text{a}^{-1}$). In large parts of southern Europe, more than 50% of the potential acid deposition is found counteracted by deposition of non-sea salt $\text{Mg}^{2+} + \text{Ca}^{2+} + \text{K}^+$ (Figure 19). In southern Portugal, southern Spain, Sardinia and the west coast of Ireland and Scotland the amount of neutralization exceeds 100%. In central and northwestern Europe base-cation deposition usually amounts less than 25% of the acid input. Smallest base-cation deposition relative to potential acid deposition is found in southern Scandinavia, Denmark, northern Germany and the Netherlands. Country average total deposition fluxes of non sea salt $\text{Mg}^{2+} + \text{Ca}^{2+} + \text{K}^+$ and potential acid are presented in Appendix 3.

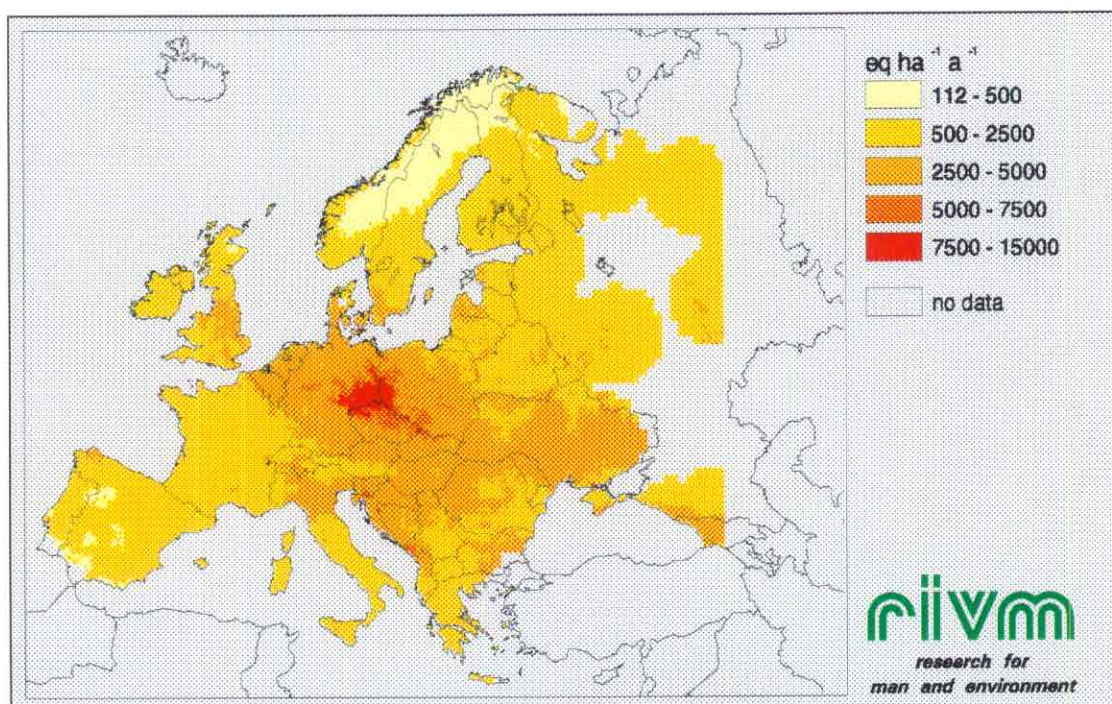


Figure 18 Total deposition of potential acid over Europe in 1989 (after Erisman *et al.*, 1995; Van Pul *et al.*, 1995).

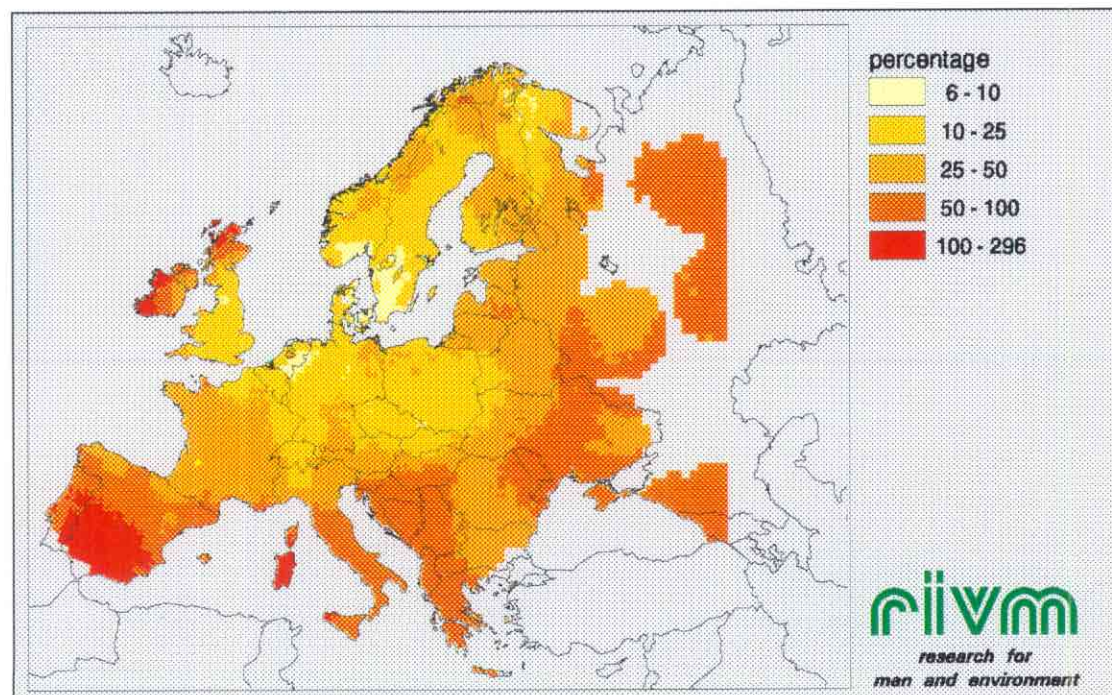


Figure 19 The percentage neutralization of potential acid deposition by deposition of base-cations over Europe in 1989 (in %), calculated according to equation [14].

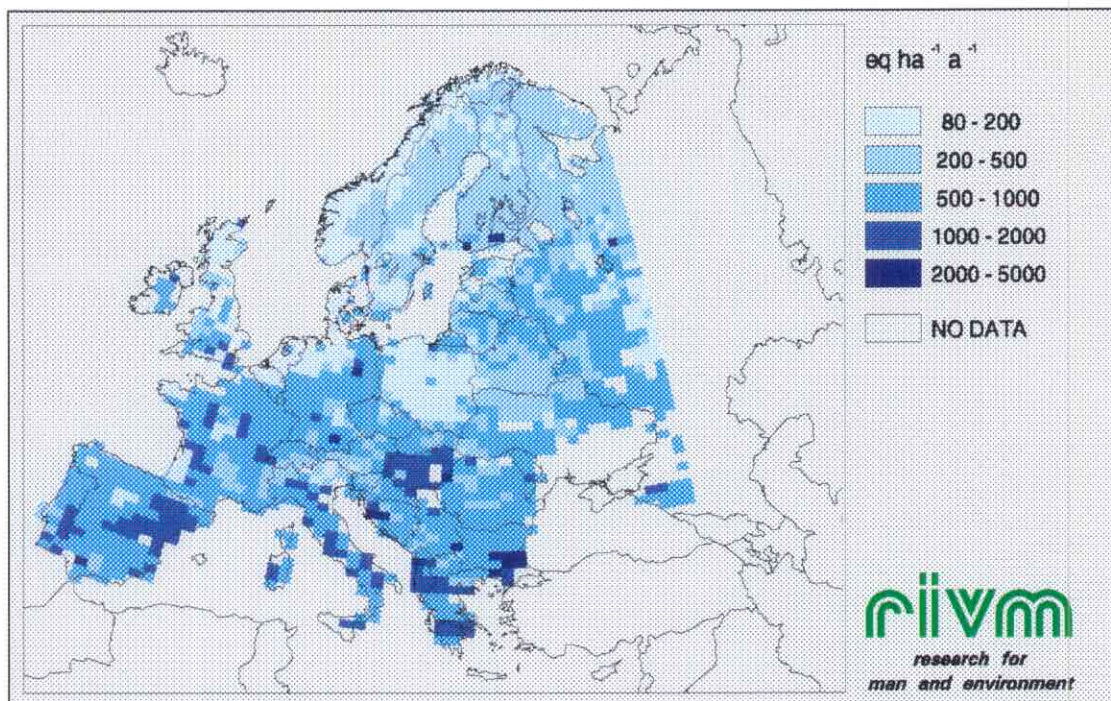


Figure 20 Weathering rates of base-cations ($Mg^{2+}+Ca^{2+}$) in the upper 0.5m of European forest soils (after De Vries *et al.*, 1993).

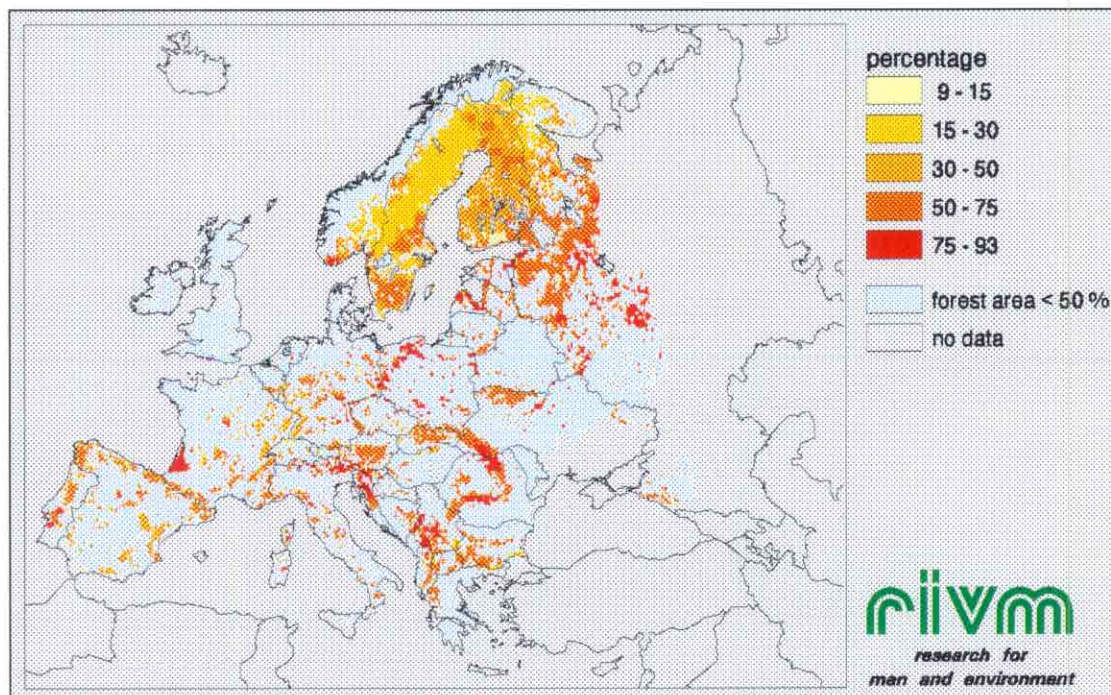


Figure 21 The percentage contribution of base-cation deposition to forest nutrition (in %), calculated according to equation [15].

5 CONTRIBUTION TO FOREST NUTRITION

Base-cations such as Mg^{2+} , Ca^{2+} and K^+ are important nutrients for forest ecosystems (in contrast, uptake of Na^+ is usually assumed negligible). To fulfill their demands plants take up base-cations from the soil solution through their root system. The supply of base-cations to the soil solution takes place through atmospheric deposition and weathering. Atmospheric deposition may be a quantitatively important source of base-cations in forest soils where the mineral content and weathering rate of base-cations are small. Weathering (= alkalinity and base-cations release) rates of soils depend on the mineral composition of the soil substrate. Weathering will be relatively large in soils with a high H^+ concentration, a high soil moisture content, a high soil temperature and/or a high CO_2 -pressure. Weathering reactions are product inhibited, i.e. decreased by high concentrations of reaction products in the soil solution such as inorganic aluminum and base-cations.

Very crude estimates of weathering rates of Mg^{2+} and Ca^{2+} in the upper 0.5 m of European forest soils have been made on a $1.0^\circ \times 0.5^\circ$ lat./long. (approx. 60×60 km) grid by De Vries *et al.* (1993) using information on parent material and soil texture. Transfer functions between parent material and texture on the one hand and weathering rate on the other hand were based on the weathering model PROFILE (Sverdrup and Warfvinge, 1988). Major input to this model are reaction rate coefficients of minerals and rocks, derived from laboratory studies. Weathering rates thus assigned have been corrected for the effect of temperature using the scheme presented by Sverdrup (1990). Weathering rates of K^+ are not considered by De Vries *et al.* (1993) as they are usually considerably smaller than those of Mg^{2+} and Ca^{2+} . The percentage contribution of base-cation deposition to forest nutrition was calculated by:

$$100 * \{2Mg^{2+}_d + 2Ca^{2+}_d + K^+_d\} / \{2Mg^{2+}_d + 2Ca^{2+}_d + K^+_d + 2Mg^{2+}_w + 2Ca^{2+}_w\} \quad [15]$$

in which d denotes deposition to forests and w weathering in forest soils. Deposition was only calculated for grids cells where forests constitute more than 50% of the total surface area within the grid. Deposition and weathering rates in equation [15] need to be expressed in $mol\ ha^{-1}\ a^{-1}$. With respect to forest nutrition it does not matter in what form base-cations are deposited (e.g. as $CaSO_4$, $Ca(NO_3)_2$, $CaCO_3$ or $CaCl_2$). In soil all these substances are soluble so plant roots encounter ions (in this case Ca^{2+}). For this reason, deposition estimates in equation [15] are not corrected for the contribution of sea salt. By neglecting weathering of K^+ in equation [15], the contribution of base-cation deposition to forest nutrition will be slightly overestimated.

Weathering rates of base-cations in the upper 0.5m of European forest soils are presented in Figure 20. A clear increase in base-cation weathering from northern to southern Europe can be observed. Values below $1000\ eq\ ha^{-1}\ a^{-1}$ mainly occur in Scandinavia, Scotland, Poland, the Netherlands and northern Germany, i.e. areas with podzolic soil types (Sverdrup and Warfvinge, 1988; de Vries *et al.*, 1993). In nutrient-rich soils (e.g. calcareous soils), base-cation release by weathering will be much larger. This is reflected in relatively large weathering rates ($>1000\ eq\ ha^{-1}\ a^{-1}$) found in, for example, Hungary and northwestern Spain. In Scandinavia weathering is usually found the dominant supplier of base-cation to forest soils, but in eastern and southern Europe, forests mainly rely on atmospheric deposition for the supply of base-cations (Figure 21).

6 UNCERTAINTY ANALYSIS

The objective of an uncertainty analysis is to define confidence intervals for the model estimates and to identify the main shortcomings in the applied methods and procedures. In this study, uncertainty analysis comprise a comparison of model results with independent field data and an error propagation analysis.

6.1 Evaluation with independent field data

Throughfall and stemflow measurements have been found useful for the evaluation of deposition models (e.g. Draaijers, 1993; Draaijers and Erisman, 1993; Erisman *et al.*, 1994; Spranger *et al.*, 1994; Draaijers *et al.*, 1996), though a major limitation is that information to distinguish between in-canopy and atmospheric sources of chemical compounds often is lacking, thereby hampering accurate deposition estimation. Another problem when using throughfall and stemflow measurements for model validation is related to the spatial scale of the estimates. Throughfall and stemflow deposition estimates usually refer to a particular forest stand or a small part of it. Deposition estimates from throughfall measurements are to some extent uncertain themselves.

Results of throughfall, stemflow and bulk precipitation measurements were obtained from national organizations responsible for throughfall and stemflow monitoring in their countries (Table IV). In total, results from 174 throughfall measurement sites were obtained. The measurement sites are reasonably well distributed over Europe although sites in southern Europe are almost lacking. The majority of the sites (71%) is situated in coniferous forest stands; only 17% in deciduous forest stands and 12% in mixed forest stands. Monitoring took place between 1987 and 1994 for a period of at least one year. Data for 1989 were used but, if not available, the average for the whole measurement period was computed and used for model validation. At most sites stemflow was not measured as it generally contributes only a small fraction of the total flux to the forest floor (Ivens, 1990). In that case, the stemflow flux was computed as a percentage of the throughfall flux using a parametrisation on tree species and stand age described by Ivens (1990). Wet deposition was estimated from bulk precipitation measurements by applying bulk to wet-only correction factors presented by Van Leeuwen *et al.* (1995).

Table IV Per country the number of throughfall monitoring locations in coniferous, deciduous and mixed forest stands, respectively, used for model validation. Moreover the measurement period is presented.

Country	No. of sites			Measurement period
	Coniferous	Deciduous	Mixed	
Czech Republic ¹⁾²⁾	6			1990-1994
Denmark ²⁾		1		1992
Finland ²⁾			9	1989-1992
France ³⁾	18	8		1993
Germany ⁴⁾²⁾	63	12	2	1989
Hungary ²⁾	1			1990-1993
Netherlands ⁵⁾	22	2	4	1987-1991
Norway ²⁾	2			1990-1993
Poland ²⁾			1	1993-1994
Russian Federation ²⁾		2		1990-1993
Sweden ²⁾			4	1989-1993
Switzerland ⁶⁾	12	5		1987-1992

1) data provided by the Czech Geological Survey, Prague (T. Paces and J. Cerný)

2) data from the ICP-Integrated Monitoring Programme provided by the Finnish Environmental Agency, Helsinki (S. Kleemola and M. Forsius)

3) data provided by the Office National des Forêts, Fontainebleau (E. Ulrich)

4) data provided by the University of Stuttgart (Th. Gauger, R. Köble and G. Smiatek)

5) data available at the National Institute of Public Health and the Environment, Bilthoven (G. Draaijers and J.W. Erisman)

6) data provided by the Institut für Angewandte Pflanzenbiologie, Schönenbuch (S. Braun)

A canopy budget model developed by Ulrich (1983) was used to estimate the impact of canopy leaching on throughfall and stemflow fluxes of Mg^{2+} , Ca^{2+} and K^+ . An extensive description and uncertainty analysis of the model is presented by Draaijers and Erisman (1995). In the model, Na^+ is assumed not to be influenced by canopy exchange through which dry deposition of Na^+ can be calculated by subtracting wet deposition from the throughfall+stemflow flux. Particles containing Mg^{2+} , Ca^{2+} and K^+ are assumed to have the same mass median diameter as Na^+ containing particles. Dry deposition of Mg^{2+} , Ca^{2+} and K^+ can subsequently be calculated according to:

$$DD_x = (TF_{Na} + SF_{Na} - BP_{Na}) / BP_{Na} * BP_x \quad [16]$$

where DD, TF, SF, and BP represent dry deposition, throughfall, stemflow and bulk-precipitation flux, respectively and x denotes Mg^{2+} , Ca^{2+} or K^+ . In equation [16] $(TF_{Na} + SF_{Na} - BP_{Na}) / BP_{Na}$ represent the so-called 'dry deposition factor'. In this study annual mean throughfall, stemflow and bulk precipitation fluxes are used through which differences in dry deposition factor caused by seasonal changes in pollution climate and canopy characteristics are neglected. Additional error will arise by using bulk precipitation data instead of wet-only deposition. The assumption that Mg^{2+} , Ca^{2+} and K^+ containing particles are deposited with equal efficiency as Na^+ containing particles introduces an error as the particle size distribution of these constituents is not necessarily the same (Milford and Davidson, 1985).

Deposition estimates derived from throughfall and bulk precipitation measurements were compared to modeled deposition estimates for the 174 measurement sites. For this purpose, the model was run using precipitation concentrations measured at the site and stand-specific roughness lengths (z_0). The latter have been found dependent on tree height (h) and canopy closure (Jarvis *et al.*, 1976). The following relationship was derived taking the average tree height of mature forests in Europe equal to 20m and assuming their average z_0 approximates 1.2m:

$$z_0 = 0.06 * h \quad [17]$$

If site-information on tree height was not available, tree height was indirectly derived using species-specific relationships between tree height and tree age presented by Schober (1987). If tree age was unknown, tree height was taken equal to the average height of other forest stands situated in the region/country. The impact of canopy closure on the roughness length could not be taken into account due to lack of data.

Results of the comparison are presented in Figure 22. Although for all base-cations significant relationships ($p < 0.05$) are found between modeled and measured total deposition, usually a considerable scatter can be observed. In part, this will be the result of uncertainties associated with the estimation of total deposition using throughfall and bulk precipitation measurements in combination with the canopy budget model. If state-of-the-art measurement and analytical techniques are used in combination with a sufficiently large number of replicate throughfall samplers, the uncertainty in base-cation deposition estimated from the canopy budget model can be estimated to amount 40% (Draaijers *et al.*, 1996). It may be expected that in this study the uncertainty will be even larger. Modeled deposition fluxes of Ca^{2+} and K^+ are on average not significantly different from measured deposition fluxes (Table V). Significant differences found for Na^+ and Mg^{2+} are attributed to the fact that the estimates not always hold for the same year. No significant differences are found if only measurement data for 1989 are used for comparison. Deposition of Na^+ and Mg^{2+} strongly depends on the suspension of sea salt particles into the atmosphere which will experience a strong year-to-year variation (e.g. Draaijers, 1993). At higher deposition levels the model seems to underestimate total deposition of Ca^{2+} and K^+ . This may be attributed to the procedure used to estimate air concentrations and, in turn, dry deposition fluxes of base-cations (Figure 23). Dry deposition generally constitutes a large fraction of the total deposition at the measurement sites. Modeled air concentrations reflect the large scale 'background' situation (see section 3.2). If forests are located near local sources such as e.g. agricultural fields or unpaved roads, they will receive an additional input of Ca^{2+} and K^+ .

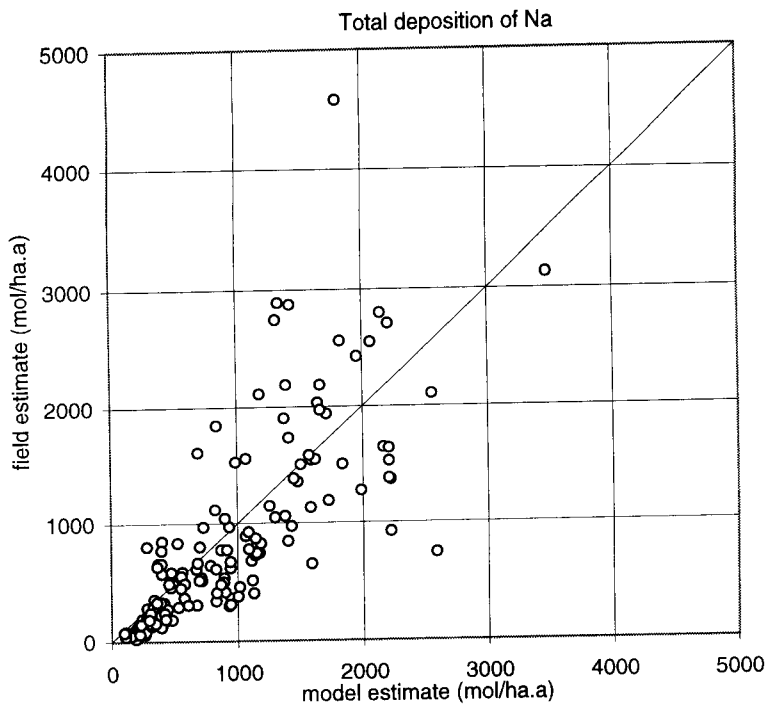


Figure 22a Relationship between modeled total deposition of Na^+ and total deposition of Na^+ estimated from throughfall and bulk precipitation measurements made at 174 sites scattered over Europe.

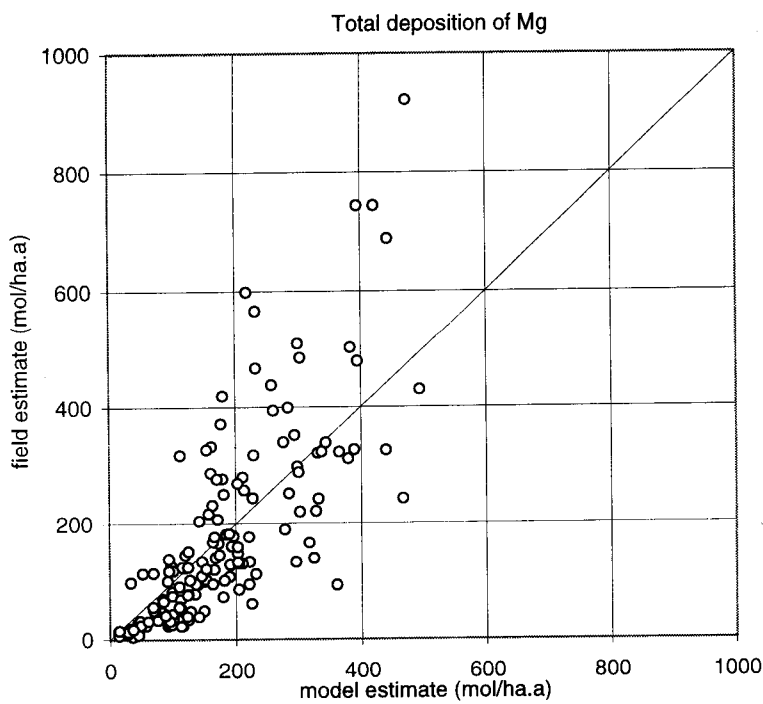


Figure 22b Relationship between modeled total deposition of Mg^{2+} and total deposition of Mg^{2+} estimated from throughfall and bulk precipitation measurements made at 174 sites scattered over Europe.

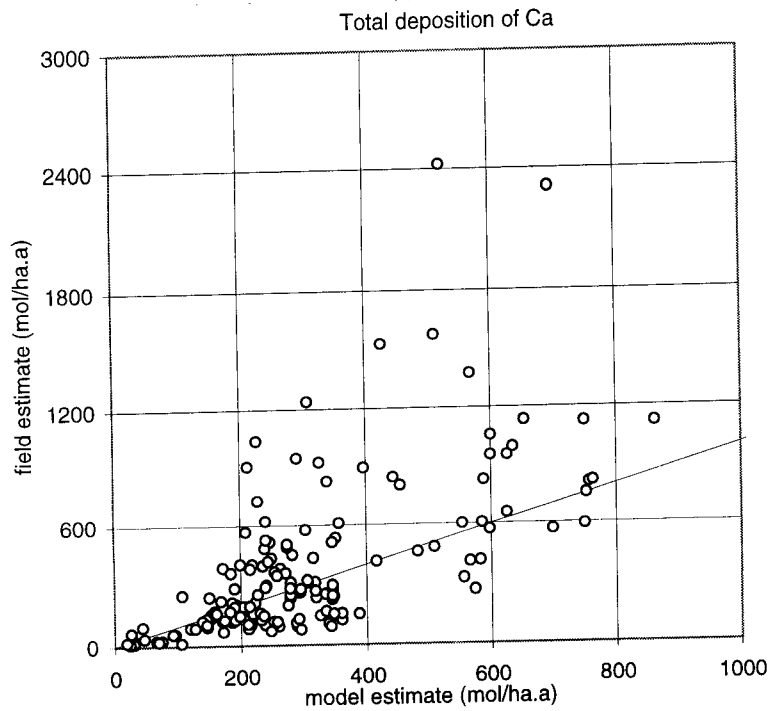


Figure 22c Relationship between modeled total deposition of Ca^{2+} and total deposition of Ca^{2+} estimated from throughfall and bulk precipitation measurements made at 174 sites scattered over Europe.

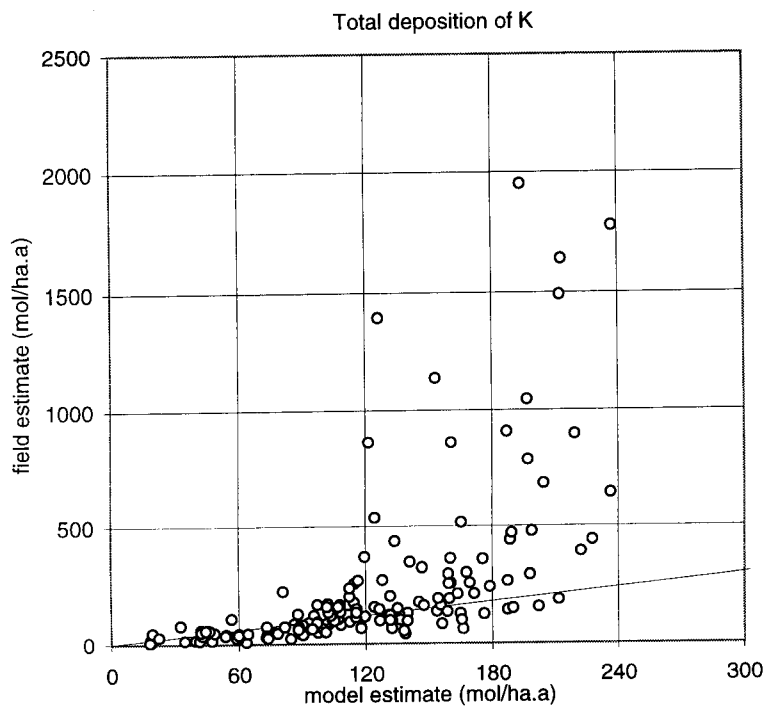


Figure 22d Relationship between modeled total deposition of K^+ and total deposition of K^+ estimated from throughfall and bulk precipitation measurements made at 174 sites scattered over Europe.

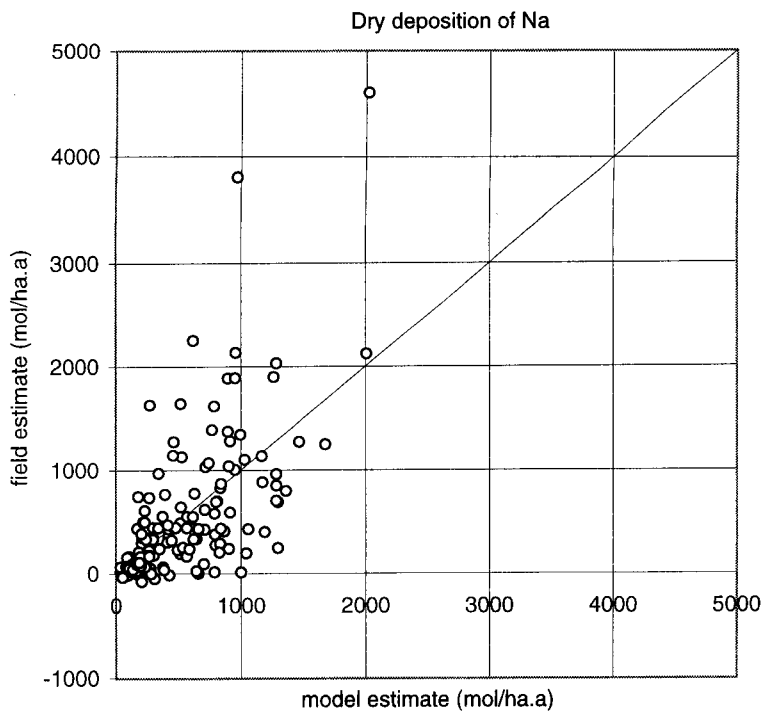


Figure 23a Relationship between modeled dry deposition of Na^+ and dry deposition of Na^+ estimated from throughfall and bulk precipitation measurements made at 174 sites scattered over Europe.

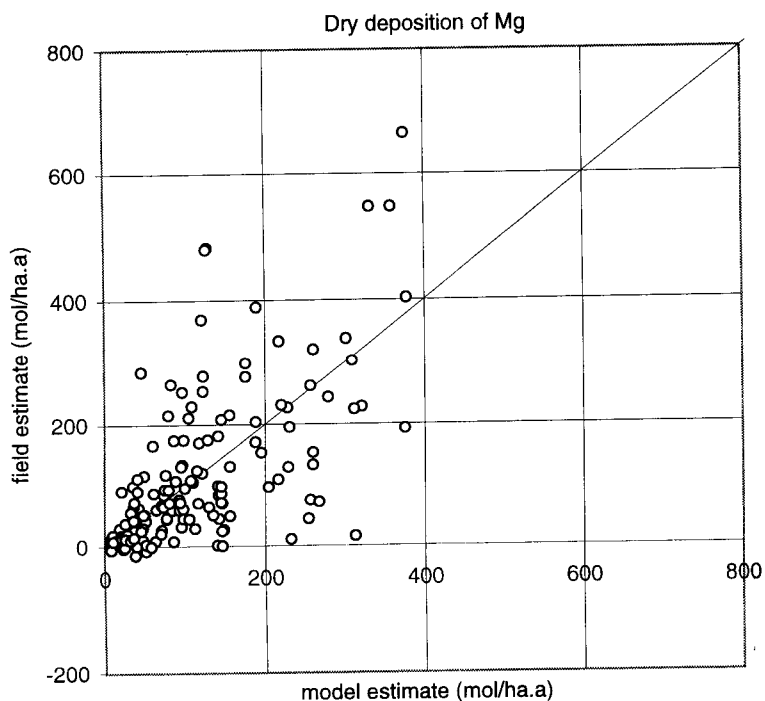


Figure 23b Relationship between modeled dry deposition of Mg^{2+} and dry deposition of Mg^{2+} estimated from throughfall and bulk precipitation measurements made at 174 sites scattered over Europe.

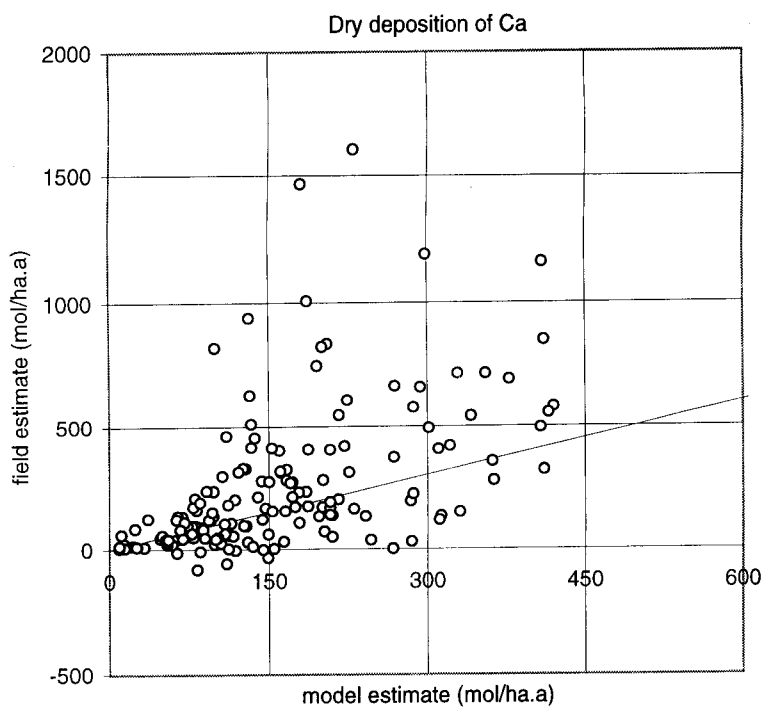


Figure 23c Relationship between modeled dry deposition of Ca^{2+} and dry deposition of Ca^{2+} estimated from throughfall and bulk precipitation measurements made at 174 sites scattered over Europe.

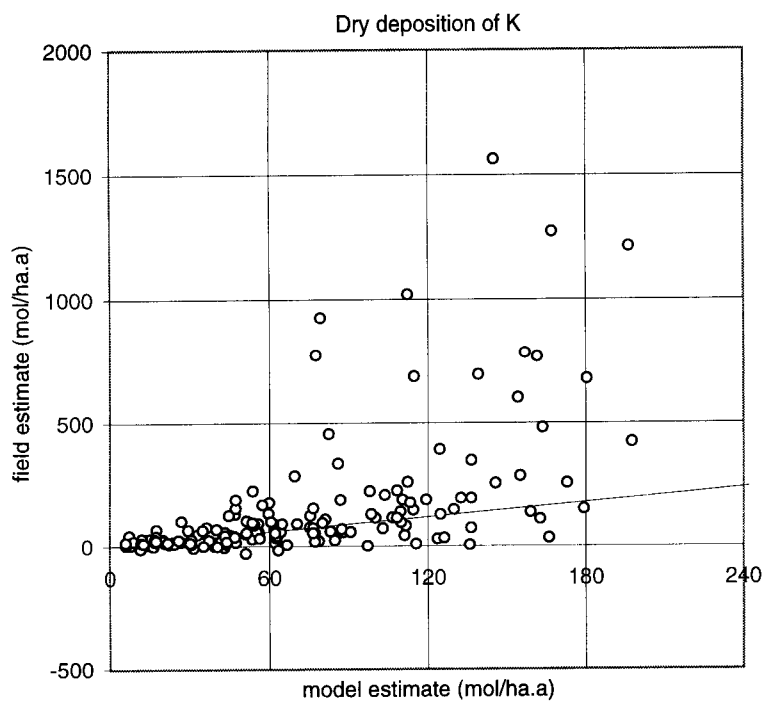


Figure 23d Relationship between modeled dry deposition of K^+ and dry deposition of K^+ estimated from throughfall and bulk precipitation measurements made at 174 sites scattered over Europe.

Table V Pearson correlation coefficients of linear regression equations between modeled and measured deposition, respectively. Moreover, results are presented of a ‘paired two sample for means’ t-test whether both estimates are equal on the average or not. * = both estimates are equal (p<0.05; n=174); n.s. = both estimates differ significantly.

		Na ⁺	Mg ²⁺	Ca ²⁺	K ⁺
<i>Total deposition</i>					
all sites	r	0.62	0.68	0.65	0.59
	t-test	n.s.	n.s.	*	*
‘1989’ sites	r	0.84	0.81	0.61	0.41
	t-test	*	*	*	*
<i>Dry deposition</i>					
all sites	r	0.53	0.55	0.53	0.57
	t-test	n.s.	n.s.	*	*
‘1989’ sites	r	0.64	0.69	0.45	0.36
	t-test	*	*	*	*

6.2 Error propagation

Uncertainties in the deposition estimates are the result of random and systematic errors. Random errors are the result of a certain variability in measured quantities and parameters due to e.g. measuring errors, correcting procedures or parametrizations. Random errors in the deposition estimates will be a function of averaging time and spatial scale. Systematic errors result from neglecting processes or variables for which knowledge is insufficient and will only partly be reduced as a result of averaging in time and space. Whereas random errors lead to variability around an average value, systematic errors may result in serious bias in the deposition estimates. The difference between random and systematic errors is not always very clear. Certain assumptions can lead to both types of errors (Erismann, 1992).

The overall uncertainty in deposition estimates can be determined by using error propagation techniques. The most difficult part when applying such a method is the definition of the uncertainty ranges in the basic measurements or theoretically derived parameters. Lack of reference or validation measurements often necessitates assumptions on uncertainty ranges. Furthermore, poor understanding of physical, chemical and biological processes related to atmospheric deposition often introduces extra uncertainty. For the determination of the overall uncertainty (U_0), the absolute (random or systematic) uncertainties for individual variables (e.g. U_a and U_b) need to be squared and added. The square root of the result is the overall uncertainty. This is only valid if no correlation between the variables exists. If variables show a significant correlation an extra term need to be added, namely $2*r*U_a*U_b$, where r is the correlation coefficient between the variables:

$$U_0 = (U_a^2 + U_b^2 + 2*r*U_a*U_b)^{0.5} \quad [18]$$

This procedure holds when the variables are added or subtracted. When variables are multiplied or divided essentially the same procedure is followed, however, relative rather than absolute uncertainties are considered (Erismann, 1992; Janssen *et al.*, 1990). For many cases the correlation coefficient is unknown.

Therefore, two cases are considered, first a propagation of errors without correlation (conservative case), and second, a propagation with full positive correlation (worst case). In the following sections the random and systematic errors in the basic parameters of both wet and dry deposition are discussed. Then the propagation of errors and the associated uncertainty in the wet, dry and total deposition is described. The uncertainty in acid neutralization capacity and contribution to forest nutrition is assessed as well. Results of the error propagation are summarized in Table VI. Numbers are presented as percentages ($x\%$) reflecting the relative deviation from the estimated value for an average grid cell in Europe in terms of one standard deviation, implying that the probability that the real value is the estimated value $\pm x\%$ is 68%. Uncertainty estimates are in many cases uncertain themselves and for this reason they have been rounded to the nearest number of five. Average values in Europe for the different variables, necessary for the error propagation calculations, are presented in Appendix 5.

6.2.1 Wet deposition

Random errors

Random errors in wet deposition are determined by the uncertainty in precipitation concentrations and precipitation amounts. The random uncertainty in precipitation concentrations will mainly be the result of measurement and interpolation errors. In Europe, two regions can be distinguished, i.e. *i*) west, northwest and central Europe where data is assumed to be of good quality and sufficient measurement sites are available, and *ii*) east, southeast and southwest Europe where data quality can be questioned and only few measurement sites are present. The total uncertainty in average precipitation concentration per grid cell is estimated 30-50% (Van Leeuwen *et al.* 1995). The uncertainty in precipitation amounts will mainly be the result of using long-term means instead of actual rainfall amounts, and equals 40-50% (Van Leeuwen *et al.*, 1995). Using error propagation the uncertainty in the wet deposition flux for an average 50x50 km grid cell in Europe due to random errors in precipitation concentrations and amounts can now be estimated to equal 50-70% in the conservative case and 70-100% in the worst case. The upper-limit values are representative for east, southeast and southwest Europe.

Systematic errors

Non-representativity of the measurement sites may lead to systematic errors in wet deposition. By neglecting the process of seeder-feeder scavenging, precipitation concentrations will be systematically underestimated in upland areas, occurring in e.g. the United Kingdom and Norway. Seeder-feeder scavenging results from the incorporation of particles into orographic clouds above hills and the scavenging of the hill cloud droplets by rain droplets falling from a higher level cloud. Dore *et al.* (1992) found an increase in precipitation concentrations of 40-75% over high ground in the United Kingdom. These areas generally represent only a small fraction of the total land area within a 50x50 km grid cell through which the underestimation of precipitation concentrations probably will be in the order of 30% at most. In high-elevation areas, i.e. areas above ~2000m a.s.l., concentrations in precipitation and snow have been found smaller compared to those at lower altitudes (e.g. Puxbaum and Kovar, 1991). Usually no measurement sites are situated in these areas due to large maintenance costs and logistic difficulties, leading to a potential overestimation of precipitation

concentrations of ~20% (Van Leeuwen *et al.*, 1995). Systematic errors in precipitation concentrations may also arise from measurements made too close to local pollutant sources and from using constant bulk to wet-only conversion factors. On a 50x50 km scale these errors are expected to be smaller than 20%. Precipitation amounts may have been underestimated in mountainous areas and in northern Europe due to inefficient capture of snow by rainfall collectors. According to Kovar *et al.* (1991), this undercatch can be as large as 30%, depending on, among others, wind speed. A systematic error in precipitation amounts may also arise from missing local shower patterns which especially will be notable in mountainous areas. It is expected, however, that on a 50x50 km scale this error is relatively small, i.e. <20%. The uncertainty in the wet deposition flux per 50x50 km grid cell due to systematic errors in precipitation concentrations and amounts can be estimated using error propagation to equal 30-40% in the conservative case and 40-60% in the worst case. The upper-limit values hold for mountainous and upland areas.

6.2.2 Dry deposition

Random errors

Random errors in dry deposition are determined by the uncertainty in dry deposition velocities and ambient air concentrations and in the parameters determining them. The uncertainty in dry deposition velocities (V_d) will be due to uncertainties in V_{da} , V_{ds} and V_s . The uncertainty in V_{da} is determined by the uncertainty in wind speed (u) and friction velocity (u_*). The random error in u as obtained from the ODS dataset is assumed equal to 10%. The wind field at 50m height can be estimated relatively accurately in situations where the assumption of the constant flux layer is valid, i.e. under near neutral conditions. In times of non-neutrality, stability corrections have been made. Especially when these corrections are large, the extrapolated wind field will be very uncertain. Largest errors will be made at night when ground temperature inversions occur. In these situations, however, fluxes will be low. These uncertainties can be considered systematic. However, because the uncertainty in the final results due to these uncertainties will be a function of averaging time intervals, these are processed as random errors. They will, however, not decrease due to spatial averaging (Erisman, 1992). The uncertainty in u at 50m height due to the uncertainty in the stability corrections is assumed equal to 100% (Erisman, 1992). Besides the uncertainty in u and stability correction, the random error in u_* depends on the uncertainty in roughness length (z_0). The latter is hard to quantify but will depend on the quality of the land use map used to derive them (Van de Velde *et al.*, 1994), on the uncertainty in the classification scheme of Wieringa (1992), and on the uncertainty in the roughness length concept itself. Here, it is assumed that the uncertainty in z_0 for an average grid cell in Europe is smaller than 50%. Locally, however, the uncertainty probably will be larger than 100%. The overall uncertainty in u_* can now be estimated to equal 20% in near-neutral conditions and 50% in very stable or unstable conditions. When averaging the stability classes throughout one year, the average uncertainty in u_* would be somewhere in between 20 and 50%. This value is assumed to be 30%. This lead to a random error in V_{da} of about 70%. The uncertainty in V_{ds} is determined in the uncertainty in u_* , wind speed at canopy height (u_h) and collecting efficiency (E). The uncertainty in E depends on the uncertainty in u_* and relative humidity (rh). Assuming the uncertainty in rh as obtained from the ODS dataset equals 10%, the random error in E can be calculated to

approximate 5% for dry surfaces and 20% for wet surfaces. Taking an uncertainty of 50% for u_h , the random error in V_{ds} can be estimated to amount 70%. The random error in V_s depends on the uncertainty in rh and equals 15%. Using error propagation the random uncertainty in V_d for an average grid cell of $1/6^\circ \times 1/6^\circ$ lat./long. in Europe can now be estimated to approximate 30%.

The random error in ambient air concentrations ($[C]_{air}$) is determined by the random error in precipitation concentrations ($[C]_{rain}$) and mass median diameters (MMD). The random error in $[C]_{rain}$ for an average grid cell in Europe was estimated 30-50% (see section 5.2.1). Largest uncertainty was found in areas with low measurement density leading to relatively large interpolation errors (i.e. southern and eastern Europe). The random error in MMD, calculated from the uncertainty in $[C]_{rain}$ using the equations presented in Table II, is smaller than 10%. The random error in $[C]_{air}$ can be estimated to approximate 35-60%. Using error propagation the uncertainty in the dry deposition flux per $1/6^\circ \times 1/6^\circ$ grid cell due to random errors in V_d and $[C]_{air}$ can now be estimated to amount 45-65% in the conservative case and 65-90% in the worst case. The upper-limit values can be considered representative for east, southeast and southwest Europe.

Systematic errors

Systematic errors in dry deposition velocities, ambient air concentrations and, in turn, dry deposition fluxes, are much harder to quantify than random errors. The model on which the parametrisation of the dry deposition velocity was based, was validated using micro-meteorological and surface wash measurement results from the Speulder forest in the Netherlands (Ruijgrok *et al.*, 1994). No significant differences were found between the mean values of modeled and measured deposition velocities. However, the model still needs to be validated for other surfaces and climates to ensure applicability everywhere in Europe. The uncertainty in grid average dry deposition velocities will mainly be determined by uncertainties associated with the determination of the roughness length (z_0), wind speed at canopy height (u_h), collecting efficiency (E), with the variation in size distribution of alkaline particles over Europe and with complex terrain effects. Uncertainty in z_0 is introduced by assuming a constant tree height over Europe and not taken into account the impact of wind penetration in terms of canopy closure or openness. Tree height is also important for accurate determination of u_h . The parametrisation of E may not automatically be considered representative for other surface types. Assuming an average mass median diameter (MMD) of 5 μm and taking a geometric standard deviation (σ_g) of 2 μm to represent the variation, the uncertainty in dry deposition velocity caused by variation in size distribution can be calculated to amount 30% (Ruijgrok *et al.*, 1994). The mean MMD of particles will depend on the distance to sources and on e.g. ambient relative humidity (Fitzgerald, 1975), and thus will show spatial variation over Europe.

To model dry deposition velocities adequately, deposition surfaces should have horizontal lengths about 100 times the reference height (Pasquill, 1972). The typical horizontal length scale of surfaces, using 50 m as the reference height, thus amounts 5 km. On this scale, however, usually considerable variation in land use is present. An area consisting of both rough and smooth terrain patches will have a higher overall roughness than the average of all patches (Wieringa, 1992). By determining turbulent exchange parameters at a height of 50 m above the receptor surface, it was assumed that the impact of enhanced turbulent exchange induced by local roughness transitions is sufficiently taken into account in the dry deposition

velocity estimates. Evaluation of modeled with measured fluxes showed that this assumption is justified (Erisman, 1992). The effects of advection, however, are not completely taken into account and may be substantial for forest edges. By neglecting advection, dry deposition velocities of coarse aerosols to forests in the Netherlands were found systematically underestimated by 20-25% (Draaijers *et al.*, 1994). For an average grid cell in Europe the effect of complex terrain on dry deposition velocities will be smaller than 20% because within a grid usually other land use categories will be present as well. The impact of topography is not taken into account in the parametrisation of the dry deposition velocity. The resulting uncertainty in grid average dry deposition velocity is hard to quantify due to lack of reference measurements in mountainous regions, but is expected to be smaller than 20%. The overall uncertainty in grid average dry deposition velocity caused by above mentioned uncertainties is assumed equal to 40-60%. Upper-limit values are assumed representative for areas close to sources, 'background' areas, and areas with high or low average ambient relative humidity.

The systematic error in ambient air concentrations ($[C]_{\text{air}}$) is determined by the systematic error in $[C]_{\text{rain}}$ and MMD. The systematic error in precipitation concentration for an average grid cell in Europe is estimated 20-30% (see section 5.2.1). The systematic error in MMD, calculated from the uncertainty in $[C]_{\text{rain}}$ using equations given in Table II, equals about 5%. The systematic error in $[C]_{\text{air}}$ can now be estimated to amount 30-45%. $[C]_{\text{air}}$ will be underestimated near local sources. In the scavenging model the impact of particle solubility, precipitation amount, precipitation rate, droplet accretion process and storm type is not taken into account. Relatively large errors in $[C]_{\text{air}}$ due to uncertainties in the scavenging model may arise in areas very close or far away from major sources, areas where sufficient mixing has not occurred and/or areas with a strongly deviating precipitation climatology. Using error propagation, the uncertainty in the dry deposition flux in a $1/6^\circ \times 1/6^\circ$ grid cell due to systematic errors in V_d and $[C]_{\text{air}}$ can be estimated to amount 50-75% in the conservative case and 70-105% in the worst case. Largest uncertainty in dry deposition estimates will be found in mountainous and upland areas, areas close to sources, 'background' areas, and areas with extremely high or low average ambient relative humidity.

Additional systematic errors in dry deposition may arise from using annual mean air concentrations and deposition velocities for flux calculation, thereby neglecting temporal correlations. Correlations may be present on a daily and seasonal time scale. The error introduced by ignoring daily correlations between concentrations and deposition velocities probably will be smaller than 20% (Van Pul and Jacobs, 1993). An indication of the error due to ignoring seasonal correlations can be obtained by calculating annual mean dry deposition fluxes using monthly mean air concentrations and dry deposition velocities (Figure 12). Averaged for the whole of Europe annual mean dry deposition of Na^+ , Mg^{2+} , Ca^{2+} and K^+ was found 2.1% larger and 0.3%, 3.2% and 2.9% lower, respectively, in comparison to dry deposition fluxes calculated using annual mean concentrations and deposition velocities.

6.2.3 Total deposition

The uncertainty in total deposition of base-cations is determined by the uncertainty in wet and dry deposition. Assuming dry deposition makes up on average 40% of the total deposition of base-cations in Europe (Appendix 5), the random error in total deposition can be calculated using error propagation to amount 35-50% in the conservative case and 50-70% in the worst case. The upper-limit values hold for east, southeast and southwest Europe. Wet and dry deposition contribute to approximately the same extent to the random error in total deposition. Systematic errors are found somewhat smaller in comparison to random errors, i.e. 25-40% in the conservative case and 40-55% in the worst case. Relatively large uncertainty in total deposition will be found in mountainous and upland areas, areas close to sources, 'background' areas, and areas with extremely high or low average ambient relative humidity. Additional errors in mountainous areas may arise due to ignoring the contribution of fog and cloud water deposition to the total deposition. The systematic uncertainty in total deposition is dominated by the systematic uncertainty in dry deposition. For both random and systematic errors, worst case estimates are more realistic as a high positive correlation may be expected between errors in wet and dry deposition.

For the total deposition of non-sea salt $Mg^{2+}+Ca^{2+}+K^+$ the random error equals 25-35% in the conservative case and 35-50% in the worst case. The systematic error in total deposition of non-sea salt $Mg^{2+}+Ca^{2+}+K^+$ amounts 20-30% in the conservative case and 25-40% in the worst case. Worst case estimates probably reflect reality better because a high correlation is expected between errors in total deposition of non-sea salt Mg^{2+} , non-sea salt Ca^{2+} and non-sea salt K^+ , respectively. In Table VI random and systematic errors are presented for the dry deposition of non-sea salt $Mg^{2+}+Ca^{2+}+K^+$ expressed as percentage of the total deposition of non-sea salt $Mg^{2+}+Ca^{2+}+K^+$ (Figure 15), and for the total deposition of non-sea salt Mg^{2+} , non-sea salt Ca^{2+} and non-sea salt K^+ expressed as percentage of the total deposition of non-sea salt $Mg^{2+}+Ca^{2+}+K^+$ (Figure 16).

6.2.4 Acid neutralization capacity

The random error in the percentage neutralization of acid in precipitation by base-cations can be calculated using error propagation to amount 30-45%. The upper-limit hold for east, southeast and southwest Europe whereas the lower-limit is probably more representative for other parts of Europe. Systematic errors are somewhat smaller, i.e. 20-25%. The upper-limit can be assumed representative for mountainous and upland areas and the lower limit for other areas in Europe.

Up to now, no detailed error analysis has been made for the total potential acid deposition as calculated with the EDACS model. Erisman (1992) estimated a random error of 40% and a systematic error of 45% for the total potential acid deposition calculated with the DEADM model. These values hold for an average grid cell of 5x5 km in the Netherlands. In EDACS a similar calculation scheme is followed as in DEADM but, instead on a 5x5 km scale, deposition is calculated on a 10x20 km scale. For this reason, it may be expected that the errors in EDACS are somewhat smaller than those in DEADM. On the other hand, input data used for EDACS are generally less reliable than the input data used for DEADM. Assuming DEADM error estimates being representative for EDACS, the random error in the percentage neutralization of potential acid by deposition of base-cations can be calculated to amount 45-55% in the

conservative case, and 65-75% in the worst case. The systematic error amounts 50-55% in the conservative case, and 65-75% in the worst case.

6.2.5 Contribution to forest nutrition

A comparison between modeled weathering rates and values estimated for individual countries has indicated that the overall (random) uncertainty in the weathering rate is generally less than 50% (De Vries, 1994). This percentage hold for an average grid cell of 60x60 km in Europe. For specific sites the deviation between modeled and actual weathering rates can be larger than 100%. The weathering rate will be systematically underestimated because weathering of K^+ has not been taken into account. For several non-calcareous acid sandy forest soils in the Netherlands, weathering of K^+ amounted, on average, ~20% of the weathering rate of $Mg^{2+}+Ca^{2+}$ (De Vries, 1994). The precipitation amount was considered irrelevant for the weathering rate which might have led to an underestimate in areas with a large precipitation excess (De Vries, 1994). The random uncertainty in the contribution of atmospheric deposition of base-cations to forest nutrition can now be calculated to amount 35-45% in the conservative case, and 50-65% in the worst case. The systematic error amounts 25-35% in the conservative case, and 35-50% in the worst case.

Table VI Overview of random and systematic errors for an average grid in Europe for different variables estimated in this study (in %). Percentages are rounded to the nearest number of five.

Variable	Grid size	Figure	Random error		System. error	
			<i>conserv. case</i>	<i>worst case</i>	<i>conserv. case</i>	<i>worst case</i>
precipitation concentration	50x50km	3	30-50 ¹⁾		20-30 ²⁾	
precipitation amount	0.5°x0.5°	4	40-50 ¹⁾		20-30 ²⁾	
wet deposition	50x50km	5	50-70 ¹⁾	70-100 ¹⁾	30-40 ²⁾	40-60 ²⁾
dry deposition velocity	1/6°x1/6°	6	30		40-60 ³⁾	
ambient air concentration	50x50km	8	35-60 ¹⁾		30-45 ²⁾	
dry deposition	1/6°x1/6°	9	45-65 ¹⁾	65-90 ¹⁾	50-75 ⁴⁾	70-105 ⁴⁾
total deposition	1/6°x1/6°	13	35-50 ¹⁾	50-70 ¹⁾	25-40 ⁴⁾	40-55 ⁴⁾
total deposition nss $Mg^{2+}+Ca^{2+}+K^+$	1/6°x1/6°	14	25-35 ¹⁾	35-50 ¹⁾	20-30 ⁴⁾	25-40 ⁴⁾
% dry deposition of total deposition	1/6°x1/6°	15	40-55 ¹⁾	55-80 ¹⁾	40-60 ⁴⁾	55-80 ⁴⁾
% individual bc to total deposition	1/6°x1/6°	16	45-60 ¹⁾	60-85 ¹⁾	30-50 ⁴⁾	45-70 ⁴⁾
% acid neutralization in precipitation	50x50km	17	30-45 ¹⁾	45-65 ¹⁾	20-25 ²⁾	25-35 ²⁾
total deposition of potential acid	1/6°x1/6°	18	40 ⁵⁾		45 ⁵⁾	
% neutralization potential acid	1/6°x1/6°	19	45-55 ¹⁾	65-75 ¹⁾	50-55 ⁴⁾	65-75 ⁴⁾
weathering rate	1.0°x0.5°	20	50		20	
% contribution to forest nutrition	1/6°x1/6°	21	35-45 ¹⁾	50-65 ¹⁾	25-35 ⁴⁾	35-50 ⁴⁾

¹⁾ upper-limit values hold for east, southeast and southwest Europe.

²⁾ upper-limit values hold for mountainous and upland areas.

³⁾ relatively large uncertainty is found in areas close to sources, 'background' areas, and areas with extremely high or low average ambient relative humidity.

⁴⁾ relatively large uncertainty is found in mountainous and upland areas, areas close to sources, 'background' areas, and areas with extremely high or low average ambient relative humidity.

⁵⁾ assumed equal to the error in total potential acid deposition calculated with the DEADM model (Erisman, 1992).

7 CONCLUSIONS

Atmospheric deposition of base-cations in Europe is mapped on a $1/6^\circ \times 1/6^\circ$ (ca 10x20 km) grid using the inferential modeling technique. Deposition fields are found to resemble the geographic variability of sources, climate and land use. For Na^+ and Mg^{2+} , a clear pattern of increasing deposition with decreasing distance to seas, in particular the Atlantic Ocean, is observed, reflecting their sea-salt origin. Large Na^+ deposition is also found e.g. northwest of the Black Sea, probably originating from wind erosion of salt containing soils. Large Mg^{2+} , Ca^{2+} and K^+ deposition in southern and south-eastern Europe results from a combination of wind erosion of calcareous and salt-containing soils, agricultural tillage practices, traffic on unpaved roads, and supply of Saharan dust. In this part of Europe, the prevalence of warm and dry conditions in the summer period enhances the suspension of alkaline particles in the atmosphere. Relatively large Ca^{2+} deposition found in the border area between Germany, Poland and the Czech Republic, as well as in e.g. Lithuania and Latvia, can be attributed to intensive industrial activity. In Europe, dry deposition constitutes on average 45% of the total deposition of non-sea salt $\text{Mg}^{2+} + \text{Ca}^{2+} + \text{K}^+$. Mg^{2+} , Ca^{2+} and K^+ contribute on average 21, 66 and 13%, respectively to the total deposition of non-sea salt $\text{Mg}^{2+} + \text{Ca}^{2+} + \text{K}^+$ in Europe.

In large parts of southern Europe, more than 50% of the potential acid deposition is found counteracted by deposition of non-sea salt $\text{Mg}^{2+} + \text{Ca}^{2+} + \text{K}^+$. In central and northwestern Europe base-cation deposition usually amounts less than 25% of the acid input. Smallest base-cation deposition relative to potential acid deposition is found in southern Scandinavia, Denmark, northern Germany and the Netherlands. A similar spatial pattern is found for the neutralization of acid anions in precipitation. Whereas in Scandinavia weathering is found the dominant supplier of base-cation to forest soils, in eastern and southern Europe forests mainly rely on atmospheric deposition for the supply of base-cations.

Modeled deposition estimates compare well with deposition estimates derived from throughfall and bulk-precipitation measurements made at 174 sites scattered over Europe, taking into account the relatively large uncertainty in both estimates. On average no significant differences are found, but the model is found to underestimate dry deposition of base-cations on forests near local sources. An extensive uncertainty analysis to assess the quality of the base-cation deposition maps revealed that for an average grid cell in Europe the random and systematic error in total deposition equals 35-50% and 25-40%, respectively. Wet and dry deposition are found to contribute to approximately the same extent to the random error in total deposition. The systematic error in total deposition is dominated by the systematic error in dry deposition. The latter depends on the systematic uncertainty in dry deposition velocity and air concentration. The parametrisation of the dry deposition velocity is based on a model only tested with results of micrometeorological measurements over forest in the Netherlands. Validation for other surfaces and climates is necessary to ensure its applicability for the whole of Europe. The parametrisation can be improved by taking into account the impact of size distribution. Relatively large uncertainty in dry deposition is introduced by using precipitation concentrations and a relatively simple scavenging model to estimate air concentrations of base-cations. The scavenging model can be improved by incorporating the effect of relative humidity on particle size and, in turn, scavenging efficiency, following findings of Fitzgerald (1975). The

impact of precipitation intensity on scavenging efficiency can be parametrised based on work of Jaffrezo and Colin (1990).

The uncertainty in deposition estimates will be reduced considerably if information on the temporal and spatial variability of base-cation air concentration and/or emission becomes available through which air concentrations can be modeled more accurately. Emission-related deposition estimates will provide the opportunity of predicting the loads to be expected in association with specific economic scenarios. With current knowledge it is not feasible to make an accurate, European-wide, inventory of base-cation emissions of natural sources. An inventory of base-cation emissions of anthropogenic sources can be set up more easily (TFM, 1996). Subtraction of 'anthropogenic' base-cation deposition from 'total' base-cation deposition as estimated in this study then gives information on the 'natural' deposition of base-cations. Ideally, the latter should be used in the critical load framework since the aim of the Convention on Long-Range Transboundary Air Pollution is to minimize acid deposition irrespective of other man-made emissions (TFM, 1996).

In this report, results for 1989 are presented. It may be expected that, due to emission reductions in particularly eastern Europe, deposition of base-cations will have been lower in more recent years. Deposition in the years 1986-1988 and 1990-1994 will be estimated within the framework of the EU project 'Assessment of critical load/level exceedance and meteorological stress parameters at ICP-forests level I sites and derivation of preliminary relationships with forest vitality' (RIVM project number 7221.). Results of this project will be published medio 1997. An uncertainty analysis using Monte Carlo sampling and simulation is foreseen. Probability ranges can be attached to model parameters and input values using e.g. the RIVM software package UNCSAM (Janssen et al., 1992; Heuberger and Janssen (1994). To reduce computing time and costs, the Monte Carlo analysis can be limited to some representative grid cells in Europe.

Acknowledgments

The authors would like to express their gratitude to Till Spranger (UBA, Germany), Wim de Vries (SC-DLO) and Frank de Leeuw, Hans van Jaarsveld and Addo van Pul (RIVM-LLO) for making valuable comments on a draft version of this report, and Gert-Jan Reinds (SC-DLO) for providing data on weathering rate in forest soils in Europe. Charlos Potma (RIVM-LLO) is acknowledged for his advise concerning data processing and Arnold Dekkers en Ferd Sauter (RIVM-CWM) for mathematical support concerning constrained non-linear optimization of multivariate functions.

References

- Andronova, A.V., Gomes, L., Smirnov, V.V., Ivanov, A.V. and Shukurova, L.M. (1993), Physico-chemical characteristics of dust aerosols deposited during the Soviet-American experiment (Tadzhikistan, 1989), *Atmospheric Environment*, 27A, 2487-2493.
- Antilla, P. (1990), Characteristics of alkaline emissions, atmospheric aerosols and deposition. In: P. Kauppi, P. Antilla and K. Kenttämies (eds.), *Acidification in Finland*. Springer Verlag, Berlin, Germany.
- Asman, W.A.H., Slanina, J. and Baard, J.H. (1981), Meteorological interpretation of the chemical composition of rain water at one measurement site, *Water, Air and Soil Pollution*, 16, 159-175.
- Barrie, L.A. (1985), Scavenging ratios, wet deposition, and in-cloud oxidation: an application to the oxides of sulphur and nitrogen, *Journal of Geophysical Research*, 90, 5789-5799.
- Barrie, L.A. (1992), Scavenging ratios: black magic or a useful scientific tool. In: S.E. Schwarz and W.G.N. Slinn (eds.), *Precipitation scavenging and atmosphere-surface exchange*, Hemisphere, New York, 403-420.
- Beljaars, A.C.M. and Holtslag, A.A.M. (1990), Description of a software library for the calculation of surface fluxes. *Environmental Software*, 5, 60-68.
- Bernard, W.R., Stensland, G.J. and Gatz, D.F. (1987), Unpaved roads as a source of alkaline materials to the atmosphere. In: R. Perry, R.M. Harrison, J.N.B. Bell and J.N. Lester (eds.), *Acid rain: scientific and technical advances. Proceedings of the International Acid Rain Conference, 1-3 September 1987, Lisbon, Portugal*, 19-24.
- Bernard, W.R., Stensland, G.J. and Gatz, D.F. (1987), Alkaline materials flux from unpaved roads: source strength, chemistry and potential for acid rain neutralization, *Water, Air and Soil Pollution*, 30, 285-293.
- Bredemeier, M. (1988), forest canopy transformation of atmospheric deposition. *Water, Air and Soil Pollution*, 40, 121-138.
- Buat Menard, P. and Duce, R.A. (1986), Precipitation scavenging of aerosol particles over remote marine regions, *Nature*, 321, 508-510.
- Buishand, T.A. and Van Montfoort, M.A.J. (1989), Changes in the chemical composition of atmospheric precipitation in the Netherlands during the period 1978-1987, Technical note no 89-02, Wageningen Agricultural University, The Netherlands.
- Cawse, P.A. (1974), A survey of atmospheric trace elements in the U.K., 1972-1973, HSMO report AERE-R7669, London.
- Clarke, A.G. and Lambert, D.R. (1987), Local factors affecting the chemistry of precipitation. In: R. Perry, R.M. Harrison, J.N.B. Bell and J.N. Lester (eds.), *Acid rain: scientific and technical advances. Proceedings of the International Acid Rain Conference, 1-3 September 1987, Lisbon, Portugal*.
- Dekkers, A.L.M. and Sauter, F.J. (1996), Een chemisch evenwichtsprobleem opgelost met niet-lineaire regressie. RIVM-CIM memo M201/96, Bilthoven, The Netherlands.
- Derrick, M.R., Moyers, J.L., Yarborough, K.A. and Warren, M. (1984), Aerosol and precipitation chemistry relationships at Big Bend National Park, *Water, Air and Soil Pollution*, 21, 171-181.

- De Vries, W., Posch, M., Reinds, G.J. and Kämäri, J. (1993), Critical loads and their exceedance on forest soils in Europe. SC-DLO report no. 58 (revised version), Wageningen, The Netherlands
- De Vries, W. (1994), Soil response to acid deposition at different regional scales. *Ph.D. thesis*, University of Wageningen, The Netherlands.
- Dore, A.J., Choularton, T.W. and Fowler, D. (1992), An improved wet deposition map of the United Kingdom incorporating the seeder-feeder effect over mountainous terrain. *Atmospheric Environment*, 26A, 1375-1381.
- Downing, R.J., Hettelingh, J.P. and De Smet, P.A.M. (1993), Calculation and mapping of critical loads in Europe. Status report 1993 Coordination Center for Effects, RIVM Report no. 259101003, Bilthoven, The Netherlands.
- Draaijers, G.P.J. (1993), The variability of atmospheric deposition to forests, *Ph.D. thesis*, University of Utrecht, The Netherlands.
- Draaijers, G.P.J. and Erisman, J.W. (1993), Atmospheric sulphur deposition onto forest stands: throughfall estimates compared to estimates from inference. *Atmospheric Environment*, 27A, 43-55.
- Draaijers, G.P.J., R. Van Ek and W. Bleuten (1994), Atmospheric deposition in complex forest landscapes. *Boundary-Layer Meteorology*, 69, 343-366.
- Draaijers, G.P.J., Van Leeuwen, E.P., Potma, C., Van Pul, W.A.J. and Erisman, J.W. (1995), Mapping of base-cation deposition in Europe on a 10x20 km grid. *Water, Air and Soil Pollution*, 85, 2389-2394.
- Draaijers, G.P.J. and J.W. Erisman (1995), A canopy budget model to estimate atmospheric deposition from throughfall measurements. *Water, Air and Soil Pollution*, 85, 2253-2258.
- Draaijers, G.P.J., Spranger, T., Erisman, J.W. and Wyers, G.P. (1996), The application of throughfall measurements for atmospheric deposition monitoring. *Atmospheric Environment*, 30 (in press).
- Driscoll, C.T., Likens, G.E., Hedin, L.O., Eaton, J.S. and Bormann, F.H. (1989), Changes in the chemistry of surface waters, *Environmental Science and Technology*, 23, 137-143.
- Eder, B.K. and Dennis, R.L. (1990), On the use of scavenging ratios for the inference of surface-level concentrations and subsequent dry deposition of Ca^{2+} , Mg^{2+} , Na^+ and K^+ , *Water, Air and Soil Pollution*, 52, 197-215.
- Erisman, J.W. (1992), Atmospheric deposition of acidifying compounds in the Netherlands, *Ph.D. thesis*, University of Utrecht, The Netherlands.
- Erisman, J.W., Draaijers, G.P.J., Duyzer, J.H., Hofschreuder, P., Van Leeuwen, N., Römer, F.G., Ruijgrok, W. and Wyers, G.P. (1994), Contribution of aerosol deposition to atmospheric deposition and soil loads onto forests. RIVM report no. 722108005, Bilthoven, The Netherlands.
- Erisman, J.W., Van Pul, W.A.J. and Wyers, G.P. (1994), Parameterization of dry deposition mechanisms for the quantification of atmospheric input to ecosystems. *Atmospheric Environment*, 28, 2595-2607.
- Erisman, J.W., Beier, C., Draaijers, G.P.J. and Lindberg, S.E. (1994), Review of deposition monitoring methods. *Tellus*, 46B, 79-93
- Erisman, J.W. and G.P.J. Draaijers (1995), Atmospheric deposition in relation to acidification and eutrophication, *Studies in Environmental Science*, 63, Elsevier, Amsterdam, The Netherlands.

- Erisman, J.W., Potma, C., Draaijers, G.P.J., Van Leeuwen, E.P. and Van Pul, W.A.J. (1995), A generalised description of the deposition of acidifying pollutants on a small scale in Europe, *Water, Air and Soil Pollution*, 85, 2101-2106.
- Evans, J.S. and D.W. Cooper (1980), An inventory of particulate emissions from open sources, *Journal of the Air Pollution Control Association*, 30, 1298-1303.
- Fitzgerald, J.W. (1975), Approximations formulas for the equilibrium size of an aerosol particle as a function of its size and composition and the ambient relative humidity, *Journal of Applied Meteorology*, 14, 1044-1049.
- Galloway, J.N., Savoie, D.L., Keene, W.C. and Prospero, J.M. (1993), The temporal and spatial variability of scavenging ratios for nss sulfate, nitrate, methanesulfonate and sodium in the atmosphere over the North Atlantic Ocean, *Atmospheric Environment*, 27A, 235-250.
- Ganor, E., Foner, H.A., Brenner, S., Neeman, E. and Lavi, N. (1991) The chemical composition of aerosols settling in Israel following dust storms. *Atmospheric Environment*, 25A, 2665-2670.
- Garland, J.A. (1978), Dry and wet removal of sulphur from the atmosphere, *Atmospheric Environment*, 12, 349-366.
- Gatz, D.F., Bernard, W.R. and Stensland, G.J. (1986), The role of alkaline materials in precipitation chemistry: a brief review of the issues, *Water, Air and Soil Pollution*, 30, 245-251.
- Gilham, C.A., Leech, P.K. and Eggleston, H. (1992), Report no LR887(AP), Warren Spring Laboratory, Hertfordshire, England.
- Gomes, L. and Gillette, D.A. (1993), A comparison of characteristics of aerosol from dust storms in central Asia with soil-derived dust from other regions, *Atmospheric Environment*, 27A, 2539-2544.
- Gorham, E. (1994), Neutralizing acid rain, *Nature*, 367, 321.
- Grace, A. (1990), Optimization toolbox for the use with MATLAB™, User's Guide, The MathWorks, Inc., MA, USA.
- Guerzoni, S., Cristini, A., Caboi, R., Le Bolloch, O., Marras, I., and Rundeddu, L. (1995), Ionic composition of rain water and atmospheric aerosols in Sardinia, southern Mediterranean, *Water, Air and Soil Pollution*, 85, 2077-2082.
- Harrison, R.M. and Pio, C.A. (1983), A comparative study of the ionic composition of rainwater and atmospheric aerosols: implications for the mechanism of acidification of rainwater, *Atmospheric Environment*, 17, 2539-2543.
- Hedin, L.O., Granat, L., Likens, G.E., Buishand, T.A., Galloway, J.N., Butler, Th.J and Rodhe, H. (1994), Steep declines in atmospheric base-cations in regions of Europe and North America, *Nature*, 367, 351-354.
- Heij, G.J. and Schneider, T. (1991), Acidification research in the Netherlands, *Studies in Environmental Science*, 46, Elsevier, Amsterdam, The Netherlands.
- Hettelingh, J.P., Downing, R.J. and De Smet, P.A.M. (1991), Mapping critical loads for Europe. RIVM report no. 259101001, Coordination Centre for Effects, Bilthoven, The Netherlands.
- Heuberger, P.S.C. en Janssen, P.H.M. (1994), UNCSAM: a software tool for sensitivity and uncertainty analysis of mathematical models. In: J. Grasman en G. van Straten (eds.), Predictability and nonlinear modelling in natural sciences and economics, Kluwer, Dordrecht, The Netherlands.
- Hicks, B.B., Baldocchi, D.D., Meyers, T.P., Hosker Jr., R.P. and Matt, D.R. (1987), A preliminary multiple resistance routine for deriving dry deposition velocities from measured quantities. *Water Air Soil Pollution*, 36, 311-330.

- Hornung, M., M.A. Sutton and R.B. Wilson (1995), Mapping and modelling of critical loads for nitrogen - a workshop report. Proceedings of the Grange-Over-Sands workshop, 24-26 October 1994.
- Ivens, W.P.M.F., Klein Tank, A., Kauppi, P. and Alcamo, J. (1989), Atmospheric deposition of sulphur, nitrogen and basic cations onto European forests: observations and model calculations. In: J. Kämäri, D.F. Brakke, A. Jenkins, S.A. Norton and R.F. Wright (eds.), *Regional acidification models: geographical extent and time development*, Springer Verlag, Heidelberg, Germany, 103-111.
- Ivens, W.P.M.F. (1990), Atmospheric deposition onto forests, *Ph.D. thesis*, University of Utrecht, The Netherlands.
- Iversen, T., Halvorsen, N., Mylona, S. and Sandnes, H. (1991), Calculated budgets for airborne acidifying components in Europe, 1985, 1987, 1988 and 1990. MSC-West, Norwegian Meteorological Institute, Oslo.
- Jaffrezo, J.L. and Colin, J.L. (1988), Rain-aerosol coupling in urban area: scavenging ratio measurement and identification of some transfer processes, *Atmospheric Environment*, 22, 929-935.
- Janssen, P.H.M., Slob, W. and Rotmans, J. (1990), Gevoeligheidsanalyse en onzekerheidsanalyse: een inventarisatie van ideeën, methoden en technieken, RIVM-report no. 958805001, Bilthoven, The Netherlands.
- Janssen, P.H.M., Heuberger, P.S.C. and Sanders, R. (1992), UNCSAM 1.1: a software package for sensitivity and uncertainty analysis: manual. RIVM-report 959101004, Bilthoven, The Netherlands.
- Jarvis, P.G., James, G.B. and Landsberg, J.J. (1976), Coniferous forest. In: J.L. Monteith, ed., *Vegetation and the atmosphere - 2*, Academic Press, New York.
- Johnson, D.W. and Lindberg, S.E. (1992), Atmospheric deposition and forest nutrient cycling, *Ecological Studies*, 91, Springer Verlag, New York.
- Kane, M.M., Rendell, A.R. and Jickells, T.D. (1994), Atmospheric scavenging processes over the North Sea, *Atmospheric Environment*, 28, 2523-2530.
- Keene, W.C., Galloway, J.N. and Holden, J.D. (1983), Measurement of weak organic acidity in precipitation from remote areas of the world. *Journal of Geophysical Research*, 88, 5122-5130.
- Kindbom, K., Sjöberg, K. and Lövblad, G. (1993), Emissioner av svavel, kväve och alkaliskt stoft i Sverige 1900-1990. IVL-report B1109, L93-166, Göteborg, Sweden.
- Kovar, A., Kasper, A., Puxbaum, H., Fuchs, G, Kalina, M. and Gregori, M. (1991), Kartierung der deposition von SO_x, NO_x, NH_x und basischen kationen in Österreich. Technische Universität Wien, Institut für Analytische Chemie, Vienna, Austria.
- Lannefors, H., Hansson, H.C. and Granat, L. (1983), Background aerosol composition in southern Sweden - Fourteen micro and macro constituents measured in seven particle size intervals at one site during one year, *Atmospheric Environment*, 17, 87-101.
- Leefflang, K.W.H. (1938), De chemische samenstelling van den neerslag in Nederland, *Chemisch Weekblad*, 35, 658-664.
- Legates, D.R. and Willmott, C.J. (1990), Mean seasonal and spatial variability in gauge-corrected, global precipitation, *International Journal of Climatology*, 10, 111-123.
- Lövblad, G. (1987), Utsläpp till luft av alkali, IVL-report no. B858, Göteborg, Sweden.

- Lövblad, G., Erisman, J.W. and Fowler, D. (1993) Models and methods for the quantification of atmospheric input to ecosystems. Report No. Nord 1993:573 Göteborg, Sweden, 3-7 November 1992. Nordic Council of Ministers, Copenhagen, Denmark.
- Løye-Pilot, M.D., Martin, J.M. and Morelli, J. (1986), Influence of Saharan dust on the rain acidity and atmospheric input to the Mediterranean, *Nature*, 321, 427-428.
- Mamane, Y., Miller, J.L. and Dzubay, T.G. (1986), Characterization of individual fly ash particles emitted from coal- and oil-fired power plants, *Atmospheric Environment*, 20, 2125-2135.
- Marquardt, W. and Ihle, P. (1988), Acidic and alkaline precipitation components in the mesoscale range under the aspect of meteorological factors and the emissions, *Atmospheric Environment*, 22, 2707-2713.
- Milford, J.B. and Davidson, C.I. (1985), The sizes of particulate trace elements in the atmosphere - a review, *Journal for Air Pollution Control and Assessment*, 35, 1249-1260.
- NAPAP (1987), National Acid Precipitation Assessment Program, C.N. Herrick and J.L. Kulp (eds.), Interim assessment: the causes and effects of acidic deposition, volume 3, US Governmental Printing Office, Washington, D.C.
- Olmez, I., Sheffield, A.E., Gordon, G.E., Houck, J.E., Pritchett, L.C., Cooper, J.A., Dzubay, T.G. and Bennet, R.L. (1988), Composition of particles from selected sources in Philadelphia for receptor modelling applications, *Journal for Air Pollution Control and Assessment*, 38, 1392-1402.
- Pannekoek, A.J. (1976), Algemene geologie, H.D. Tjeenk Willink bv, Groningen, The Netherlands.
- Pasquill, F. (1971), Atmospheric dispersion of pollutants. *Quaternary Journal of the Royal Meteorological Society*, 97, 369-395.
- Posch, M., De Smet, P.A.M., Hettelingh, J.P. and Downing, R.J. (1995), Calculation and mapping of critical thresholds in Europe. Status report 1995, Coordination Center for Effects, RIVM Report no. 259101004, Bilthoven, The Netherlands.
- Potma, C.J.M. (1993), Description of the ECMWF/WMO Global Observational Data Set, and associated data extraction and interpolation procedures. RIVM report no. 722401001, Bilthoven, The Netherlands.
- Powell, M.J.D. (1978), The convergence of variable metric methods for nonlinearly constrained optimization calculations. In: Mangasarian, Meyer, R.R. and Robinson, S.M. (eds.), *Nonlinear programming 3*, Academic Press, London.
- Pratt, G.C. and Krupa, S.V. (1985), Aerosol chemistry in Minnesota and Wisconsin and its relation to rainfall chemistry, *Atmospheric Environment*, 19, 961-971.
- Puxbaum, H and Kovar, A. (1991), Seasonal trend of snowfall composition at the high alpine observatory Sonnblick (3106m a.s.l., eastern Alps). In: Borrell, P.M., Borrell, P., Cvitas, T and Seiler, W. (eds.), *Proceedings Eurotrac Symposium '90*, SPB Academic Publishing bv., 61-66.
- RIVM (1993), data obtained from the National Air Quality Monitoring Network, The Netherlands (unpublished).
- RIVM (1994), data obtained from the National Precipitation Monitoring Network, The Netherlands (unpublished).
- Roda, F., Bellot, J., Avila, A, Escarré, A., Pinol, J. and Terrades, J. (1993), Saharan dust and the atmospheric inputs of elements and alkalinity to mediterranean ecosystems, *Water, Air and Soil Pollution*, 66, 277-288.

- Rodhe, H., Grennfelt, P., Wisniewski, J., Ågren, C., Bengtsson, G., Hultberg, H., Johansson, K., Kauppi, P., Kucera, V., Oskarsson, H., Karlsson, G. P., Rasmussen, L., Rosseland, B., Schotte, L., Selldén and Thörnelöf, E. (1995), Acid Reign '95? - Summary statement from the 5th International conference on acidic deposition science and policy, Göteborg, Sweden, 26-30 June 1995.
- Römer, F.G. and Te Winkel, B.W. (1994), Dry deposition of aerosols on vegetation: acidifying components and basic cations, KEMA report no. 63591-KES/MLU 93-3243, Arnhem, The Netherlands.
- Ruijgrok, W., Tieben, H. and Eisinga, P. (1994), The dry deposition of acidifying and alkaline particles to Douglas fir: a comparison of measurements and model results. KEMA report no. 20159-KES/MLU 94-3216, Arnhem, The Netherlands.
- Savoie, D.L., Prospero, J.M. and Nees, R.T. (1987), Washout ratios of nitrate, non-sea-salt sulfate and sea-salt on Virginia Key, Florida and on Mamerican Samoa, *Atmospheric Environment*, 21, 103-112.
- Schaug, J., Pedersen, U. and Skjelmoen, J.E. (1991), Data report 1989, part 2: monthly summaries, EMEP Co-operative programme for monitoring and evaluation of the long-range transmission of air pollutants in Europe, Norwegian Institute for Air Research, EMEP/CCC-Report 2/91.
- Schober, R. (1987), Ertragstafeln wichtiger Baumarten, 3. Auflage. Sauerländer Verlag, Frankfurt a. M., Germany.
- Schroeder, W.H., Dobson, M., Kane, D.M. and Johnson, N.D. (1987), Toxic trace elements associated with airborne particulate matter: a review, *Journal for Air Pollution Control and Assessment*, 37, 1267-1285.
- Schütz, L. and Sebert, M. (1987), Mineral aerosols and source identification, *Journal of Aerosol Science*, 18, 1-10.
- Schütz, L. and Rahn, K.A. (1982), Trave-element concentrations in erodible soils, *Atmospheric Environment*, 16, 171-176.
- Scott, B.C. (1981), Sulfate washout ratios in winter storms, *Journal of Applied Meteorology*, 20, 619-625.
- Semb, A., Hanssen, J.E., Francois, F., Maenhout, W. and Pacyna, J.M. (1995), Long range transport and deposition of mineral matter as a source for base-cations. *Water, Air and Soil Pollution*, 85, 1933-1940.
- Slanina, J., Römer, F.G. and Asman, W.A.H. (1983), Investigation of the source regions for acid deposition in the Netherlands. In: Beilke, S. and Elshout, A.J. (eds.), Acid deposition, Reidel, 129-141.
- Slanina, J., Baard, J.H., Broersen, B.C., Möls, J.J. and Voors, P.I. (1987), The stability of precipitation samples under field conditions. *International Journal of Environmental Analytical Chemistry*, 28, 247-261.
- Slinn, W.G.N. (1977), Some approximations for the wet and dry removal of particles and gases from the atmosphere, *Water, Air and Soil Pollution*, 7, 513-543.
- Slinn, W.G.N., Hasse, L., Hicks, B.B., Hogan, A.W., Lal, D., Liss, P.S., Munnich, K.O., Sehmel, G.A. and Vittori, O. (1978), Some aspects of the transfer of atmospheric trace constituents past the air-sea interface, *Atmospheric Environment*, 12, 2055-2087.
- Slinn, W.G.N. (1982), Predictions for particle deposition to vegetative surfaces., *Atmospheric Environment*, 16, 1785-1794.

- Slinn, W.G.N. (1983), Air to sea transfer of particles. In: P.S. Liss and W.G.N. Slinn (eds.), Air sea exchange of gases and particles, Reidel, Dordrecht, The Netherlands.
- Spranger, T, E. Hollwurtel, F. Poetzsch-Heffter and A. Branding (1994), Dry deposition estimates from two different inferential models as compared to net throughfall measurements. In: P.M. Borrell, P. Borrell, T. Cvitaš and W. Seiler (eds.), Transport and transformation of pollutants in the troposphere. Proceedings of EUROTRAC symposium in Garmisch Partenkirchen, Germany, 11-15 April 1994, 615-619.
- Stedman, J.R., C.J. Heyes, J.G. Irwin (1990), A comparison of bulk and wet-only precipitation collectors at rural sites in the United Kingdom. *Water, Air and Soil Pollution*, 52, 377-395.
- Stelson, A.W. and Seinfeld, J.H. (1981), Chemical mass accounting of urban aerosol, *Environmental Science and Technology*, 15, 671-679.
- Stevenson, C.M. (1967), An analysis of the chemical composition of rain-water and air over the British Isles and Eire for the years 1959-1964, *Tellus*, 19, 56-70
- Sverdrup, H.U. and Warfvinge, P.G. (1988), Chemical weathering of minerals in the Gardsjön catchment in relation to a model based on laboratory rate coefficients. In: J. Nilsson and P. Grennfelt (eds.), critical loads for sulphur and nitrogen, Copenhagen, Nordic Council of Ministers, Miljørapport 1988, 15, 131-149.
- Swap, R., Garstang, M. and Greco, S. (1992), Saharan dust in the Amazon Basin. *Tellus*, 44B, 133-149.
- TFM (1996), Manual on methodologies for mapping of critical loads/levels and geographical areas where they are exceeded. Final draft prepared for the 12th meeting of the Task Force on Mapping, Budapest, 22 March 1996.
- UBA (1992), Facts and figures on the environment of Germany, Umweltbundesamt, Berlin, Germany.
- Ulrich, B. (1983), Interaction of forest canopies with atmospheric constituents: SO₂, alkali and earth alkali cations and chloride. In: B. Ulrich and J. Pankrath, eds., Effects of accumulation of air pollutants in forest ecosystems, Reidel, Dordrecht, The Netherlands, 33-45.
- Ulrich, E. and Williot, B. (1993), Les depots atmospheriques en France de 1850 à 1990. Report of the Office National des Forêts, France.
- Van Breemen, N., Burrough, P.A., Velthorst, E.J., Dobben, H.F. van, Wit, T. de, Ridder, T.B., Reinders, H.F.R. (1982) Soil acidification from atmospheric ammonium sulphate in forest canopy throughfall. *Nature*, 299, 548-550.
- Van de Velde, R.J., Faber, W., Katwijk, V., Scholten, H.J., Thewessen, T.J.M., Verspuy, M. and Zevenbergen, M. (1994), The preparation of a European land use database. RIVM report no. 712401001, Bilthoven, The Netherlands.
- Van Leeuwen, E.P., Potma, C., Draaijers, G.P.J., Erisman, J.W. and Van Pul, W.A.J. (1995), European wet deposition maps based on measurements. RIVM report no. 722108006, Bilthoven, The Netherlands.
- Van Leeuwen, E.P., Erisman, J.W. and Draaijers, G.P.J. (1996), Mapping wet deposition of acidifying components and base-cations over Europe using measurements. *Atmospheric Environment*, 30, 2495-2511.
- Van Pul, W.A.J. and Jacobs, A.F.G. (1993), The conductance of a maize crop and the underlying soil to ozone under various environmental conditions. *Boundary-Layer Meteorology*, 69, 83-99

- Van Pul, W.A.J., Potma, C., Van Leeuwen, E.P., Draaijers, G.P.J. and Erisman, J.W. (1995), EDACS: European Deposition maps of Acidifying Components on a Small scale. Model description and results. RIVM report no. 722401005, Bilthoven, The Netherlands.
- Veldkamp, J.G., Faber, W.S., Van Katwijk, V.F. and Van de Velde, R.J. (1996), Enhancements of the 10x10 minutes pan-European land use data base. RIVM-report in preparation, Bilthoven, The Netherlands.
- Weast, R.C. (1975), Handbook of chemistry and physics, 56th edition, CRC-press, Cleveland, Ohio.
- Wedding, J.B., Macfarland, A.R. and Cermak, J.E. (1977), Large particle collection characteristics of ambient aerosol samplers. *Environmental Science and Technology*, 11, 387-392.
- Wieringa, J. (1992), Updating the Davenport roughness classification. *Journal of Wind Engineering and Industrial Aerodynamics*, 41.
- Williams, P.T., Radojevic, M. and Clarke, A.G. (1988), Dissolution of trace metals from particles of industrial origin and its influence on the composition of rain water, *Atmospheric Environment*, 22, 1433-1442.

Appendix 1

For the calculation and mapping of critical loads in Europe, very crude estimates of base-cation dry deposition were made by Downing *et al.* (1993) and De Vries *et al.* (1993). Downing *et al.* (1993) assumed dry deposition of base-cations (BC_d) to be related to the wet deposition amount according to:

$$\begin{aligned} BC_d &= 2 * BC_w && \text{if } BC_w < 250 \text{ eq ha}^{-1} \text{ a}^{-1} \\ BC_d &= BC_w + 250 && \text{otherwise} \end{aligned} \quad [19]$$

in which BC_w amounts the wet deposition estimated by the EMEP MSC-West for a 150x150 km grid. De Vries *et al.* (1993) assumed dry deposition of base-cations to forests situated with such a grid linearly related to wet deposition according to:

$$BC_d = (1-f_d) * BC_w \quad [20]$$

in which f_d denotes a dry deposition factor, which was derived from the ratio of Na^+ in bulk precipitation (bp) and throughfall (tf) (Ulrich, 1983; Bredemeier, 1988):

$$f_d = (Na_{tf} - Na_{bp}) / Na_{bp} \quad [21]$$

Based on a literature survey of Ivens *et al.* (1989) for 47 sites scattered over Europe, De Vries *et al.* (1993) took f_d equal to 0.6 for deciduous forest and 1.1 for coniferous forest. Data were based on results in areas sparsely occupied with forests. For this reason, it was expected that the dry deposition factor will decrease with an increase of the forested areas within a grid, since dry deposition of base-cations increases considerably at forest edges (Draaijers *et al.*, 1994). De Vries *et al.* (1993) took this effect into account by a linear relationship between f_d and the coverage fraction of open land (f_0) according to:

$$f_d = \alpha * f_0 \quad [22]$$

where $\alpha = 0.6$ for deciduous forests and $\alpha = 1.1$ for coniferous forests.

As ecosystems of different species and roughness receive pollutants at different rates, it is necessary to define atmospheric dry deposition in relation to land use type. At UN-ECE workshops held in Gothenburg (Lövblad *et al.*, 1993), Grange-Over-Sands (Hornung *et al.*, 1995) and Geneva (TFM, 1996) it was concluded that dry deposition factors or 'filter factors' attempt to simulate the effects of atmospheric roughness but lack a rigorous scientific basis and should therefore not be used. It was stated that the best current approach to estimate dry deposition of base-cations is the inferential technique in which dry deposition velocities estimated from land use and meteorological information using the scheme of Slinn (1982) are multiplied with air concentrations estimated from rain chemistry data using scavenging ratios (Hornung *et al.*, 1995; TFM, 1996).

Appendix 2

Table VII presents an overview of site characteristics and measurement methods used by several authors for the simultaneous measurement of base-cation concentrations in precipitation and surface-level air. Bulk precipitation data from Stevenson (1967) were corrected for the contribution of dry deposition on the collectors, using the wet-only to bulk ratios derived by Stedman *et al.* (1990) and Clark and Lambert (1988) for the United Kingdom. One measurement site of Stevenson (1967), i.e. 'Lerwick', was situated very close to the sea. Wet-only to bulk ratios of Stedman *et al.* (1990) and Clark and Lambert (1988) do not hold for this situation. Moreover, large-sized maritime aerosols at this site most probably did not enter the air sampling system. For this reason, data from Lerwick were not used in estimating scavenging ratios. Galloway *et al.* (1993) mention that scavenging ratios should ideally be based on volume-weighted mean precipitation concentrations and mean aerosol concentrations. All mentioned authors have published their results in this way, Stevenson (1967), presenting median precipitation concentrations, being the only exception. At one measurement site of Galloway *et al.* (1993), i.e. 'Ireland', a few storms deposited disproportionately large amounts of Na^+ , resulting in extremely high volume-weighted mean precipitation concentrations. This site was therefore not used in the estimation of scavenging ratios.

Using the scavenging model described in section 3.2, surface-level air concentrations will probably be overestimated in forested areas and/or areas far from major sources. In such areas, the surface-level air will be 'cleaned' as a result of dry deposition. In Figure 7, this is demonstrated by data from Harrison and Pio (1983), Pratt and Krupa (1985), Eder and Dennis (1990) and Römer and te Winkel (1994). Sites situated in agricultural areas (Stevenson, 1967; Pratt and Krupa, 1985; Kane *et al.*, 1994) usually show higher air concentrations of Mg^{2+} , Ca^{2+} and K^+ than would have been predicted using the scavenging model. Most probably, this is the result of local base-cation emissions due to agricultural tillage practices. The same reasoning hold for sites situated in coastal areas (Savoie *et al.*, 1987; Galloway *et al.*, 1993) which experience higher air concentrations of Na^+ than predicted by the model.

Table VII An overview of site characteristics and measurement methods used by several authors for the simultaneous measurement of base-cation concentrations in precipitation and surface-level air.

Reference	Country	No of sites	Site characteristics
Stevenson (1967)	United Kingdom	9	agricultural area, away from local industrial pollution
Harrison & Pio (1983)	United Kingdom	1	open pasture land, appreciably distant from major source regions
Derrick <i>et al.</i> (1984)	USA	1	large open area with no large vegetation or buildings
Pratt & Krupa (1985)	USA	6	agricultural area (4 sites) or predominantly forested area (2 sites)
Savoie <i>et al.</i> (1987)	Miami, Samoa, Bermuda	3	coastal area
Jaffrezo & Colin (1988)	France	1	build up area (Paris)
Eder & Dennis (1990)	Canada	17	rocky desert, away from roads, agricultural activity or other sources
RIVM (1993)	The Netherlands	6	open pasture land, away from local industrial pollution
Galloway <i>et al.</i> (1993)	Barbedos, Bermuda, Ireland	3	coastal area
Kane <i>et al.</i> (1994)	United Kingdom	1	agricultural area
Römer & te Winkel (1994)	The Netherlands	1	above a 21m tall forest stand, 5km distant from agricultural area
Guerzoni <i>et al.</i> (1995)	Sardinia (Italy)	1	coastal area

Reference	Components analysed	Measurement period	Air concentration sampler	Height of inlet	Collecting efficiency	Precipitation sampler
Stevenson (1967)	Na, Mg, Ca, K	5 years, on monthly basis	medium-volume sampler	1.2m	<17 μm	bulk
Harrison & Pio (1983)	Na, Mg, Ca, K	2 years, 17 periods of 24h	high-volume sampler	1.8m	<100 μm ¹⁾	wet-only
Derrick <i>et al.</i> (1984)	Na, Mg, Ca, K	1 year, on weekly basis	high-volume samplers	1.5m	<40 μm ¹⁾	wet-only
Pratt & Krupa (1985)	Ca	0.5 year, on weekly basis	dichotomus sampler	?	<15 μm	wet-only
Savoie <i>et al.</i> (1987)	Na	1 year, on daily basis	high-volume samplers	?	?	wet-only
Jaffrezo & Colin (1988)	Na, Mg, Ca, K	1 year, 82 periods	?	25m	?	wet-only
Eder & Dennis (1990)	Na, Mg, Ca, K	3 years, on monthly basis	low-volume sampler	2.0m	<10 μm	wet-only
RIVM (1993)	Ca	1-4 years, on monthly basis	low-volume sampler	?	<5 μm	wet-only
Galloway <i>et al.</i> (1993)	Na	2 years, on daily basis	high-volume samplers	2-23m	?	wet-only
Kane <i>et al.</i> (1994)	Na, Ca	1 year, on weekly basis	high-volume sampler	?	?	wet-only
Römer & te Winkel (1994)	Na, Mg, Ca, K	0.5 year, on monthly basis	dichotomus sampler	29m	<15 μm	wet-only
Guerzoni <i>et al.</i> (1995)	Na, Mg, Ca, K	1 year, 31 periods	high-volume sampler	?	?	wet-only

¹⁾ The collecting efficiency of particles larger than 15 μm was less than 100% due to non-isokenetic sampling and dependent on wind speed and direction (Wedding *et al.*, 1977).

Appendix 3

Table VIII Average total deposition of Na⁺, Mg²⁺, Ca²⁺, K⁺ (in mol ha⁻¹ a⁻¹), non sea salt Mg²⁺+Ca²⁺+K⁺ and potential acid (in eq ha⁻¹ a⁻¹) in 1989 in different pan-European countries. Moreover, the average percentage neutralization of acid deposition by deposition of base-cations is presented.

Country	Na ⁺	Mg ²⁺	Ca ²⁺	K ⁺	Mg ²⁺ +Ca ²⁺ +K ⁺	Nss	Potential acid	% neutralization
Albania	997	291	713	153		1876	2750	68
Andorra	528	126	374	46		897	1696	53
Austria	216	84	291	63		753	2810	27
Belgium	1233	165	260	88		589	3576	16
Belorussia	385	163	221	101		763	2268	34
Bosnia-Herzegowina	905	314	719	209		2016	3203	63
Bulgaria	560	143	406	86		1026	2557	40
Croatia	796	352	836	177		2326	3650	64
Czech Republic	280	110	295	71		802	5750	14
Denmark	2209	245	166	86		316	2669	12
England	1909	233	150	197		434	1858	23
Estonia	543	114	205	132		619	1872	33
Finland	201	36	90	52		251	978	26
France	810	131	250	65		603	1728	35
Georgia	857	465	464	266		1881	3298	57
Germany	639	141	303	86		804	4202	19
Greece	812	158	474	100		1140	1983	58
Hungary	307	200	516	103		1450	3002	48
Ireland	4234	612	356	206		949	1047	91
Italy	700	185	499	95		1265	2231	57
Latvia	850	154	341	167		926	2150	43
Lichtenstein	256	54	204	56		500	2290	22
Lithuania	753	129	340	136		862	2275	38
Luxembourg	876	136	213	93		544	3100	18
Macedonia	456	133	424	88		1075	1934	56
Moldavia	1017	355	579	371		1950	2820	69
Netherlands	1452	187	169	79		381	3396	11
Norway	879	115	50	37		124	634	20
Poland	414	110	274	78		731	4052	18
Portugal	1002	158	285	85		686	726	95
Romania	867	168	503	129		1228	2642	46
Russian Federation	348	189	263	101		895	1597	56
Servia	558	241	635	126		1720	2647	65
Slovak Republic	221	104	264	87		761	4087	19
Slovenia	416	187	682	102		1723	3448	50
Spain	576	104	303	54		706	960	74
Sweden	297	45	44	29		125	904	14
Switzerland	261	45	223	61		525	2246	23
Turkey	612	202	422	97		1172	2304	51
Ukraine	743	353	328	213		1366	2823	48

Appendix 4

To calculate the percentage in which specific anions are related to the various cations in precipitation, constrained non-linear multiple regression analysis was used. The following set of multiple regression equations and constraints was numerically solved:

$$\begin{aligned}
 [\text{SO}_4^{2-}] &= a_1[\text{NH}_4^+] + a_2[\text{H}^+] + a_3[\text{Na}^+] + a_4[\text{Mg}^{2+}] + a_5[\text{Ca}^{2+}] + a_6[\text{K}^+] \\
 [\text{NO}_3^-] &= b_1[\text{NH}_4^+] + b_2[\text{H}^+] + b_3[\text{Na}^+] + b_4[\text{Mg}^{2+}] + b_5[\text{Ca}^{2+}] + b_6[\text{K}^+] \\
 [\text{Cl}^-] &= c_1[\text{NH}_4^+] + c_2[\text{H}^+] + c_3[\text{Na}^+] + c_4[\text{Mg}^{2+}] + c_5[\text{Ca}^{2+}] + c_6[\text{K}^+] \\
 [\text{PO}_4^{3-}] &= d_1[\text{NH}_4^+] + d_2[\text{H}^+] + d_3[\text{Na}^+] + d_4[\text{Mg}^{2+}] + d_5[\text{Ca}^{2+}] + d_6[\text{K}^+] \\
 [\text{HCO}_3^-] &= e_1[\text{NH}_4^+] + e_2[\text{H}^+] + e_3[\text{Na}^+] + e_4[\text{Mg}^{2+}] + e_5[\text{Ca}^{2+}] + e_6[\text{K}^+] \\
 [\text{F}^-] &= f_1[\text{NH}_4^+] + f_2[\text{H}^+] + f_3[\text{Na}^+] + f_4[\text{Mg}^{2+}] + f_5[\text{Ca}^{2+}] + f_6[\text{K}^+]
 \end{aligned}$$

Constraints:

$$\begin{aligned}
 a_1 + b_1 + c_1 + d_1 + e_1 + f_1 &= 1 \\
 a_2 + b_2 + c_2 + d_2 + e_2 + f_2 &= 1 \\
 a_3 + b_3 + c_3 + d_3 + e_3 + f_3 &= 1 \\
 a_4 + b_4 + c_4 + d_4 + e_4 + f_4 &= 1 \\
 a_5 + b_5 + c_5 + d_5 + e_5 + f_5 &= 1 \\
 a_6 + b_6 + c_6 + d_6 + e_6 + f_6 &= 1 \\
 a_1, b_1, c_1, \dots, d_6, e_6, f_6 &\geq 0
 \end{aligned}$$

Similarly, the percentage in which specific cations are associated to the various anions in precipitation was calculated by solving:

$$\begin{aligned}
 [\text{NH}_4^+] &= a_1[\text{SO}_4^{2-}] + a_2[\text{NO}_3^-] + a_3[\text{Cl}^-] + a_4[\text{PO}_4^{3-}] + a_5[\text{HCO}_3^-] + a_6[\text{F}^-] \\
 [\text{H}^+] &= b_1[\text{SO}_4^{2-}] + b_2[\text{NO}_3^-] + b_3[\text{Cl}^-] + b_4[\text{PO}_4^{3-}] + b_5[\text{HCO}_3^-] + b_6[\text{F}^-] \\
 [\text{Na}^+] &= c_1[\text{SO}_4^{2-}] + c_2[\text{NO}_3^-] + c_3[\text{Cl}^-] + c_4[\text{PO}_4^{3-}] + c_5[\text{HCO}_3^-] + c_6[\text{F}^-] \\
 [\text{Mg}^{2+}] &= d_1[\text{SO}_4^{2-}] + d_2[\text{NO}_3^-] + d_3[\text{Cl}^-] + d_4[\text{PO}_4^{3-}] + d_5[\text{HCO}_3^-] + d_6[\text{F}^-] \\
 [\text{Ca}^{2+}] &= e_1[\text{SO}_4^{2-}] + e_2[\text{NO}_3^-] + e_3[\text{Cl}^-] + e_4[\text{PO}_4^{3-}] + e_5[\text{HCO}_3^-] + e_6[\text{F}^-] \\
 [\text{K}^+] &= f_1[\text{SO}_4^{2-}] + f_2[\text{NO}_3^-] + f_3[\text{Cl}^-] + f_4[\text{PO}_4^{3-}] + f_5[\text{HCO}_3^-] + f_6[\text{F}^-]
 \end{aligned}$$

Constraints:

$$\begin{aligned}
 a_1 + b_1 + c_1 + d_1 + e_1 + f_1 &= 1 \\
 a_2 + b_2 + c_2 + d_2 + e_2 + f_2 &= 1 \\
 a_3 + b_3 + c_3 + d_3 + e_3 + f_3 &= 1 \\
 a_4 + b_4 + c_4 + d_4 + e_4 + f_4 &= 1 \\
 a_5 + b_5 + c_5 + d_5 + e_5 + f_5 &= 1 \\
 a_6 + b_6 + c_6 + d_6 + e_6 + f_6 &= 1 \\
 a_1, b_1, c_1, \dots, d_6, e_6, f_6 &\geq 0
 \end{aligned}$$

Other ions present in precipitation were excluded from analysis because they generally constitute only a very small fraction of the total amount of cations or anions present in precipitation. Precipitation concentrations, expressed in eq l^{-1} , for De Bilt (The Netherlands) were used as input. Results of 39 wet-only precipitation collections made during the period 02/01/92-28/12/94 were obtained (RIVM, 1994). Due to extremely high Na^+ and Cl^- concentrations, 3 periods were excluded from analysis because they would otherwise have had a disproportionately large effect on the regression results. To find the minimum of the constrained multivariable functions, the CONSTR option in MATLAB™ (Grace, 1990) was used. The method used is generally referred to as constrained non-linear optimization (Powell, 1978). CONSTR uses a sequential quadratic programming method in which a quadratic programming subproblem is solved at each iteration (Grace, 1990). Derived regression coefficients ($a_1, b_1, c_1, \dots, d_6, e_6, f_6$), concentrations calculated from the regression equations, and measured values are presented in Table IX. Very small differences are found

indicating that the fit of the multiple regression models is reasonable. Regression equations are found less reliable for PO_4^{3-} , HCO_3^- and F^- concentrations. The percentage anions are connected to the various cations, and vice versa, is presented in Table III. Inconsistencies which can be examined in Table III and IX (e.g. in the upper part of the table Mg^{2+} is only connected to Cl^- whereas in the lower part Mg^{2+} is also related to SO_4^{2-} and HCO_3^-) are probably inherent to the numerical procedure followed and the generally very low concentrations together with some exceptionally large values measured for certain ions (Dekkers, personal communication). A detailed description of the methodology used can be found in Dekkers and Sauter (1996).

Table IX Derived regression coefficients ($a_1, b_1, c_1, \dots, d_6, e_6, f_6$) using constrained non-linear optimization. Average concentrations calculated from the regression equations, and average measured values are presented as well (in $\mu\text{eq l}^{-1}$).

	NH_4^+	H^+	Na^+	Mg^{2+}	Ca^{2+}	K^+	calculated	measured
SO_4^{2-}	0.5421	0.6537	0.1313	0	0.8310	0	79.59	81.86
NO_3^-	0.4012	0.3256	0	0	0.1690	0	44.81	45.98
Cl^-	0	0.0207	0.8687	1.0000	0	0	63.34	64.09
PO_4^{3-}	0.0502	0	0	0	0	0.0173	4.84	2.84
HCO_3^-	0	0	0	0	0	0.9827	6.77	4.59
F^-	0.0065	0	0	0	0	0	0.61	0.91

	SO_4^{2-}	NO_3^-	Cl^-	PO_4^{3-}	HCO_3^-	F^-	calculated	measured
NH_4^+	0.7005	0.7284	0	1.0000	0.4680	1.0000	96.73	94.11
H^+	0	0.1306	0.0848	0	0	0	11.44	14.35
Na^+	0.0826	0	0.7790	0	0.0386	0	56.86	57.14
Mg^{2+}	0.0500	0	0.1363	0	0.0166	0	12.90	13.41
Ca^{2+}	0.1051	0.1410	0	0	0.0275	0	15.21	14.07
K^+	0.0619	0	0	0	0.4492	0	7.13	6.89

Appendix 5

Table X Mean, standard deviation, minimum and maximum values in Europe for different variables estimated in this study.

Variable	Grid size	Figure	Mean	St.dev	Min.	Max.
Na ⁺ concentration in precipitation (mg l ⁻¹)	50x50km	3	1.04	1.00	0.07	8.69
Mg ²⁺ concentration in precipitation (mg l ⁻¹)	50x50km	3	0.35	0.33	0	1.67
Ca ²⁺ concentration in precipitation (mg l ⁻¹)	50x50km	3	0.86	0.59	0.04	4.36
K ⁺ concentration in precipitation (mg l ⁻¹)	50x50km	3	0.33	0.35	0	2.96
precipitation amount (mm a ⁻¹)	0.5°x0.5°	4	915	432	87	3272
Na ⁺ wet deposition (mol ha ⁻¹ a ⁻¹)	50x50km	5	420	587	18	6264
Mg ²⁺ wet deposition (mol ha ⁻¹ a ⁻¹)	50x50km	5	114	113	5	1089
Ca ²⁺ wet deposition (mol ha ⁻¹ a ⁻¹)	50x50km	5	169	131	7	1547
K ⁺ wet deposition (mol ha ⁻¹ a ⁻¹)	50x50km	5	69	69	3	602
dry deposition velocity (m s ⁻¹)	1/6°x1/6°	6	0.019	0.005	0.001	0.056
Na ⁺ ambient air concentration (µg m ⁻³)	50x50km	8	1.25	0.87	0.11	4.28
Mg ²⁺ ambient air concentration (µg m ⁻³)	50x50km	8	0.34	0.19	0.04	1.02
Ca ²⁺ ambient air concentration (µg m ⁻³)	50x50km	8	0.82	0.39	0.09	1.62
K ⁺ ambient air concentration (µg m ⁻³)	50x50km	8	0.52	0.25	0.07	1.49
Na ⁺ dry deposition (mol ha ⁻¹ a ⁻¹)	1/6°x1/6°	9	293	237	22	2962
Mg ²⁺ dry deposition (mol ha ⁻¹ a ⁻¹)	1/6°x1/6°	9	76	42	8	456
Ca ²⁺ dry deposition (mol ha ⁻¹ a ⁻¹)	1/6°x1/6°	9	115	49	8	409
K ⁺ dry deposition (mol ha ⁻¹ a ⁻¹)	1/6°x1/6°	9	38	19	5	236
Na ⁺ total deposition (mol ha ⁻¹ a ⁻¹)	1/6°x1/6°	13	647	676	81	7532
Mg ²⁺ total deposition (mol ha ⁻¹ a ⁻¹)	1/6°x1/6°	13	174	126	14	1435
Ca ²⁺ total deposition (mol ha ⁻¹ a ⁻¹)	1/6°x1/6°	13	282	166	18	1683
K ⁺ total deposition (mol ha ⁻¹ a ⁻¹)	1/6°x1/6°	13	102	67	13	532
nss Mg ²⁺ +Ca ²⁺ +K ⁺ total deposition (eq ha ⁻¹ a ⁻¹)	1/6°x1/6°	14	836	513	41	4961
% dry dep. to total dep. nss Mg ²⁺ +Ca ²⁺ +K ⁺	1/6°x1/6°	15	45.0	11.7	2.9	75.5
% nss Mg ²⁺ to total dep. nss Mg ²⁺ +Ca ²⁺ +K ⁺	1/6°x1/6°	16	21.4	12.9	0	65.6
% nss Ca ²⁺ to total dep. nss Mg ²⁺ +Ca ²⁺ +K ⁺	1/6°x1/6°	16	65.7	13.7	20.3	93.7
% nss K ⁺ to total dep. nss Mg ²⁺ +Ca ²⁺ +K ⁺	1/6°x1/6°	16	13.0	7.4	0.9	63.7
% acid neutralization in precipitation	50x50km	17	45.4	23.9	0.3	93.4
total deposition of potential acid (eq ha ⁻¹ a ⁻¹)	1/6°x1/6°	18	2064	1299	113	14984
% neutralization potential acid	1/6°x1/6°	19	44.0	26.2	5.7	296
weathering rate in forest soils (eq ha ⁻¹ a ⁻¹)	1.0°x0.5°	20	596	520	79	5000
% contribution to forest nutrition	1/6°x1/6°	21	52.2	18.8	9.0	92.7